Universidad de La Laguna

Behavioral Consequences of Electrical Versus Chemical Synapse Restoration in a Drosophila Model of Neurodegeneration

Ninovska Romero Luis

FACULTAD DE CIENCIAS DE LA SALUD
DEPARTAMENTO DE CIENCIAS MÉDICAS BÁSICAS

DISSERTATION TITLE:

BEHAVIORAL CONSEQUENCES OF ELECTRICAL *VERSUS* CHEMICAL SYNAPSE RESTORATION IN A *DROSOPHILA* MODEL OF NEURODEGENERATION

by

Ninovska Romero Luis

July 2019

BEHAVIORAL CONSEQUENCES OF ELECTRICAL *VERSUS* CHEMICAL SYNAPSE RESTORATION IN A *DROSOPHILA* MODEL OF NEURODEGENERATION

by

Ninovska Romero Luis

B. Sc in Chemistry

M. Sc in Biomedicine

A dissertation submitted to the Faculty of Health Sciences at the University of La Laguna in fulfillment of the requirement for the degree of Doctor in Health Sciences

Supervisor: Ángel Acebes Vindel, PhD

July 2019

This Project was funded by IMBRAIN,
Agencia Canaria de Investigación and
Ministerio de Economía y Competetitividad

"Enamórate de una actividad y ¡házlo!
Nunca nadie se da cuenta de lo que se trata la vida en realidad.
Explora el mundo. Prácticamente todo a nuestro alrededor,
es realmente interesante, si lo observas profundamente.
Trabaja duro y cuanto puedas,
en las cosas que más te gusta hacer.
No pienses en lo que quieres ser,
sino en lo que TÚ quieras hacer."

Richard Feynman

A mis padres

SUMMARY

In this thesis we have documented the behavioral consequences of synapse restoration employing *Drosophila melanogaster* as a genetic model. Here, we have characterized the role of electrical synapses in olfactory perception after eliminating the electrical connections in fly brain or by attenuating them in the whole brain and in selected neuronal populations of the olfactory pathway. Besides, we have also analyzed fly olfactory responses after their restoration. Our findings revealed that alterations in electrical connections yield to behavioral changes in an odorant- and concentration- manner and how their selective restoration allows the rescue of normal olfactory responses.

In addition to their role in olfaction, this thesis also highlights the relevance of electrical synapses in life expectancy and locomotion. Again, the selective restoration of electrical synapses in whole fly brain and in selected neuronal populations improves fly viability and locomotor activity.

Furthermore, this thesis also describes the beneficial synaptogenic and neuroprotective effects triggered by phosphoinositide 3 Kinase (PI3K) activation in a *Drosophila* model of neurodegeneration, based on the expression of a human variant of Aβ42 peptide. Our findings reveal that negative effects on olfaction, locomotion and life expectancy elicited by Aβ42 peptide are ameliorated by PI3K expression in *Drosophila* neurons.

RESUMEN

Esta tesis ha tenido como objetivo el análisis de las consecuencias funcionales de la restauración de sinapsis empleando la mosca de la fruta, *Drosophila melanogaster*, como modelo genético. En este trabajo se ha caracterizado el papel de las sinapsis eléctricas en la percepción olfativa tras eliminar las conexiones eléctricas en todo el cerebro de la mosca o atenuándolas en poblaciones neuronales seleccionadas de la vía olfativa. Además, se han analizado las respuestas olfativas de las moscas tras restaurar las sinapsis eléctricas. Nuestros datos revelan que las alteraciones en las conexiones eléctricas conducen a cambios en el comportamiento que son dependientes del olor y de la concentración y cómo su restauración selectiva permite el rescate de las respuestas olfativas normales.

Además de su papel en la olfacción, esta tesis ha caracterizado también la importancia de las sinapsis eléctricas en la esperanza de vida y la locomoción. Una vez más, la restauración selectiva de las sinapsis eléctricas en todo el cerebro de las moscas y en poblaciones neuronales seleccionadas mejora la viabilidad y la actividad locomotora de las moscas.

Por último, en esta tesis se describen los efectos sinaptogénicos y neuroprotectores inducidos por la expresión de la enzima fosfoinositol 3-quinasa (PI3K) en un modelo de neurodegeneración en *Drosophila,* basado en la sobreexpresión de una variante humana del péptido Aβ42. Nuestros datos muestran que los efectos negativos sobre la olfacción, la locomoción y la esperanza de vida provocados por el péptido Aβ42 mejoran tras la expresión de PI3K en neuronas de *Drosophila.*

INDEX

ABBREVIATIONS

Aβ	Amyloid β-peptide
AD	Alzheimer´s disease
Akt	Protein kinase B
AL	Antennal lobe
APP	Amyloid precursor transmembrane protein
cAMP	Cyclic adenosine monophosphate
Cha	Choline acetyl-transferase
CNS	Central nervous system
CFS	Cerebrospinal fluid
Cx	Connexin
CX	Central complex
DLMn	Dorsal longitudinal muscle motor neuron
EB	Ethyl-butyrate
EEG	Electroencephalography
ECE-1	Endothelin-converting enzyme
eLN	Excitatory local interneuron
GABA	γ-Amino-butyric acid
GFP	Green fluorescent protein
GFP^{nls}	Green fluorescent protein – nuclear localization sequence
GFS	Giant fiber system
GJ	Gap junction
GSK3	Glycogen synthase kinase 3
IAA	Isoamyl-acetate
IDE	Insulin degrading enzyme
iLN	Inhibitory local interneuron
Inx	Innexin
JO	Johnston´s organ
LAL	Lateral accesory lobe
LH	Lateral horn
LN	Local interneuron
LTM	Long-term memory
MB	Mushroom body
mTOR	Mammalian target for rapamycin
NEP	Neprilysin
NFl	Neurofilament light polypeptide
NFT	Neurofibrillary tangle
NMJ	Neuromuscular junction
OB	Olfactory bulb
OI	Olfactory index
OR	Olfactory receptor
ORN	Olfactory receptor neuron
PBS	Phosphate buffered saline
PD	Parkinson´s disease
PDK1	3-phosphoinositide-dependent kinase 1
PET	Positron emission tomography
PI3K	Phosphoinositide-3 kinase
PIP2	Phosphatidylinositol-(4,5)-biphosphate
PIP3	Phosphatidylinositol-(3,4,5)-triphosphate
PN	Projection neuron
p-tau	Phosphorilated tau
PSI	Peripherally synapsing neuron
RNAi	Interference RNA

trkB	Tropomyosin receptor B/Tyrosine receptor kinase B
TTMn	Tergotrochanteral neuron
VNC	Ventral nerve cord
UAS	Upstream activating sequence
1-HEX	1-hexanol

INTRODUCTION

1.Synaptic transmission types

Transference of information is carried out through cellular specializations called synapses. The chemical or electrical nature of neuronal connectivity has caused a strong controversy in the past. Nowadays, both chemical and electrical transmissions are considered the two modalities of neuronal communication.

Chemical transmission was the first synaptic type identified (Fatt, 1954). In a chemical connection, the information is directionally transferred from a pre-synaptic to post-synaptic membrane. Both cell membranes are not physically bound but separated by a gap called synaptic cleft, mostly containing extracellular matrix proteins (Zuber et al., 2005). In the pre-synaptic neuron, neurotransmitters stored in small vesicles are released into synaptic cleft by exocytosis upon the arrival of an action potential (Bear et al., 2007). The nature of the postsynaptic response depends on the type of neurotransmitter released by pre-synaptic neuron, either excitatory or inhibitory, and the receptor type (ionotropic and metabotropic receptors) in the post-synaptic neuron (**Fig. I-1**). Then, intracellular signaling cascades are triggered after post-synaptic receptor activation, modulating the conversion of synaptic activity into gene expression (Bear et al., 2007).

However, physiological analysis in crayfish (Furhspan & Potter, 1957), in birds (Martin & Pilar, 1963) and later in mammals (Llinas et al., 1974; Hinrichsen & Larramendi, 1970; Baker & Llinás, 1971), demonstrated the presence of electrical transmission as an alternative modality of neuronal communication.

Many years later, Goodenough and Paul identified the structural basis of this connection: the gap junction (GJ) (Goodenough & Paul, 2009). This structure consists of intercellular channels aggregated in clusters that directly allow the flux of electrical current and small molecules (Ca^{2+}, cAMP, IP3 amongst others) from the cytoplasm of one cell to the next (**Fig. I-1**). Each intercellular channel is formed by the apposition of two hemichannels or connexons situated each one in one of the coupled cells (Goodenough & Paul, 2009). Despite of sharing similar functions, vertebrate and invertebrate GJs are structurally different: in invertebrates, hemichannels are hexamers and octamers of proteins known as innexins (Inx) while in vertebrates, they are formed by hexamers known as connexins (Cx). Whereas mammalian´s genome encodes around twenty Cx-encoding genes, in *Drosophila´s* genome, there are only eight Inx-encoding genes (Söhl et al., 2005; Phelan & Starich, 2001).

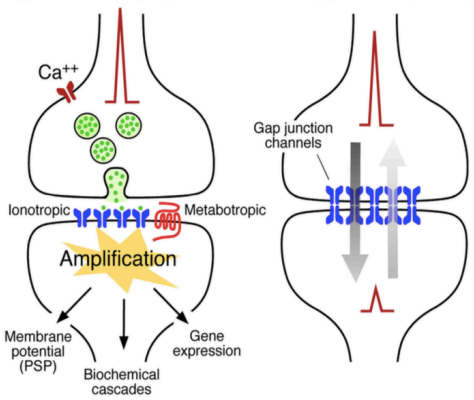

Fig. I-1. The two synaptic transmission types. Schematic cartoon representing the chemical and electrical synapses. Chemical synapses (on the left) requires presynaptic molecules to regulate the neurotransmitter release into postsynaptic membrane after the arrival of an action potential. Electrical synapses (on the right) are mediated by clusters of proteins called gap junctions, allowing the bi-directional flux of ionic current and small molecules (Extracted from Pereda, 2014).

In the past, electrical transmission was considered as a simple, static and rigid form of neuronal communication. Nowadays, it is well known that electrical synapses are more complex and dynamic than previously thought (Pereda, 2014). The main functional property of electrical connection relies on their bidirectionality, which allows them to coordinate the activity of several interconnected neurons, participating in processes such as lateral excitation in cerebellar interneurons (Vervaeke et al., 2012) or increasing the sensitivity in sensory systems (DeVries et al., 2002). Besides, due to their reliability and the absence of synaptic delay which facilitates an instantaneous transmission, electrical synapses are also relevant in escape response networks in both vertebrate and invertebrates (Faber et al., 2011; Herberholz et al.. 2002; Edwards et al., 1999); Phelan et al., 1996).

Furthermore, studies in goldfish Mauthner cells documented that both synaptic transmission types are intimately related (Faber et al., 2011; Pereda et al., 2011). This interaction is called mixed synapses and facilitates the combinatorial ability to induce plasticity, relevant in chemical synapses with the speed and reliability of electrical transmission (Pereda, 2014). These mixed synapses were first reported in cold-vertebrates (Pereda et al., 2004) and thanks to technical developments in electrophysiology, transgenesis, cell labeling, imaging and molecular cloning, many studies have documented their existence in the mammalian brain, including hippocampal mossy fibers (Hamzei-Sichani et al., 2012; Vivar et al., 2012), dendrites of hippocampal inhibitory interneurons (Haider, 2007) and spinal cord (Rash et al., 1996).

Many efforts during the last years have been directed to find out the interaction between chemical and electrical synapses during development. Remarkably, at early stages of development the connections are prominently electrical albeit at later stages their presence becomes weaker (Kandler & Katz, 1995; Montoro & Yuste, 2004). Several research works have

reported their initial relevance in both invertebrate (Marin-Burgin et al., 2006; Wolszon, 1995; Chuang et al., 2007) and vertebrate nervous systems (Volff, 2005; Montoro & Yuste, 2004; Penn et al., 1994; Bittman et al., 1997).

Additionally, some studies have demonstrated the correlation between the formation and elimination of electrical coupling with the appearance of chemical synapses during development in invertebrate species (Marin-Burgin, 2005; (Szabo, 2004); Todd et al., 2010). For instance, mutations in the *Drosophila* fly innexin gene *ShakB* prevent to establish functional synaptic connections in visual system. This developmental disruption could only be rescued in pupal stages but not in subsequent developmental stages (Curtin et al., 2002). Another evidence of this relationship has also been found in studies with motor neurons in *Helisoma snail* (Szabo, 2004). Indeed, this chemical-electrical correlation has also been reported in vertebrates, in developing spinal motoneurons (Mentis et al., 2002) in mice olfactory bulb (Maher et al., 2009) and in developing neocortex (Yu et al., 2012).

Conversely, chemical transmission is also crucial to regulate the presence and elimination of electrical connections during development (Arumugam et al., 2005; Park et al., 2011; Belousov & Fontes, 2013). For instance, *in vitro* cultures of cortical and hypothalamic neurons have shown specific Cx at early stages regulating the activation of specific receptors for chemical neurotransmitters prior to the establishment of a proper chemical synapse (Park et al., 2011). Likewise, findings in rat hypothalamus have reported that an activation of glutamate receptors reduces the electrical coupling at later developmental stages delaying the appearance of chemical connections, suggesting that glutamatergic transmission regulates the electrical uncoupling (Arumugam et al., 2005).

Thereby, the relationship between both synaptic types in the formation of neuronal networks is essential during development, resulting in a dynamic reconfiguration of hardwired circuit in the mature brain (Pereda, 2014). This closely interaction is pretty susceptible to disruptions which might yield to pathologies having neurological or behavioral consequences (Pereda, 2014). Thus, dysfunctions in the Cx36 gene have been associated with epilepsy in early adolescence (juvenile myoclonic epilepsy) although the mechanism remains unknown (Mas et al., 2004; Hempelmann et al., 2006). Further, disruptions in glutamatergic transmissions decrease the gap-junction communication leading to variations of electrical coupling levels in some brain areas that might rises neuronal synchrony and seizures (Dudek et al., 1986). In turn, inhibitory neurons are relevant to generate the gamma-frequency oscillatory activity which is related to cognitive processing (Buzsáki & Wang, 2012; Mas et al., 2004) and studies in mice have revealed that Cx36 is determinant to raise this rhythm (Hormuzdi et al., 2001). Finally, several studies have identified the role of alterations in these oscillatory activities in the pathophysiology of schizophrenia (Nakazawa et al., 2012), Parkinson's disease (Hammond et al., 2007) and autism (Welsh et al., 2005) as well as disruptions in glutamatergic (Moghaddam, 2003; Moghaddam & Javitt, 2012) and dopaminergic (Nieoullon, 2002; Penzes et al., 2013) transmissions.

1.1.ShakB^2 mutation

Electrical transmission is mediated by GJs between neurons facilitating a fast information transfer in many neural circuits. These GJs are present in several tissues in all developmental stages indicating a great variety of functions besides their mainly established roles in synchronizing the electrical activity (Brink et al., 1996). The sophisticated genetic tools available in simpler models like *Drosophila* or *C. elegans* have unveiled other functions of GJs (Phelan et al., 1998; Phelan & Starich, 2001; Starich et al., 1996; Li et al., 2003). Amongst these functions, GJs are essential in processes related to increase the sensitivity of sensory systems as well as to regulate the ionic coupling, regulation pattern and growth or cellular coordination (Zhang et al., 1999).

In *Drosophila,* a group of 8 genes coding for innexins have been previously indentified (Phelan & Starich, 2001). One of them, the *ShakingB* locus (also called *ShakB* and previously named *Passover*) is one of the most thoroughly studied (Baird et al., 1990) and coding for structural molecules of gap junctions in *Drosophila* flies.

ShakB locus produces at least 5 transcripts by alternative splicing which are translated into three proteins: *ShakB(neural)*, *ShakB(neural+16)* and *ShakB(lethal)* (Krishnan et al., 1993; Crompton et al., 1995; Zhang et al., 1999; Krishnan et al., 1993). These three *ShakB* transcripts are identical in their 3´ exons whereas 5´ coding exons are exclusively for each transcript and responsible for their N-terminal sequence differences. Indeed, both *ShakB(neural)* and *ShakB(neural+16)* are 96% identical only differing in an N-terminal tail of 16 amino acids. By contrast, *ShakB(lethal)* protein shares 88% identity with other *ShakB* proteins differing in their N-terminus, first trans-membrane domain and first loop (Phelan, 2005).

The different *ShakB* transcripts can be found in different cells at developmental stages of the nervous system and in non-neural tissues. Thus, both *ShakB neural* transcripts are found in later stage embryos in central and peripheral nervous systems (Stebbings et al., 2002; Zhang et al., 1999), in retinal photoreceptors and in lamina neurons during pupal development (Curtin et al., 2002). Additionally, other studies in adult flies identified *ShakB neural* transcripts in specific neurons in the giant fiber system (GFS) and haltere sensory neurons: tergotrochanteral motoneurons (TTMns) which innervate the jump muscles and peripherally synapsing interneurons (PSIs) which connect to the dorsal longitudinal flight muscle motor neurons (DLMns) controlling the movement of wings (Krishnan et al., 1993; Crompton et al., 1995; Zhang et al., 1999; Phelan et al., 1996; Blagburn et al., 1999; Trimarchi & Murphey, 1997). By contrast, *ShakB(lethal)* is expressed along the brain and ventral central nervous system (CNS) during pupation, when many postembryonic neurons are establishing connections.

Together, these evidences have strongly supported the role of the *ShakB* gene in the formation, functionality and regulation of electrical synapses. Indeed, these works have also pointed out the possible relevance of GJs at developmental stages in the posterior establishment of chemical transmission.

Mutations at *ShakB* locus have been extensively known to provoke defective gap junctions, disrupting electrical transmission. *ShakB*^{2} mutation is characterized as an X-chromosome mutation which lies in an exon common to *ShakB(neural)* and *ShakB(neural+16)* transcripts generating the loss of function of both *neural* transcripts (Krishnan et al., 1993; Zhang et al., 1999). This mutation generates a single base pair substitution in exon 6, inserting a stop codon within the signal sequence (Zhang et al., 1999).

The *ShakB*^{2} mutation severely interferes in the electrical transmission of the giant fiber escape pathway (Phelan et al., 1996; Sun & Wyman, 1996; Homyk et al., 1980; Krishnan et al., 1993), the optic lobe (Shimohigashi et al., 1998) and in auditory neurons of the antenna (Pézier et al., 2016). This *ShakB*^{2} mutation is also associated to other several phenotypes such as: behavioral defects in grooming and feeding (Thomas & Wyman, 1984; Philis et al. 1993; Balakrishnan et al., 1991), lack of escape jump as well as abnormalities in fly legs during the flight (Phelan et al., 1996; Sun & Wyman, 1996; Krishnan et al., 1993; Homyk et al., 1980) and increase of seizure susceptibility (Song & Tanouye, 2005).

2. Olfaction

Chemoreception is a crucial sensory modality for animal survival. Concerning olfaction, the ability to encode the identity and intensity of odorants in natural environments represents vital information to detect predators, dangers, location of food sources as well as to develop social and mating interactions (Su et al., 2009; Masse et al., 2009).

Sensory systems produce internal representations of external stimuli. In the case of odorants, there is no a single or continuous function provided by wavelength or frequency parameters. Rather, odorants have specific molecular structures differing in their physicochemical properties (Su et al., 2009; Haddad et al., 2008; Khan et al., 2007). In fact, natural odors are usually complex mixtures with variable concentration and persistence. Thus, these features confer olfaction as a particularly fascinating field of study. Many efforts have been carried out to reveal the organization of olfactory system and the molecular and cellular bases of olfaction since the Nobel Prize winning research of Richard Axel and Linda Buck in 2004, for their findings of a novel multigene family in rodents encoding odorant receptors (ORs) (Linda Buck & Richard Axel, 1991).

Remarkably, the functional organization of olfactory system is similar in organisms ranging from insects to mammals (Rubin & Katz, 1999; Uchida et al., 2000; Wachowiak & Cohen, 2001; Ng et al., 2002; Wang et al., 2004; Wilson et al., 2004; Su et al., 2009; Masse et al., 2009). For this reason, the fruit fly *Drosophila melanogaster* has become a suitable model to study the olfactory system thanks to its simplicity, manageable size and accessibility to powerful genetic and molecular tools (Masse et al., 2009; Vosshall, 2007). Besides, the comprehensive descriptions of olfactory receptors (ORs) and the connectivity between olfactory receptor neurons (ORNs) and central neuronal populations in the fly brain have provided valuable information about the underlying mechanisms of olfactory information processing (Grabe & Sachse, 2018).

2.1. The olfactory system of *Drosophila*

The detection of smell starts with the binding of volatile molecules to ORs located on the dendrites of ORNs (Hallem & Carlson, 2006). These neurons are harbored into three morphological types of sensory hairs (or sensilla) named as basiconic, coeloconic and trichoid. These sensilla cover the two *Drosophila* olfactory organs, antenna and maxillary palps whereas in vertebrates, these neurons are housed in olfactory epithelium. Each sensillum contains the dendrites of up to four ORNs of different specificities (Su et al., 2009).

ORs are seven-transmembrane-domain proteins encoded by a large gene family. The molecular identity of the receptors has been thoroughly described in *Drosophila*, with a number around 60-63 ORs expressed in different subsets of ORNs (Vosshall et al., 1999) compared to the 1000 ORs or 400 ORs expressed in mice and humans respectively (Niimura, 2012). In all phyla, the stimuli detected by ORNs needs to be orderly processed in sensory organs and relayed to higher areas of the brain.

The ORNs axons from the antenna project to the antennal lobe (AL), the primary olfactory center in insects, equivalent to the olfactory bulb (OB) in mammals (Masse et al., 2009). In the AL, axons from ORNs expressing the same OR converge and target to discrete neuropil units called glomeruli. The number of glomeruli strongly oscillates throughout species and roughly depends on the number of OR: whereas there are 52 glomeruli in the fruit fly, in mice and humans this number increased to 1800 and 5500 ORs, respectively (Grabe & Sachse, 2018).

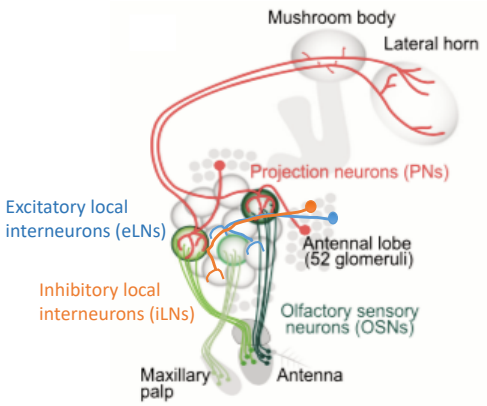

Fig. I-2. *Drosophila* olfactory system. Schematic diagram of *Drosophila* olfactory pathway from the antennal lobe to higher brain centers such as: Mushroom body and Lateral horn (Adapted from Seki et al., 2017).

Each glomerulus is enabled to code a set of odorants provided by the range of OR expressed in ORNs dendrites. Odor identity is the result of a combinatorial process where odorant is

internally coded by specific combinations of active ORNs (Bhandawat et al., 2007). In the glomerulus, the axon terminals of ORNs establish synapses with dendrites of projection neurons (PNs). In *Drosophila*, there are from 150 to 200 PNs (Seki et al., 2017) (**Fig. I-2**). Most of these neurons are cholinergic and mainly receive inputs from only one type of ORNs, expressing one odor receptor type. Outside the AL, PNs relay the information to higher brain areas such as: mushroom body (MB) where they form synapses with around 2500 intrinsic MB neurons (Kenyon cells), and lateral horn (LH) in the lateral protocerebrum (**Fig. I-2**). A small number of PNs are inhibitory (GABAergic neurons) which innervate multiple glomeruli and directly send the information to the LH, establishing synapses with LH neurons. The structure of MB is involved in olfactory learning and memory processes whereas the LH is linked to innate behaviors as olfactory discrimination (Liang et al., 2013; Heisenberg, 2003; Wong et al., 2002; Tanaka et al., 2008).

An important feature of ORNs to PNs connections is the high convergence of many ORNs on a smaller number of PNs. Even though there is variability among glomerulus, the number of PNs innervating the same glomerulus is on average three (Su et al., 2009; Vosshall et al., 2000). These three PNs facilitate the integration and amplification of weak signals in individual glomerulus.

The activity of PNs is also regulated by another subset of neurons whose function is decisive to olfactory processing: local interneurons (LNs). These neurons are primarily inhibitory (iLNs), releasing GABA but there are also excitatory neurons (eLNs), releasing acetyl choline. These LNs receive inputs from ORNs and PNs. Indeed, both types of LNs are interconnecting each glomerulus throughout the AL (Shang et al., 2007; Olsen et al., 2007; Yaksi & Wilson, 2010).

In summary, ORNs expressing the same OR target to specific glomerulus in the AL, establishing synapses with PNs and LNs and generating a spatial and also temporal pattern of odor-specific glomerular activation, constituting the internal representation of the odorant in the brain (Ng et al., 2002; Wang et al., 2003; Wilson, 2004; Lin et al., 2006; Masse et al., 2009; Su et al., 2009).

2.1. Electrical and chemical coupling in *Drosophila* olfactory processing

In recent years, electrophysiological studies have been directed to characterize the synaptic connectivity in the AL to establish how electrical and chemical coupling transforms the sensory input into behavioral responses (Wilson, 2013; Yaksi & Wilson, 2010; Kazama & Wilson, 2008). However, to the date, the specific weight of one synapse type *versus* the other remains unclear.

In one single glomerulus, both chemical and electrical connections are formed among all olfactory neurons: ORNs, PNs, eLNs and iLNs (**Fig. I-3**). Within the AL, two relevant phenomena take place: lateral inhibition and lateral excitation being both relevant to achieve a correct smell processing.

Lateral inhibition has been interpreted as a mechanism to enhance contrast and facilitate discrimination between stimuli. This phenomenon is predominantly presynaptic, at the ORN axon terminal and the overall level of inhibition rises with increasing stimulus intensity (Olsen

et al., 2010; Silbering & Galizia, 2007; Silbering et al, 2008). In fact, high ORNs levels of activation decreasing the activity in PNs preventing their saturation (Root et al., 2008). However, although ORNs are the most functionally target of inhibition, PNs and LNs also receive synaptic inhibition (Olsen et al., 2007; Root et al., 2007; Shang et al., 2007; Yaksi & Wilson, 2010). Thus, lateral inhibition improves the ability to identify odorants allowing PNs to encode changes in concentration (Luo et al., 2010; Olsen et al., 2010). Indeed, an odorant-induced depolarization of ORNs and PNs in a glomerulus suppresses the activity in other glomeruli due to iLNs activity.

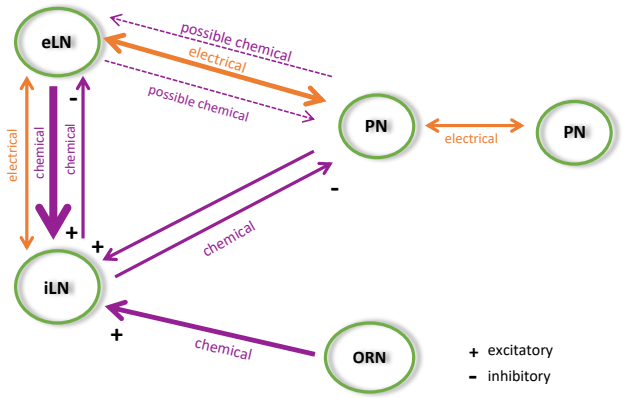

Fig. I-3. Electrical *versus* chemical synapses. Schematic diagram representing the specific weight of electrical *versus* chemical synapses among different neuronal populations of *Drosophila* olfactory pathway based on the published data at the present time.

In turn, the neural substrate of lateral excitation is the subset of eLNs. This phenomenon has been identified as a mechanism to maintain a state of basal activity (Shang et al., 2007). Previous findings indicate that lateral excitation is mediated by an electrical transmission formed by eLNs onto PNs, instead of chemical coupling (Yaksi & Wilson, 2010). Thereby, the stimulation of eLNs elicits a selective electrical coupling between eLNs and PNs. These authors, using the *ShakB*^{2} mutation, disrupted the electrical eLNs-PNs connections by blocking pharmacologically the phenomenon of lateral excitation in the AL (Yaksi & Wilson, 2010). Therefore, in the AL, excitatory and inhibitory LNs are connected by electrical coupling acting as a softener in the system but, due to eLNs can also interact to iLNs by chemical transmission, eLNs increased the total level of excitation in iLNs and thereby, leading to an indirect inhibition of PNs depending on the odor intensity. In addition, due to the strong chemical coupling between eLNs and iLNs, eLNs are able to increase the iLNs level of activation, leading to an indirect inhibition of PNs.

These authors (Yaksi & Wilson, 2010) have proposed that an excitation and indirect inhibition of PNs depends on stimulus intensity. In this way, the activity of eLNs does not considerably increase with high stimulus intensity and PNs inputs to iLNs are growing as ORNs activity is

raising (Olsen et al., 2010; Olsen & Wilson, 2008). Besides, the reciprocal connections between PNs within the AL have been determined as a synaptic purely electric connection (Yaksi & Wilson, 2010).

Thanks to an extensive knowledge about the organization of olfactory system and the large collection of available tools to manipulate and drive genes in certain subsets of neurons, *Drosophila* has become a suitable model to study the established electrical connections in olfactory system.

3. Alzheimer´s disease

Alzheimer´s disease (AD) was first identified by Alois Alzheimer in 1906. AD is the most prevalent neurodegenerative illness and the leading cause of dementia among the elderly, affecting an estimated population of 50 million people around the world. Recently, the World Alzheimer's Report in 2018 published that these numbers will be expected to rise until 152 millions of AD patients by 2050 suffering this disease. Mainly, age is the most relevant risk factor representing a 10% risk at the age of 65 to develop AD (Scheltens et al., 2006) which increases to 45% above the age of 85 (Bird, 2008).

This irreversible disease is characterized by a progressive neuronal loss and impairment of memory, besides personality changes, patient dependence and neuropsychiatric symptoms as depression, anxiety, sleep alterations and hallucinations (Sheng et al., 2012). Nowadays, AD can be diagnosed by using biomarkers related to neurodegeneration and blood-brain barrier dysfunction (Preische et al., 2019). For instance, the measurement of Aβ or tau protein concentration is performed by cerebrospinal fluid (CFS), magnetic resonance imaging and positron emission tomography (PET). Additionally, a new biomarker is recently under study, the measurement in blood of an intrinsic protein of axonal cytoskeleton, the neurofilament light polypeptide (NFl), a neurofilament protein that in humans is encoded by NEFL gene (Zetterberg & Schott, 2019).

AD is a devastating and multifactorial disease. For this reason, a huge effort is being directed to discern its underlying mechanisms in order to prevent its detrimental effects. Historically, AD classical hallmarks have been based on the accumulation of two above-mentioned proteins: extracellular amyloid plaques composed by amyloid-β peptide (Aβ42) and neurofibrillary tangles (NFTs) enriched by intracellular aggregates of hyperphosphorylated tau protein (p-tau) (Scheltens et al., 2006). However, it is still a matter of controversy whether both proteins are the only causing agents of AD (Molinuevo et al., 2018). Unfortunately, amyloid-β accumulation in the brain is produced decades before the appearance of the first signs of cognitive decline in patients and the diagnosis at early stages of the disease is severely impaired due to the absence of clinical identifiable markers.

Under this scenario, Aβ peptide still remains as a critical player to the pathogenesis of AD, becoming in one of the few biomarkers of this disease. This peptide is generated from the amyloid precursor transmembrane protein (APP) which is processed in two sequential cleavages

by β and γ secretases in the amyloidogenic pathway (Corbett and Hooper, 2018; De Strooper et al., 2010). These cleavages lead to the formation of two forms of Aβ long peptides of 40 and 42 amino acids (Aβ40 and Aβ42) being the relative amount of Aβ42 determinant in AD progression.

Interestingly, the amyloidogenic proteolytic pathway of APP is also produced under non-pathological conditions. The main Aβ-degrading enzymes are neprilysin (NEP), insulin-degrading enzyme (IDE) and endothelin-converting enzyme (ECE-1). However, when there is an imbalance on the production of amyloidogenic processing of APP, which can be degraded by these three mentioned enzymes (Turner et al., 2004), the amyloid cascade is produced and Aβ is considered as toxic (Hardy & Higgins, 1992).

Further, Aβ peptide can accumulate, oligomerize and aggregate forming plaques causing inflammation, oxidative stress and apoptosis (De Felice et al., 2007; Sakono and Zako, 2010; Tomiyama et al., 2010). This aggregation process seems to be critical for AD development and progression with different Aβ assemblies differing in their toxicity (Goure et al., 2014). There are three different species which may cause from non-deleterious effects to toxic damage in cells. Monomers are inoffensive if they do not associate into oligomers whereas pre-fibrillar accumulation is toxic. However, insoluble Aβ plaques are considered innocuous species which could act as oligomers, even though plaques also represent a potential source of toxic aggregates (Moreth et al., 2013; Stefani, 2010; Caughey & Lansbury, 2003). The amyloid cascade hypothesizes that plaques can sequester Aβ oligomers until reaching a physical limit after which the oligomers diffuse again to the surrounding membranes and hydrophobic cell surfaces (Esparza et al., 2013).

Many evidences have shown that Aβ synaptotoxicity elicits progressive synaptic alterations that later continue into degeneration of neural tissue, especially starting in areas involved in memory and cognition such as hippocampus and cortex at early events of AD (Braak and Braak, 1998). Further evidence has shown that loss of glutamatergic neurons in these brain areas is clearly affecting cognitive functions (Revett et al., 2013). Moreover, electrophysiological recordings in excitatory projection neurons have also determined negative effects on cholinergic synaptic transmission caused by Aβ expression (Fang et al., 2012).

On the other hand, other researchers have revealed how inhibitory neurons are much more sensitive to Aβ (Palop & Mucke, 2010). Moreover, β-amyloids could inhibit the network excitation by suppressing synaptic transmission strength and plasticity (Palop & Mucke, 2010). Besides, another study in human APP transgenic mice have revealed epileptic activity after Aβ exposure and conversely, studies in cell culture and cortical slices have shown an increase in their activity after Aβ treatment (Palop et al., 2007).

Thereby, the toxic effect of Aβ generates damage in synapses depending on its own abundance, the synapse nature and their vulnerability to Aβ (Palop & Mucke, 2010). Multiple synaptic, metabolic and cellular aspects are affected in the progression of AD pathology. Unfortunately, the absence of identifiable biomarkers makes the diagnosis at pre-clinical stages very difficult.

3.1. *Drosophila* as a model to study neurodegeneration

Over decades, many efforts have been directed to identify possible behavioral changes which facilitate the prediction of AD in a preclinical state before the appearance of the first symptoms. Besides, limitations in the work with human patients have prompted the use of model systems to analyze early affected genes, pathways and mechanisms underlying the shift form normal aging to neurodegenerative illness.

In addition to synapse loss, several studies in the field of brain illnesses have reported the relevance of smell in pathophysiology evidencing the existence of olfactory deficits at early stages of neurodegenerative diseases such as AD and Parkinson´s disease (PD), but also in multiple sclerosis, Lewy Body disorders, schizophrenia and depression (Sheng et al., 2012; William et al., 2009). These data strongly suggest that olfaction could be considered as a potential biomarkers source not only for AD but also, for other disorders. In addition to anosmia, there are also studies reporting defaults in other senses such as visual and auditory in AD patients (Cronin-Golomb et al., 1991; Cacace, 2007). Further studies developed in these patients have demonstrated that brain regions associated to olfactory system (hippocampus, entorhinal cortex) are highly impaired (Kovacs, 2004; Wilson et al., 2007; Attems et al., 2006) preventing odorant identification and discrimination (Rahayel et al., 2012).

Therefore, the development of olfactory assays could be useful to predict certain brain illnesses contributing to a better understanding of specific cognitive domains affected by aging and neurodegenerative diseases. All of these observations provide solid arguments to believe that an olfactory marker may serve as a complementary tool for the early screening of patients. Unfortunately, despite of these evidences, the investigation of its clinical relevance it is still today quite limited due to the complexity of olfactory function and the high variability within the human population.

Another clear signal of functional decline in the nervous system is related to a significant reduction of motor activity as well as an increased difficulty to balance (Camicioli et al., 1999).

In comparison to other animal models, *Drosophila* has become in an excellent model to mimic neurodegenerative diseases such as AD and aging. Thanks to the easy maintenance, the lower cost, their simplicity, short lifespan and most importantly, the extensive collection of available genetic tools which allow to manipulate gene expression with extraordinary precision (Rincon-Limas et al., 2012; Hirth, 2010). For instance, studies using a fly model of AD have reported olfactory memory defaults performing a Pavlovian olfactory classical test (Iijima et al., 2004; Iijima et al., 2008; Martín-Peña et al., 2018; Martin-Peña et al., 2017). On the other hand, most aging studies employing *Drosophila* flies have also focused on climbing, flight or other locomotor behaviors trying to understand the age-dependent relevance of functional decline to be posteriorly compared with other pathological and neurodegenerative conditions.

Fly models of AD have been generated applying different strategies. Some studies have expressed human APP and BACE (β-secretase) to describe the consequences of the amyloid plaques formation and age-dependent neurodegeneration (Greeve, 2004) producing a

reduction of pre-synaptic connection, alterations in mitochondrial localization and a decrease of post-synaptic protein levels (Mhatre et al., 2014). In addition, other models express the human β-amyloid peptide by developing several Aβ constructions: UAS-Aβ40, which produces no plaque formation but induces age-dependent learning defects (Iijima et al., 2004), the UAS-Aβ42, which elicits alterations on synaptic transmission, locomotion, survival and learning impairments (Iijima et al., 2008; Martin-Peña et al., 2017; López-Arias et al., 2017; Arnés et al., submitted). More, other Aβ constructs associated to human AD mutations like UAS- Aβ42-Arc (Crowther et al., 2005; Iijima et al., 2008). Additionally, a construct generated by two tandem copies of human Aβ42 fused to a secretion signal leads to stronger neurotoxic effects than one single copy model (Casas-Tinto et al., 2011).

3.2. Synapse restoration in an AD *Drosophila* model

In the last years, the search for new tools to restore the neuronal damage in neurodegenerative diseases has been very intensive. Unfortunately, Pharma companies have heavily invested in disease-tackling drugs failing one after the other (Mehta et al., 2017).

In this deep search of candidates, protein kinases are implicated in plasticity mechanisms like neurogenesis, modulation of excitability or synaptogenesis. Concerning this last issue, the class I phosphoinositide 3 kinase (PI3K) is involved in a signaling pathway that leads to synapse formation in *Drosophila* (Martin-Pena et al., 2006) and mammals (Cuesto et al., 2011).

Particularly, PI3K is an intracellular lipid kinase that promotes the phosphorylation of phosphatidylinositol-(4,5)-biphosphate (PIP2) to phosphatidylinositol-(3,4,5)-triphosphate (PIP3) activating PDK1 (3-phosphoinositide-dependent kinase 1) and Akt, both downstream elements of the canonical PI3K/Akt pathway. The activation of PI3K is regulated by tyrosine kinase receptors like the BDNF receptor trkB. This activation is crucial for long-term memory (LTM) formation as the impairment of PI3K/Akt signaling in trkB mutants suppress LTM (Musumeci et al., 2009). On the other hand, two downstream effectors of PI3K/Akt pathway, mTOR (mammalian target for rapamycin) and GSK3-β, have also important functions in LTM, memory consolidation and retrieval (Bekinschtein et al., 2007; Hooper et al., 2008; Hong et al., 2012; Huang et al., 2013). This synaptogenic pathway is different from the canonical insulin signaling pathway (Martin-Pena et al., 2006).

Previous studies developed in flies have demonstrated the age-independent synaptogenic effects of PI3K, producing an increase in the number of functional synapses in larval neuromuscular junctions (NMJs) and a population of interneurons and PNs in adult fly brain (Martin-Pena et al., 2006; Acebes et al., 2011; Acebes et al., 2012). Regarding to this, inhibitors of the PI3K/Akt pathway like GSK3-β reduced the number of synapses in both types of neurons (Cuesto et al., 2015). Recent findings have also revealed the neuroprotective effects of PI3K in a pathological context expressing an extremely toxic variant of human Aβ42 peptide in adult NMJ and non-neuronal cells (López-Arias et al., 2017; Arnés et al., 2017). Besides, these works have also reported how PI3K leads to restore the toxic effects induced by Aβ42 on locomotion and lifespan (López-Arias et al., 2017; Doctoral Thesis Mercedes Arnés; Arnés et al., submitted). In summary, these results have pointed PI3K as a good candidate to generate new and fully

functional synapses in a pathological context. Exploring the possible restoration of behavioral tasks such as olfaction and locomotion but also life expectancy, strongly damaged in AD, by expressing PI3K would be of potential therapeutic interest, especially in the early onset of AD.

HYPOTHESIS AND OBJECTIVES

Selective synapse restoration could represent a potential help in the treatment of neurodegenerative diseases characterized by synaptic loss, early anosmia, locomotor defaults and reduced life expectancy.

This thesis has mainly focused on the following aims:

1. To characterize the role of electrical synapses in olfactory processing of *Drosophila melanogaster*
2. To determine the role of electrical synapses in locomotion and life expectancy in health conditions and in a *Drosophila* model of Alzheimer´s disease
3. To analyze the behavioral consequences after restoring the chemical synapses by expressing PI3K in an Aβ42-induced neurodegeneration model

MATERIALS AND METHODS

MATERIALS

***Drosophila* genetics, stocks and maintenance**
Gal4/UAS system
Gal80ts system
Fly stocks

METHODS

Olfactory behavioral assay
Negative geotaxis assay
Lifespan assay
RNA isolation and cDNA preparation
PCR
Immunostaining
Statistical Analysis

MATERIALS

Drosophila genetics, stocks and maintenance

Fly strains were maintained at 25°C (except those specified) on a 12-12 hours light/dark cycle at constant humidity in standard medium (4% glucose, 55 g/L yeast, 0.65% agar, 28 g/L wheat flour and 5 mL/L propionic acid).

Gal4/UAS system

The Gal4/UAS system is the most used genetic system to drive the expression of selected genes in a great variety of tissues and cells types (Brand & Perrimon, 1993). This basic tool is based on the specificity of the yeast transcriptional factor *Gal4*, which is randomly inserted into Drosophila´s genome under the yeast regulatory sequence *UAS* (Upstream Activating Sequence) allowing the expression of a gene of interest. These *UAS* sequences are fused to genes of interest and reporters (**Fig. M-1**).

In this system, the gene of interest is silent in absence of *Gal4* protein. Thus, its activation is only accomplished by crossing two independent parent transgenic lines, a Gal4 driver line and an *UAS* line. In the progeny of this cross, the interest gene is expressed downstream of *UAS* sequence in the same tissue-specific pattern as *Gal4* factor.

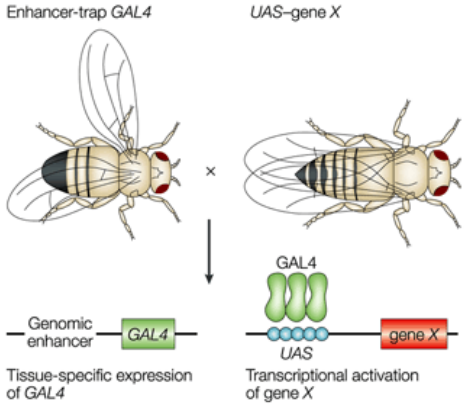

Fig. M-1. *Gal4/UAS* genetic system. Schematic cartoon of *Gal4/UAS* system expression (Extracted from St Johnston, 2002).

Gal80^{ts} system

The Gal4/UAS system presents another element, the *Gal80* repressor factor. This yeast protein is specifically used to bind and block *Gal4* function. This construct is extremely useful when it is necessary to restrict the study at specific times in the fly biological cycle.

Additionally, the use of a temperature-sensitive allele of *Gal80* repressor serves to regulate the expression of interest gene by shifting the temperature. As an example, at permissive temperature (18°C), the *Gal80^{ts}* protein is repressing the *Gal4* factor. By contrast, at restrictive temperature (30°C), the *Gal80^{ts}* protein is not functional and *Gal4* factor is active, allowing the gene expression (McGuire et al., 2003) (**Fig.M-2**).

Gal80^{ts} constructs are very useful in experiments where gene expression must be temporally controlled and restricted to later stages of development. Particularly in this work, *Gal80^{ts}* was used to study the effects of *ShakB^{Neural}* construct and human Aβ42 peptide in a ShakB^{2} background (Chapter 2, section 2.5 and Chapter 3) and the effects of PI3K expression in an Aβ42-induced neurodegeneration model (Chapters 4 and 5).

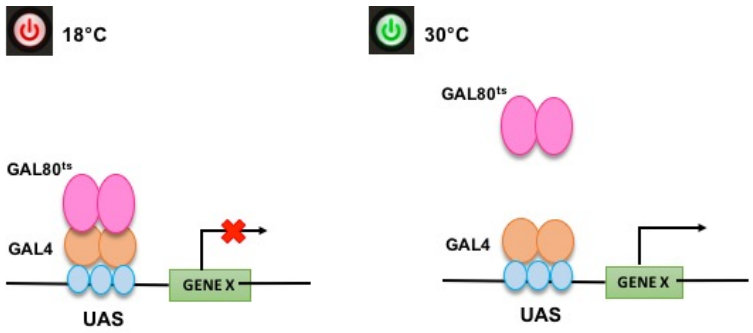

Fig. M-2. Gal80 thermosensitive system. Schematic cartoon of *Gal80^{ts}* system, a temperature-dependent Gal4 repressor factor (Adapted from McGuire et al., 2003).

Fly stocks

The *Gal4* and *UAS* lines employed in this work are compiled in the following tables:

Gal4 Lines	Source	Reference
GH298-Gal4	Dr. R.F. Stocker (University of Fribourg, Switzerland)	(Wong et al., 2002)
MZ19-Gal4	Dr. Davis RL. (Scripps Research Institute, Florida)	(Berdnik et al., 2006; Jefferis et al., 2004)
GH146-Gal4	Dr. Davis RL. (Scripps Research Institute, Florida)	(Stocker et al., 1997)
Elav-Gal4 (Chr. X)	BL-458	(Lin and Goodman, 1994)
LN2-Gal4	Dr. S. Sachse (Max Planck Institute, Germany)	(Okada et al., 2009; Tanaka et al., 2009)
Krasavietz-Gal4	Dr. G. Miessenbock (Oxford University, UK)	(Dubnau et al., 2003; Shang et al., 2007)
MBGal80	Dr. Davis RL. (Scripps Research Institute, Florida)	(McGuire et., 2003; Wang et al., 2003; Krashes et al., 2007)
THGal80	Dr. Scott Wadell (Massachusetts Medical School University, Worcester)	(Sitaraman et al., 2008)

UAS Lines	Source	Reference
UAS-ShakingB^{RNAi}	Dr. Rachel Wilson (Harvard University, Boston, USA)	GD26801
UAS-ShakingB^{Neural}	Dr. Rachel Wilson (Harvard University, Boston, USA)	(Curtin et al., 2002)
UAS-PI3K^{CAAX}	BL-8294	(Parrish et al., 2009)
UAS-Aβ42(2X)	Dr. Pedro Funez (Florida College of Medicine University, Florida)	(Casas-Tintó et al., 2011)
UAS-GFP^{nls}	BL-4775	(Shiga et al., 1996)
UAS-CD8-GFP	Dr. J.F. Ferveur (CGSA, Dijon)	(Kitamoto et al., 1992)
UAS-nsyb-GFP	BL-6921	(Zhang et al., 2002)

In this work, a mutant was also employed:

Mutant	Source	Reference
ShakB^{2}	Dr. Rachel Wilson (Harvard University, Boston, USA)	(Baird et al., 1990; Homyk et al., 1980)

Finally, the following fly lines were previously generated and employed in this work:

- *LN2-Gal4; Gal80^{ts}* (Dr. Ángel Acebes)
- *THGal80; UAS-ShakingB^{RNAi}* (Dr. Alberto Ferrús)
- *MBGal80; krasavietz-Gal4* (Dr. Ángel Acebes)
- *ShakB^{2}; UAS-ShakingB^{Neural}* (Dra. Rachel Wilson)
- *ShakB^{2}; UAS-Aβ42(2x)* (Dra. Mari-Cruz Marín)
- *UAS-Aβ42(2x); UAS-GFP^{nls}* (Dra. Mercedes Arnés)
- *UAS-Aβ42(2x); UAS-CD8GFP* (Dr. Ángel Acebes)

- *UAS-PI3K^{CAAX}; UAS-Aβ42(2x)* (Dr. Ángel Acebes)

Gal4 lines were crossed with the respective *UAS* and *Gal80* lines and the F1 used for experiments.

METHODS

Olfactory behavioral assay

Fly olfactory perception was evaluated performing an olfactory behavioral test using an odorant choice chamber, named T-maze, represented in the cartoon (**Fig. M-3**) (Tully & Quinn, 1985; Acebes & Ferrús, 2001). Prior to the behavioral experiment, each group of twenty to thirty adult flies, were kept overnight in a humidified chamber at room temperature in vials containing a soaked paper. Flies were allowed 30 seconds to choose between a vial containing a filter paper (4 x 1 cm) soaked in 75 µL of odorant diluted in paraffin oil (Odorant) and another just containing the solvent, paraffin oil (Control). Both soaked papers were added just at the start of the behavioral test. The three tested odorants, 1-hexanol (1-HEX), isoamyl-acetate (IAA) and ethyl-butyrate (EB) were of the maximum available purity (Fluka, purity >95%) and tested in a range of concentrations from 10^{-3} to 10^{-1} (vol/vol). All experiments were performed in darkness at room temperature randomizing control and experimental fly genotypes.

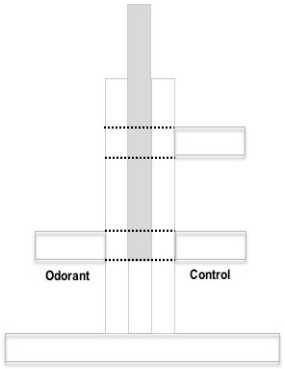

Fig. M-3. T-Maze apparatus. Schematic cartoon of T-Maze used in olfactory tests.

Olfactory index (OI) was calculated as the subtraction between number of flies trapped in the odorant vial and the number of flies trapped in the control vial divided by the total. Olfactory values range from full attraction (+1) to full repulsion (-1) whereas values close to 0 are considered as an equilibrium between attraction and repulsion or indifference (Ayyub et al., 1990). Odorant assays in which more than one-third of the flies did not make any choice were not quantified to discard any motor impairment bias. Each data point indicates the olfactory response of 300-400 individuals distributed in 14-16 replicates of 25 flies that were subjected just once to one odorant concentration choice.

However, depending on the genetic of fly lines employed, there are some variations in performing olfactory behavioral tests. In Chapter 2, the olfactory experiments were performed with male and female flies of 5- to 7-days old. Each group of flies was tested separately. Our data showed that results are gender-independent, thus allowing data pooling.

However, in experiments from Chapters 2 (section 2.5) and Chapter 4, due to genetic reasons, only female flies were tested. To develop our study, we used a protocol to achieve a temporal control of *Gal4* driver expression (**Fig. M-4**). Thus, crosses were maintained at 18°C and we only collected female flies after hatching. At day 7, flies were shifted to 30°C, inactivating the termo-sensitive *Gal80^{ts}* factor and allowing the expression of interest gene. Females remained at this temperature for 15 days. At the age of 22- to 23-days old (on twenty-second day of experiment), olfactory tests were only performed for ethyl-butyrate odorant. In order to compare all fly groups, the same procedure was applied to control genotypes. Each group of flies was tested separately and only once.

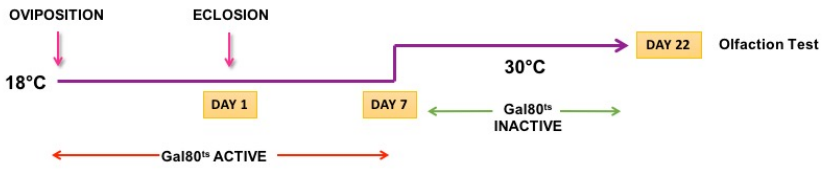

Fig. M-4. Diagram of temporal control of *Gal4* expression. Crosses were maintained at 18°C. After eclosion, only female flies were collected. They stayed at 18°C until sixth day in order to keep inactive the Gal4/UAS system. At day 7, flies were shifted to 30°C allowing the inactivation of Gal80^{ts} factor and consequently, the expression of interest gene to be active. Females remained at this temperature for 15 days. On twenty-second day, at the age of flies of 22- to 23-days old, olfactory perception is evaluated.

Negative geotaxis assay

A total number of 30-35 female flies (1- to 3-days old) per genotype were grown at 18°C. Only females were separated and placed in plastic vials (28.5 x 95 mm) containing ten to twelve flies. Flies were gently tapped down to the bottom of the vial and they were observed and scored during 8 seconds of climbing performance (**Fig. M-5**). Eight trials were completed for each sample.

The counting was done at room temperature every two days annotating the number of flies reaching the 4 cm high threshold line and at the same time, the number of flies that started to climb but did not reach the line. The assay for each genotype was repeated at least three times.

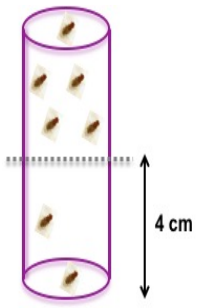

Fig. M-5. Climbing assay. Schematic cartoon of climbing assay, indicating the proportions of flies considered.

To develop our study and due to genetic reasons, another protocol based on temporal control of Gal4 was applied (**Fig. M-6**). After hatching, flies were kept at 18°C during 7 days of life and

then, they were shifted to 30°C allowing the inactivation of the Gal80^{ts} repressor factor and the consequent activation of Gal4/UAS system.

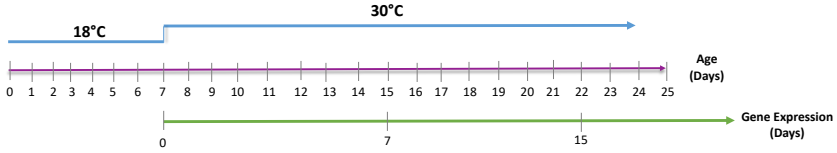

Fig. M-6. Diagram of the temperature shift schedule to activate *Gal4* expression. Female flies (1- to 3-days old) were collected and maintained at 18°C until seventh day in order to keep inactive the Gal4/UAS system. At day 7, flies were shifted to 30°C allowing the inactivation of Gal80^{ts} factor and the expression of the gene driven by *Gal4*. The climbing effects were examined every two days.

Lifespan assay

A total number of 30-35 female flies per genotype were grown at 18°C in order to keep inactive the Gal4/UAS system. As above, females were separated and placed in food vials in groups of ten to twelve flies.
Lifespan assays were carried out following the similar protocol shown in **Fig.M-6**. Food vials were changed every 3 days and the dead flies were counted and annotated at that time. The study was carried out in triplicates.

RNA Isolation and cDNA preparation

Total number of 15 female fly heads per genotype was used to extract RNA following Trizol protocol (Purezol, Bio-Rad). To synthesize cDNA was used the iScript cDNA Synthesis (Bio-Rad).

PCR

PCR analysis was performed using a thermal cycler C1000 (Bio-Rad) connected to CFX-96 optical detector module (Bio-Rad) with cycling conditions of 94°C for 2 min, 30 cycles of 94°C for 20 sec and 60°C for 20 sec.

All primer pairs employed are compiled in the following table:

Gene/Transcript	Primer pair (Sequence 5´- 3´)
ShakB[2] (Mutation)	Forward: GCAACTCGTGAAAAGGTGGC Reverse: CACAGCAATCGAGAATGTGATCAGTA
ShakB[2] (Variant C)	Forward: GCAACTCGTGAAAAGGTGGC Reverse: CACAGCAATCGAGAATGTGATCAGTT
Cha 1 (Housekeeping)	Forward: CCTGCAACTGGCTCACTACA Reverse: GCATTATGTCCAGCGAGTCC
Cha 2 (Housekeeping)	Forward: GCTGCGTAGACTGCATCAGA Reverse: GGCACTCGTATCCTCACAGG

Immunostaining

Single neuron mosaics were obtained as FRT/FLP recombinants in the construct *UAS-frtCD2y+frtCD8-GFP/hsflp* by applying a mild heat-shock (37°C during 55 min) in late third instar larvae and also early pupae stages (Lee & Luo, 2001). Different pulses of FLP were assayed during metamorphosis to achieve a high frequency of single neuron clones.

For whole-mount immunostainings, brains were dissected in PBS and fixed in PLP fixative (2% paraformaldehyde, 0.075M lysine, 0.037M sodium phosphate) for 1 hour at room temperature, washed in PBT (PBS + 0.5% Triton X-100) and pre-incubated in 90% PBT in 10% Normal Goat Serum. Fly brains were then incubated with primary antibodies anti-GFP (1:500, Molecular Probes), anti-amyloid beta (6E10) (1:1500, Covance) and monoclonal antibody nc82 (1:10, DSHB, Iowa) overnight at 4°C and secondary fluorescent antibodies Alexa 488 and Alexa 568 (Molecular probes) for two hours at room temperature. Specimens were finally mounted in Vectashield mounting medium (Vector Labs, USA).

Preparations were imaged in a Leica TCS-SP5 confocal microscope. Serial optical sections (512x512 pixels) were taken at 1 µm intervals using 40x or 63x objectives. Laser settings were maintained throughout all the genotypes analyzed.

Statistical Analysis

All data are represented as mean ± standard deviation of the mean (SDM).

In olfaction experiments, statistical significance was calculated using Unpaired t-test with Welch´s correction. In climbing assays, statistical significance was calculated using Two-Way RM ANOVA with Multiple Comparisons Tukey´s Test. Statistical significance for lifespan analysis was calculated using a Mantel-Cox Test. Significant differences between groups noted by: * $p < 0.05$, ** $p < 0.01$ and *** $p < 0.001$. All statistical analysis was done with GraphPad program.

CHAPTER 1:

Validation of genetic constructs and *Gal4* expression domains

1.1. Validation of *ShakB*^{2} mutant and *ShakingB* constructs
1.2. Expression patterns of *Gal4* drivers

In this work we have thoroughly employed the *ShakB²* mutants and genetic constructs allowing the attenuation of electrical synapses by using *UAS-ShakingB^{RNAi}* or their restoration by employing *ShakB²;UAS-ShakingB^{Neural}*. In addition, we have also employed several specific *Gal4* lines to drive gene expression to selected neurons in olfactory pathway. In this first chapter, we have validated the genetic tools used for electrical synapses and we have documented the expression pattern domain of olfactory *Gal4* lines.

1.1.Validation of *ShakB²* mutant and *ShakingB* constructs

In order to check the absence of *ShakB* gene in *ShakB²* mutants and validate the genetic constructs employed, we have performed a qualitative PCR with primers designed to identify the normal variant C of *ShakB* gene (shown in graphs as Variant C) as well as the mutation at the end of the sequence (shown in graphs as Mutation). As a positive control, we verified that our flies contain transcripts for choline acetyltransferase gene (shown in graphs as *Cha 1* and *Cha 2*).

In this experiment, we combined the previously mentioned constructs with the pan-neural driver (*Elav*) in order to express both *UAS-ShakingB* transcripts. Then, we have extracted cDNA from female adult fly heads of the following genotypes: *ShakB²* mutants, *Elav-Gal4/UAS-ShakingB^{RNAi}* (shown in graphs as *Elav/UAS-ShakingB^{RNAi}*), *ShakB²;UAS-ShakingB^{Neural};Elav-Gal4* (shown in graphs as *ShakB²;Neural;Elav)* and as a control, *Elav-Gal4.* The number of heads per group was 15 and the age of flies under study was 1-to-3 days old. Experiments were carried out in triplicates.

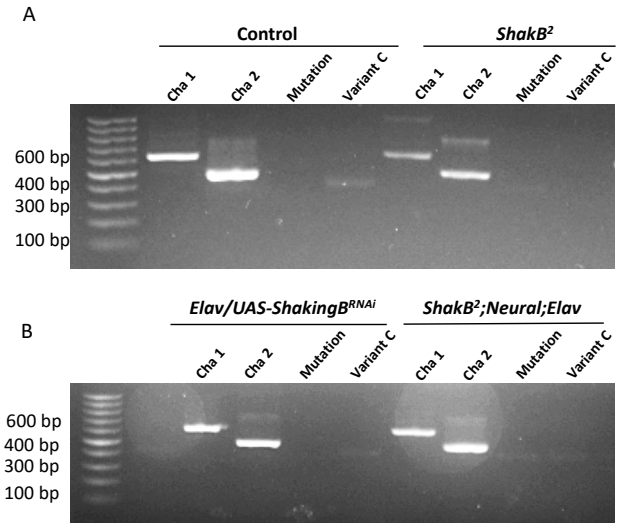

Fig. R1. **Expression of *ShakB* transcripts in whole brain. (A,B)** Agarose gel electrophoresis of PCR products from the following genotypes: Elav-*Gal4* and *ShakB*^{2} **(A)** and *Elav/UAS-ShakingB*^{RNAi} and *ShakB*^{2}*;Neural;Elav-Gal4* **(B).** PCR product of Cha 1, 605 bp; Cha 2, 482 bp; Variant C; 398 bp and Mutation; 398 bp. DNA ladder marker is shown on the left.

First, we detected that all genotypes under study contained the transcripts for *Cha* (**Fig. R1**). As expected, we found that control flies did not contain the *ShakB*^{2} mutant transcript, whereas the normal variant C of *ShakB* gene is present (**Fig. R1-A**). Conversely, we appreciated a weak band for *ShakB*^{2} mutant genotype in the mutation. In addition, the variant C of *ShakB* genes was not either detected in these mutants, indicating that they are not expressing the *ShakB* gene (**Fig. R1-A**).

In fly heads from *Elav/UAS-ShakingB*^{RNAi} flies in which the *ShakB* gene is attenuated, we detected a weak band corresponding to the normal variant C of the gene, whereas the mutant band is totally absent (**Fig. R1-B**).This result indicated that our *UAS-ShakingB*^{RNAi} construct was able to attenuate the expression of the normal transcript of the *ShakB* gene.

Notably, when we analyzed by PCR fly heads from *ShakB*^{2}*;Neural;Elav* genotype we detected the presence of both transcripts: the mutant and the normal variant C of the gene (**Fig. R1-B**). The presence of the mutant band was due to the ShakB^{2} background in these flies allows the expression of the mutant transcript, whereas the band corresponding to the normal variant C of the gene was produced by the *Elav-Gal4* driven expression of the *UAS-ShakingB*^{Neural} construct in all the neurons of these flies.
Together, these data validated the use of *ShakB*^{2} mutants and the two *UAS-ShakingB* constructs to attenuate (*UAS-ShakingB*^{RNAi}) or restore (*UAS-ShakingB*^{Neural}) electrical synapses.

1.2. Expression patterns of *Gal4* lines

Here we have characterized the expression domain of several *Gal4* lines by using: a) a nuclear reporter *UAS-GFP*^{nls}, b) a synaptic reporter *UAS-nSyb-GFP* and c) a membrane-bound *UAS-CD8-GFP* marker, together with a monoclonal antibody nc82 to visualize the synapses.

First, we analyzed the expression pattern of *GH298-Gal4* line, expressed in a population of 30-32, mostly corresponding to GABA-immunopositive inhibitory LNs (Ng et al., 2002) (**Fig. R2**). The expression of these iLNs is restricted to the AL.

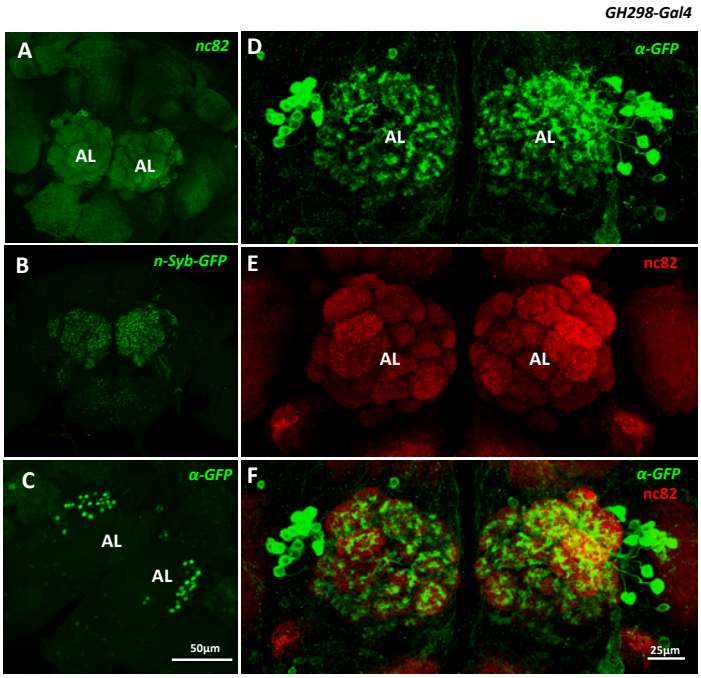

Fig. R2. **Expression domain of *GH298-Gal4* line. (A)** Neuropile of the brain of a *GH298-Gal4* fly visualized by the nc82 antibody. **(B)** *GH298* domain labeled by the synaptic marker n-Syb-GFP. Note that the expression pattern of this line is restricted to local interneurons projecting to the antennal lobe **(C)** Nuclei from all *GH298* domain neurons visualized by nuclear reporter GFP^{nls}. **(D)** Antennal lobe labeled by CD8-GFP to visualize local interneuron projections to the AL. **(E)** Antennal lobe visualized by nc82. **(F)** Merge of both CD8-GFP and nc82 labeling. Scale bars A-C (in C), 50 µm; D-F (in F), 25 µm.

We have also addressed another *Gal4* domain of inhibitory LNs: the subset of 30-37 neurons from *LN2-Gal4* domain (Okada et al., 2009) (**Fig. R3**).

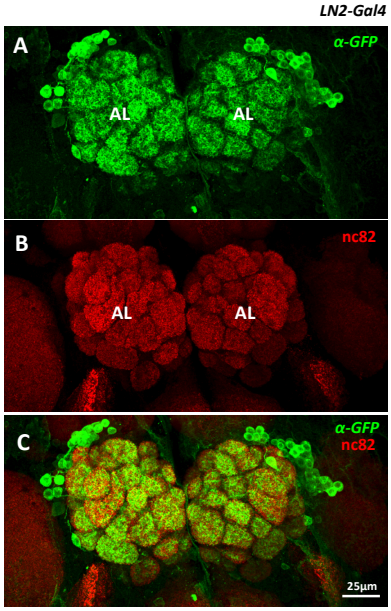

Fig. R3. **Expression domain of *LN2-Gal4 line*.** Each panel shows representative confocal sections of LN2 neurons visualized by CD8-GFP reporter **(A)**, nc82 monoclonal antibody to reveal AL synapses **(B)** and combined CD8-GFP reporter and nc82 staining **(C).** Scale bar A-C, (in C), 25 µm.

Then, we have also documented the expression domain of two neuronal subsets of PNs: *GH146-Gal4* line, expressed in 83-90 PNs (Berdnik, 2006) (**Fig. R4**) and *MZ19-Gal4*, expressed in 12-15 PNs (Stocker et al., 1997) (**Fig. R5**). Olfactory projection neurons send their dendrites to particular glomeruli in the AL and project their axons to higher brain centers as Mushroom bodies (MB) and Lateral Horn (LH).

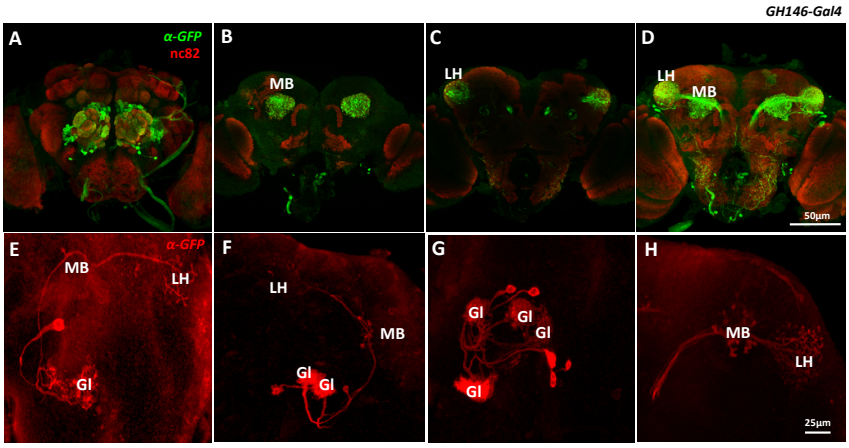

Fig. R4. Expression domain of *GH146-Gal4* line. Anterior **(A)** and posterior **(C-D)** view of a brain expressing the membrane-bound reporter CD8-GFP (green) counterstained with nc82 antibody (red). *GH146-Gal4* neurons have their dendrites in several AL glomeruli **(A)** and send their axons to Mushroom body (MB) **(B)** and lateral horn (LH) **(C)** brain centers. Single **(E)** and multiple **(F)** *GH146-Gal4* projection neurons. Detail of around 10 *GH146-Gal4* neurons projecting to 4 glomeruli of the AL **(G)** and their projections to MB and LH higher centers **(H)**. Bars: A-D (in D), 50 µm); E-H (in H), 25 µm.

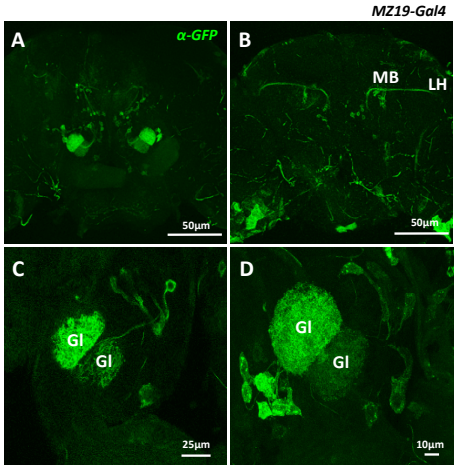

Fig. R5. Expression domain of *MZ19-Gal4* line. Dendrites of *MZ19-Gal4* neurons expressing CD8-GFP reporter showing their dendrites in several AL glomeruli **(A)** and sending their axons to Mushroom body (MB) and lateral horn (LH) brain areas **(B)**. Detail of the projection of several *MZ19* neurons to different subsets of glomeruli in the AL **(C-D)**. Scale bars A-B, 50 µm); C, 25 µm; E, 10 µm.

Finally, we analyzed the *krasavietz-Gal4* domain, expressed in a population of 6-8 excitatory LNs, restricted to the AL, in a subset of neurons projecting to the MB and in a group of TH-expressing dopaminergic neurons (Shang et al., 2007) (**Fig. R6**).

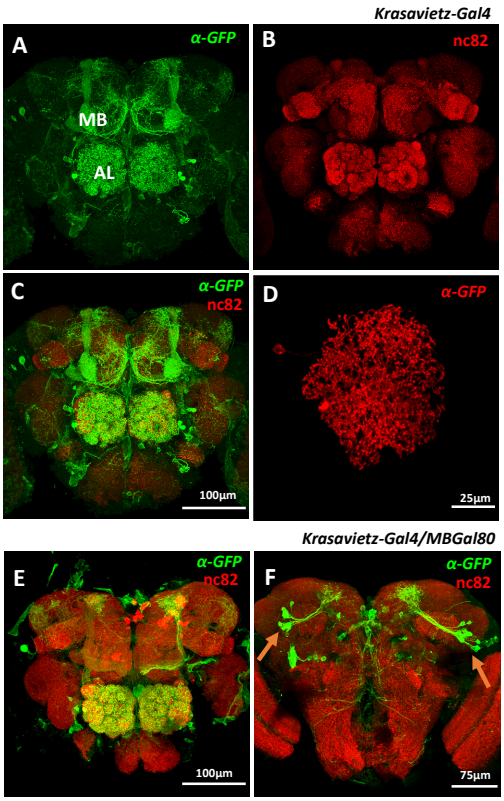

Fig. R6. Expression domain of *krasavietz-Gal4* line. (A) *krasavietz* neurons projecting to the AL and other brain areas visualized by the CD8-GFP reporter. **(B)** Brain synapses revealed by the nc82 monoclonal antibody. **(C)** Merge of a krasavietz fly brain expressing the nuclear GFP marker counterstained with nc82 antibody. **(D)** Single clone of a *krasavietz* excitatory local interneuron. **(E)** The repressor MB-Gal80 suppresses Gal4 expression in the *krasavietz* neurons. **(F)** Some *krasavietz* neurons in defined clusters are TH-expressing cells (orange arrow heads). Scale bars: A–C (in C), 100µm; D, 25µm; E, 100 µm; F, 75 µm.

CHAPTER 2:

Role of electrical synapses in olfactory processing of *Drosophila melanogaster*

2.1. Total loss of electrical synapses does not produce anosmia

2.2. Brain attenuation of electrical synapses modifies olfactory perception

2.3. Attenuation of electrical synapses in different subsets of PNs yields to olfactory perception changes

2.4. Attenuation of electrical synapses in excitatory and inhibitory LNs generates changes in olfactory perception

2.5 Electrical synapse restoration in the whole brain and in selected LNs populations rescues normal olfaction

Understanding signal propagation has a fundamental significance to decipher olfactory processing cues. Previous studies using optogenetic and electrophysiological approaches have shed light on how and where the electrical and chemical coupling is established among different olfactory neuronal populations (Wilson, 2013; Yaksi & Wilson, 2010; Kazama & Wilson, 2008). However, little is known about the specific weight of each synapse type, their importance to carry out a normal smell processing and how imbalances in any of these synapse types alter the olfactory circuit.

In this chapter, we aimed to study the role of electrical synapses in olfactory processing. To address this issue, the *ShakB* gene, required for formation and functional of electrical synapses is abolished and attenuated. We have employed a large collection of *Gal4* driver lines to selectively drive this attenuation to specific neurons of *Drosophila* olfactory pathway. Combination of *Gal4* drivers with an *UAS* construct, allowed us to attenuate the *ShakB* gene by interference RNA, employing the *UAS-shakingB*^{RNAi} construct (shown in graphs as *UAS* line). We also wondered whether selective restoration of electrical synapses, by using *UAS-ShakingB*^{Neural} construct in a *ShakB*^{2} background, is able to rescue normal olfactory perception.

To evaluate potential changes in olfactory perception, a behavioral assay is required. Flies were exposed to volatiles of different chemical nature: an alcohol as 1-hexanol (1-HEX) and two esters as isoamyl-acetate (IAA) and ethyl-butyrate (EB) in a range of 10^{-3} to 10^{-1} (v/v) concentration. Olfactory index (OI) was measured for each volatile and a dose-response curves were obtained for every control and experimental fly groups (see Material and Methods for details).

2.1.Total loss of electrical synapses does not produce anosmia

Firstly, we wondered whether the absence of electrical synapses in the brain leads to the loss of smell (anosmia) in *ShakB*^{2} mutant flies.

Interestingly, *ShakB*^{2} mutants yielded a significantly more attractive response to the lowest and intermediate stimulus concentration (10^{-3} and 10^{-2}, respectively) of 1-HEX compared to control flies (**Fig. R7-A**). By contrast, although the highest stimulus concentration (10^{-1}) was also detected as an attractive response, it was significantly less repulsive than control (**Table R1**).

By contrast, in their olfactory responses to IAA, *ShakB*^{2} flies showed the opposite effects to 1-HEX (**Fig. R7-B**). In this case, mutant olfactory reactions shifted toward repulsion to two of tested concentrations (10^{-2} and 10^{-1}) in comparison to control flies. However, no differences in olfactory responses were detected to 10^{-3} concentration between mutant and control fly groups (**Table R2**).

In the case of EB, an odorant with the same functional group as IAA, , *ShakB*^{2} individuals only presented differences to the highest stimulus concentration (10^{-1}), shifting mutant olfactory responses to less repulsive values compared to those obtained for IAA throughout the whole range of concentrations (**Fig. R7-C**,**Table R3**).

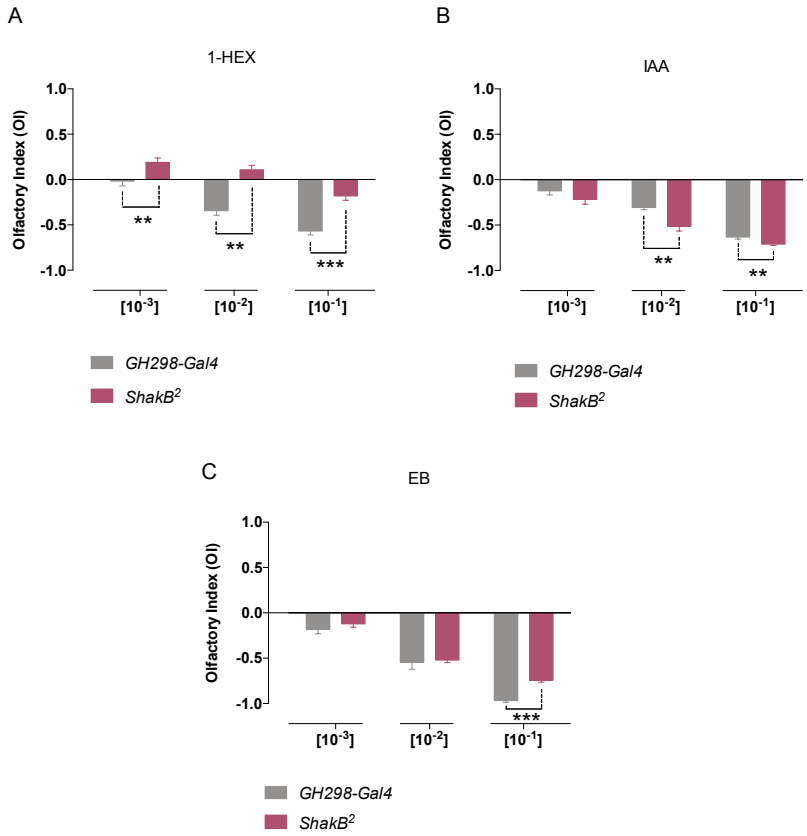

Fig. R7. Total loss of electrical synapses does not produce anosmia. Dose-response curves to: **(A)** 1-HEX, **(B)** IAA and **(C)** EB for *ShakB²* mutants (in pink) and *GH298-Gal4* as control (in grey). Each data point represents the average ± SEM. For all genotypes N=350-400 per data point. Statistical t-test results are indicated with: *** $p < 0.001$, ** $p < 0.01$ for control group comparison.

[1-HEX]	Genotype	OI value	Statistical Analysis (vs. Control)
[10^{-3}]	*GH298-Gal4 (control)* *ShakB²*	-0.02 ± 0.05 -0.19 ± 0.05	** $p < 0.01$
[10^{-2}]	*GH298-Gal4 (control)* *ShakB²*	-0.34 ± 0.05 0.11 ± 0.05	** $p < 0.01$
[10^{-1}]	*GH298-Gal4 (control)* *ShakB²*	-0.57 ± 0.04 -0.18 ± 0.04	*** $p < 0.001$

Table R1. Statistical analysis of 1-HEX dose-response curve (Fig. R7-A) for *ShakB²* mutants and *GH298-Gal4*.

[IAA]	Genotype	OI value	Statistical Analysis (vs. Control)
[10^{-3}]	*GH298-Gal4 (control)*	-0.12 ± 0.04	ns
	ShakB²	-0.22 ± 0.05	
[10^{-2}]	*GH298-Gal4 (control)*	-0.31 ± 0.02	** p < 0.01
	ShakB²	0.51 ± 0.05	
[10^{-1}]	*GH298-Gal4 (control)*	-0.63 ± 0.02	** p < 0.01
	ShakB²	-0.71 ± 0.04	

Table R2. Statistical analysis of IAA dose-response curve (Fig. R7-B) for *ShakB²* mutants and *GH298-Gal4*.

[EB]	Genotype	OI value	Statistical Analysis (vs. Control)
[10^{-3}]	*GH298-Gal4 (control)*	-0.18 ± 0.05	ns
	ShakB²	-0.12 ± 0.04	
[10^{-2}]	*GH298-Gal4 (control)*	-0.54 ± 0.08	ns
	ShakB²	-0.52 ± 0.03	
[10^{-1}]	*GH298-Gal4 (control)*	-0.90 ± 0.02	*** p < 0.001
	ShakB²	-0.75 ± 0.02	

Table R3. Statistical analysis of EB dose-response curve (Fig. R7-C) for *ShakB²* mutants and *GH298-Gal4*.

Considering all our data together, we conclude that the abolishment of electrical synapses does not prevent neither recognition nor processing of odorants at central level. Interestingly, *ShakB²* flies ability to discriminate along the whole range of stimulus concentration is maintained in all dose-response curves as well as the potential to develop odorant-specific responses depending on the chemical nature of the odorant. Our results demonstrate that these mutant flies are not anosmic and their ability to detect different odorants and concentrations is unaltered.

2.2. Brain attenuation of electrical synapses modifies olfactory perception

Secondly, we set out to analyze if the attenuation of electrical component in the whole brain affects the olfactory perception. To this end, the pan-neural Gal4 driver (*Elav*) was combined to the genetic *UAS-shakingB^{RNAi}* construct.

Experimental *Elav-Gal4/UAS-ShakingB^{RNAi}* flies shifted to attractive responses in two concentrations (10^{-3} and 10^{-2}) of 1-HEX compared to control, being only statistically significant to the intermediate one, 10^{-2} (**Fig. R8-A**). In addition, the highest stimulus evoked repulsive responses to experimental flies although no olfactory differences compared to control flies were found (**Table R4**).

In turn, experimental flies evoked less repulsive responses to IAA compared to control flies (**Fig. R8-B**), being statistically significant to the intermediate stimulus concentration, 10^{-2} (**Table R5**).

Finally, olfactory responses to EB for experimental flies were coincident with the control flies to the lowest and intermediate concentration tested. Remarkably, experimental flies evoked more

repulsive responses than control flies along the whole range of tested concentrations, being statistically significant to the highest stimulus concentration (**Fig. R8-C**, **Table R6**).

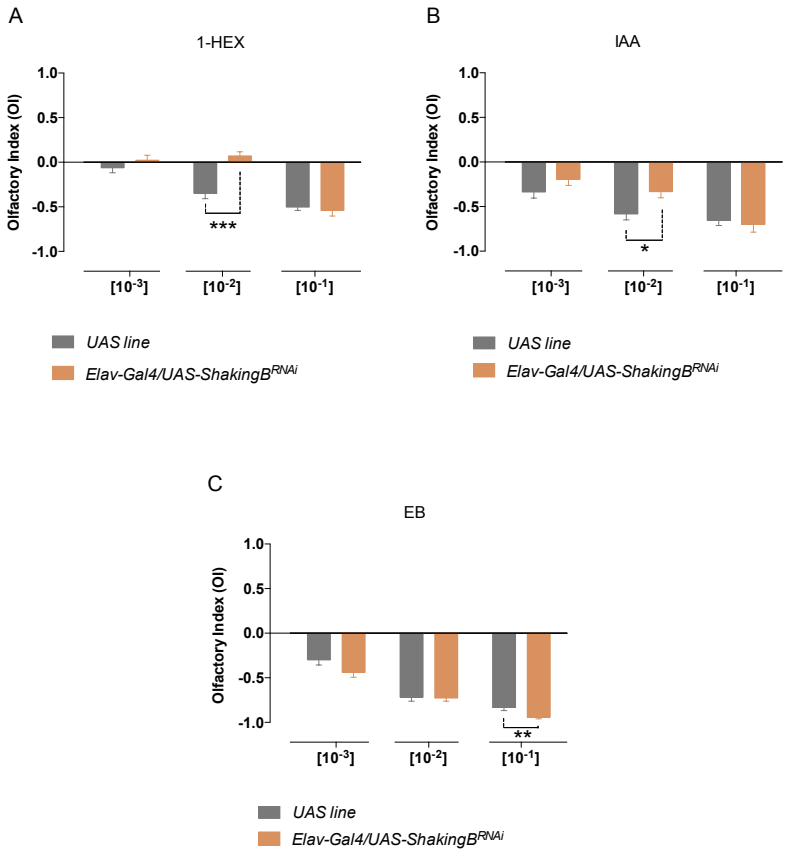

Fig. R8. Attenuation of total electrical synapses in the brain modifies the olfactory perception. Dose-response curves to: **(A)** 1-HEX, **(B)** IAA and **(C)** EB for *Elav-Gal4/UAS-ShakingB*^{RNAi} as experimental flies (in orange) and *UAS line* as control (in grey). Each data point represents the average ± SEM. For all genotypes N=350-400 per data point. Statistical t-test results are indicated with: *** $p < 0.001$, ** $p < 0.01$, * $p < 0.05$ for control group comparison.

[1-HEX]	Genotype	OI value	Statistical Analysis (vs. Control)
[10^{-3}]	*UAS-line (control)*	-0.06 ± 0.06	ns
	Elav-Gal4/UAS-ShakingB^{RNAi}	0.02 ± 0.06	
[10^{-2}]	*UAS-line (control)*	-0.35 ± 0.06	*** p < 0.001
	Elav-Gal4/UAS-ShakingB^{RNAi}	0.06 ± 0.05	
[10^{-1}]	*UAS-line (control)*	-0.50 ± 0.04	ns
	Elav-Gal4/UAS-ShakingB^{RNAi}	-0.54 ± 0.06	

Table R4. Statistical analysis of 1-HEX dose-response curve (Fig. R8-A) for *Elav-Gal4/UAS-ShakingB^{RNAi}* and *UAS-line*.

[IAA]	Genotype	OI value	Statistical Analysis (vs. Control)
[10^{-3}]	*UAS-line (control)*	-0.20 ± 0.07	ns
	Elav-Gal4/UAS-ShakingB^{RNAi}	-0.34 ± 0.07	
[10^{-2}]	*UAS-line (control)*	-0.33 ± 0.07	* p < 0.05
	Elav-Gal4/UAS-ShakingB^{RNAi}	-0.58 ± 0.07	
[10^{-1}]	*UAS-line (control)*	-0.70 ± 0.09	ns
	Elav-Gal4/UAS-ShakingB^{RNAi}	-0.65 ± 0.06	

Table R5. Statistical analysis of IAA dose-response curve (Fig. R8-B) for *Elav-Gal4/UAS-ShakingB^{RNAi}* and *UAS-line*.

[EB]	Genotype	OI value	Statistical Analysis (vs. Control)
[10^{-3}]	*UAS-line (control)*	-0.30 ± 0.06	ns
	Elav-Gal4/UAS-ShakingB^{RNAi}	-0.44 ± 0.05	
[10^{-2}]	*UAS-line (control)*	-0.72 ± 0.04	ns
	Elav-Gal4/UAS-ShakingB^{RNAi}	-0.73 ± 0.04	
[10^{-1}]	*UAS-line (control)*	-0.83 ± 0.03	** p < 0.01
	Elav-Gal4/UAS-ShakingB^{RNAi}	-0.94 ± 0.02	

Table R6. Statistical analysis of EB dose-response curve (Fig. R8-C) for *Elav-Gal4/UAS-ShakingB^{RNAi}* and *UAS-line*.

Together, these observations indicate that total attenuation of electrical connections in the whole fly brain prevents a normal olfactory processing in a concentration and odorant manner. Indeed, these flies have not lost their ability to detect odorants and discriminate among different stimulus concentration.

2.3. Attenuation of electrical synapses in different subsets of PNs yields to olfactory perception changes

After analyzing the effects of attenuating the electrical synapses in the whole brain, we wonder if the attenuation of electrical connections in specific subsets of central olfactory neurons produces different outcomes in the olfactory perception.

Here, *UAS-shakingB^{RNAi}* construct was combined to two specific subsets of projection neurons (PNs) by using the following Gal4 drivers: *MZ19* and *GH146* in which *Gal4* expression is restricted to around 12-15 and 83-90 neurons per AL, respectively.

Firstly, we analyzed the perception of 1-HEX in experimental *GH146-Gal4/UAS-ShakingB^{RNAi}* flies in which electrical synapses of around 83-90 PNs were attenuated (*GH146* domain) (**Fig. R9-A**). These experimental flies did not show any olfactory change compared to control flies throughout the whole range of concentrations (**Table R7**). By contrast, experimental *MZ19-Gal4/UAS-ShakingB^{RNAi}* flies, where the selective electrical attenuation was directed to a smaller subset of neurons (12-15 PNs), evoked less repulsive olfactory responses to the intermediate and highest concentration (10^{-2} and $10^{-1,}$ respectively). These differences were significantly higher than control. Interestingly, significant differences to the same concentrations were also found between both experimental fly groups (**Table R7**).

Then, we evaluated the dose-response curves of experimental and control groups to IAA (**Fig. R9-B**). Olfactory changes were strongly different from those obtained in 1-HEX. On one hand, the attenuation of electrical component in the PNs of *GH146* domain elicited more repulsive OI values than control group in response to the lowest and intermediate concentration (10^{-3} and 10^{-2}, respectively) (**Table R8**). On the other hand, the attenuation in PNs of *MZ19* domain did not produce changes in olfactory perception for IAA odorant for none of tested concentrations. Additionally, any changes in olfactory responses were detected between both experimental and control flies to the highest concentration, 10^{-1}. Besides, pretty similar OI values were obtained to 10^{-3} and 10^{-2} for experimental *GH146-Gal4/UAS-ShakingB^{RNAi}* flies (**Table R8**), pointing the possible role of these 83 neurons to discriminate among odorant concentrations, specifically to IAA odorant.

Finally, the perception of EB did not reveal a discernible effect for experimental *GH146-Gal4/UAS-ShakingB^{RNAi}* flies along the whole range of concentrations (**Fig. R9-C**). By contrast, just for the intermediate concentration, 10^{-2}, *MZ19-Gal4/UAS-ShakingB^{RNAi}* flies evoked highly significant more repulsive responses than control and experimental *GH146-Gal4/UAS-ShakingB^{RNAi}* flies (**Table R9**). Moreover, both experimental fly groups detected the other tested concentrations (10^{-3} and 10^{-1}) in a similar way, presenting OI values very close among them (**Table R9**). In addition, according to the dose-response curve to IAA, olfactory responses also shifted to repulsion.

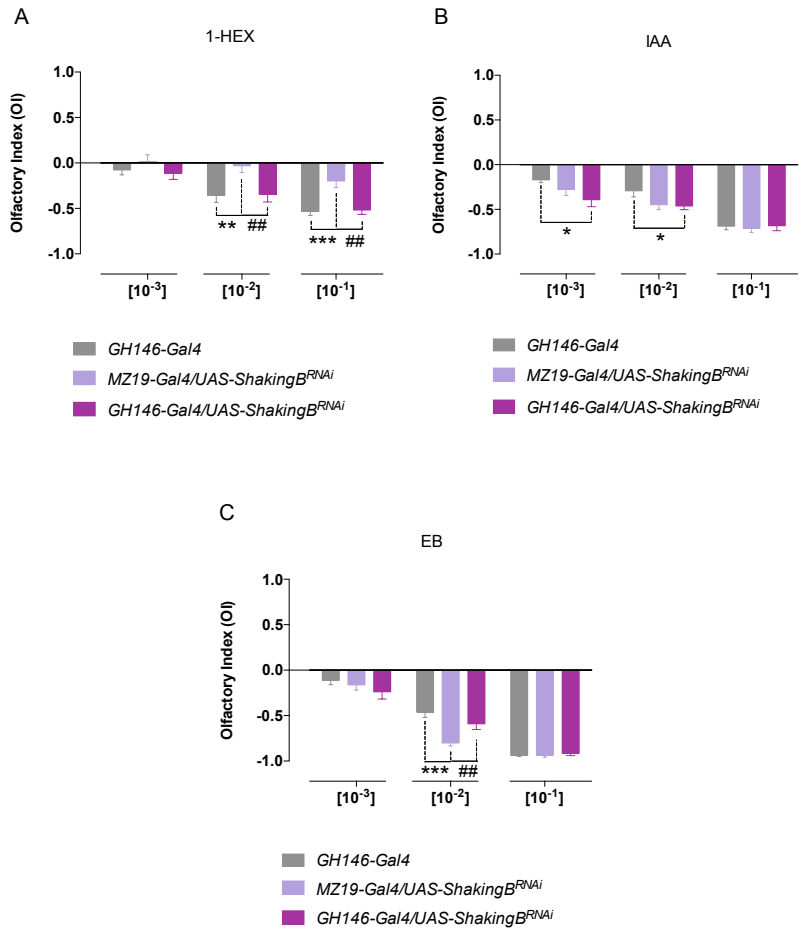

Fig. R9. Olfactory perception is affected depending on the number of PNs electrically attenuated. Dose-response curves to: **(A)** 1-HEX, **(B)** IAA and **(C)** EB for experimental flies: 1) *MZ19-Gal4/UAS-ShakingB^{RNAi}* (in light purple) and 2) *GH146/UAS-ShakingB^{RNAi}* (in dark purple); and as a control: *GH146-Gal4* (in grey). Each data point represents the average ± SEM. For all genotypes N=350-400 per data point. Statistical t-test results are indicated with: *** $p < 0.001$; ** $p < 0.01$ and * $p < 0.05$ for control group comparison and ## $p < 0.01$ for experimental group comparison.

[1-HEX]	Genotype	OI value	Statistical Analysis (*vs. control*)	Statistical Analysis (*vs. GH146-Gal4/UAS-ShakingB^{RNAi}*)
[10^{-3}]	*GH146-Gal4 (control)*	-0.08 ± 0.05		
	GH146-Gal4/UAS-ShakingB^{RNAi}	-0.11 ± 0.07	ns	
	MZ19-Gal4/UAS-ShakingB^{RNAi}	0.02 ± 0.07	ns	ns
[10^{-2}]	*GH146-Gal4 (control)*	-0.36 ± 0.08		
	GH146-Gal4/UAS-ShakingB^{RNAi}	-0.34 ± 0.09	ns	
	MZ19-Gal4/UAS-ShakingB^{RNAi}	-0.03 ± 0.07	** p < 0.01	## p < 0.01
[10^{-1}]	*GH146-Gal4 (control)*	-0.53 ± 0.04		
	GH146-Gal4/UAS-ShakingB^{RNAi}	-0.52 ± 0.05	ns	
	MZ19-Gal4/UAS-ShakingB^{RNAi}	-0.20 ± 0.07	*** p < 0.001	## p < 0.01

Table R7. Statistical analysis of 1-HEX dose-response curve (Fig. R9-A) for experimental genotypes: *GH146-Gal4/UAS-ShakingB^{RNAi}* and *MZ19-Gal4/UAS-ShakingB^{RNAi}* and as control: *UAS-line*.

[IAA]	Genotype	OI value	Statistical Analysis (*vs. control*)	Statistical Analysis (*vs. GH146-Gal4/UAS-ShakingB^{RNAi}*)
[10^{-3}]	*GH146-Gal4 (control)*	-0.17 ± 0.03		
	GH146-Gal4/UAS-ShakingB^{RNAi}	-0.39 ± 0.08	* p < 0.05	
	MZ19-Gal4/UAS-ShakingB^{RNAi}	-0.28 ± 0.07	ns	ns
[10^{-2}]	*GH146-Gal4 (control)*	-0.29 ± 0.07		
	GH146-Gal4/UAS-ShakingB^{RNAi}	-0.46 ± 0.04	* p < 0.05	
	MZ19-Gal4/UAS-ShakingB^{RNAi}	-0.45 ± 0.06	ns	ns
[10^{-1}]	*GH146-Gal4 (control)*	-0.69 ± 0.04		
	GH146-Gal4/UAS-ShakingB^{RNAi}	-0.68 ± 0.06	ns	
	MZ19-Gal4/UAS-ShakingB^{RNAi}	-0.71 ± 0.04	ns	ns

Table R8. Statistical analysis of IAA dose-response curve (Fig. R9-B) for experimental genotypes: *GH146-Gal4/UAS-ShakingB^{RNAi}* and *MZ19-Gal4/UAS-ShakingB^{RNAi}* and as control: *UAS-line*.

[EB]	Genotype	OI value	Statistical Analysis (*vs. control*)	Statistical Analysis (*vs. GH146-Gal4/UAS-ShakingB^{RNAi}*)
[10^{-3}]	*GH146-Gal4 (control)*	-0.11 ± 0.05		
	GH146-Gal4/UAS-ShakingB^{RNAi}	-0.24 ± 0.08	ns	
	MZ19-Gal4/UAS-ShakingB^{RNAi}	-0.16 ± 0.06	ns	ns
[10^{-2}]	*GH146-Gal4 (control)*	-0.46 ± 0.06		
	GH146-Gal4/UAS-ShakingB^{RNAi}	-0.59 ± 0.06	ns	
	MZ19-Gal4/UAS-ShakingB^{RNAi}	-0.80 ± 0.03	*** p < 0.001	## p < 0.01
[10^{-1}]	*GH146-Gal4 (control)*	-0.94 ± 0.01		
	GH146-Gal4/UAS-ShakingB^{RNAi}	-0.91 ± 0.03	ns	
	MZ19-Gal4/UAS-ShakingB^{RNAi}	-0.93 ± 0.02	ns	ns

Table R9. Statistical analysis of EB dose-response curve (Fig. R9-C) for experimental genotypes: *GH146-Gal4/UAS-ShakingB^{RNAi}* and *MZ19-Gal4/UAS-ShakingB^{RNAi}* and as control: *UAS-line*.

Altogether, our results indicate that the selective attenuation of electrical synapses in PNs modifies the olfactory perception of flies. Indeed, these olfactory changes crucially depend on the attenuated electrical connections and the chemical nature of the given odorant.

2.4. Attenuation of electrical synapses in excitatory and inhibitory LNs generates changes in olfactory perception

After evaluating the potential changes in olfactory perception in the whole fly brain and in two subsets of PNs, we focused our analysis on another two populations of central neurons, excitatory and inhibitory local interneurons (LNs).

To address this issue, we combined the genetic *UAS-shakingB*^{RNAi} construct to the following Gal4 drivers: *krasavietz-Gal4* and *LN2-Gal4* which are expressed in 6-8 excitatory LNs (eLNs) and 30-37 inhibitory LNs (iLNs) per AL, respectively. Since *krasavietz-Gal4* line presents a Gal4 expression pattern in other fly brain areas as Mushroom Bodies (MB) and in a subset of dopaminergic neurons expressing tyrosine hydroxylase (TH) enzyme, a Gal80 repressor factor was employed to assure the selective attenuation in those 6-8 eLNs per AL. Hence, using *MBGal80* and *THGal80* constructs (shown in graphs as *MBGal80 line* and *THGal80 line*), we prevented Gal4 expression in MB and dopaminergic neurons (Material and Methods for details).

Firstly, the perception to 1-HEX produced a strong shift toward attraction for experimental *MBGal80/THGal80;krasavietz-Gal4/UAS-ShakingB*^{RNAi} flies compared to control groups in all range of tested concentrations (**Fig. R10-A**). In fact, whereas control flies detect the lowest concentration (10^{-3}) as indifferent, experimental flies sensed it even more attractive. Remarkably, OI values were close to each other, meaning that these experimental flies might have lost their ability to discriminate among different odorant concentrations (**Table R10**).

Surprisingly, the perception of 1-HEX was affected in the same way as in the case of eLNs, after the attenuation of electrical connections in iLNs (*LN2* domain), yielding statistically significant responses toward attraction in comparison to control flies (**Fig. R10-B**). Again, the OI values in these experimental *LN2-Gal4/UAS-ShakingB*^{RNAi} flies remained strikingly similar to 10^{-3} and 10^{-1} concentrations (**Table R11**). This evidence suggests, at least to 1-HEX, that the ability to discern odorant concentrations is affected in both groups of LNs-attenuated flies (**Fig. R10**, **Table R10** and **Table R11**).

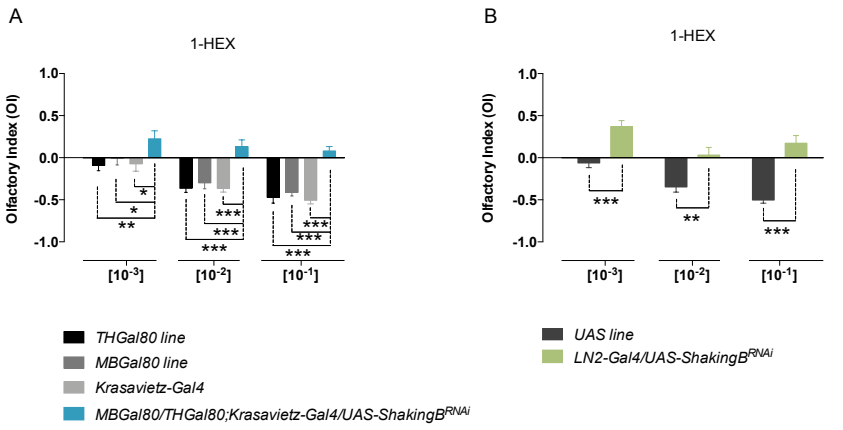

Fig. R10. Attenuation of electrical synapses in LNs modifies olfactory perception. (A-B) Dose-response curves for 1-HEX. **(A)** Dose-response curve for eLNs experimental flies: *MBGal80/THGal80;krasavietz-Gal4/UAS-ShakingB^{RNAi}* (in blue); and controls: 1) *THGal80 line* (in black), 2) *MBGal80 line* (in grey) and 3) *krasavietz-Gal4* (in light grey). **(B)** Dose-response curve for iLNs experimental flies: *LN2-Gal4/UAS-ShakingB^{RNAi}* (in green) and control: *UAS line* (in grey). Each data point represents the average ± SEM. For all genotypes N=350-400 per data point. Statistical t-test results are indicated with: *** p < 0.001, ** p < 0.01, * p < 0.05 for control group comparison.

[1-HEX]	Genotype	OI value	Statistical Analysis (vs. THGal80)	(vs. MBGal80)	(vs. krasavietz-Gal4)
[10^{-3}]	*THGal80 (control)*	-0.09 ± 0.06			
	MBGal80 (control)	-0.01 ± 0.08			
	krasavietz-Gal4 (control)	-0.07 ± 0.09			
	MBGal80/THGal80; krasavietz-Gal4/ UAS-ShakingB^{RNAi}	0.23 ± 0.09	** p < 0.01	* p < 0.05	* p < 0.05
[10^{-2}]	*THGal80 (control)*	-0.36 ± 0.05			
	MBGal80 (control)	-0.30 ± 0.07			
	krasavietz-Gal4 (control)	-0.37 ± 0.04			
	MBGal80/THGal80; krasavietz-Gal4/ UAS-ShakingB^{RNAi}	0.13 ± 0.08	*** p < 0.001	*** p < 0.001	*** p < 0.001
[10^{-1}]	*THGal80 (control)*	-0.47 ± 0.07			
	MBGal80 (control)	-0.41 ± 0.04			
	krasavietz v-Gal4 (control)	-0.51 ± 0.04			
	MBGal80/THGal80; krasavietz -Gal4/ UAS-ShakingB^{RNAi}	0.08 ± 0.05	*** p < 0.001	*** p < 0.001	*** p < 0.001

Table R10. Statistical analysis of 1-HEX dose-response curve: (Fig. R10-A) Experimental genotype *MBGal80/THGal80;krasavietz-Gal4/UAS-ShakingB^{RNAi}* and *THGal80, MBGal80* and *krasavietz-Gal4* as control genotypes.

[1-HEX]	Genotype	OI value	Statistical Analysis (vs. Control)
[10^{-3}]	*UAS-line (control)*	-0.06 ± 0.06	*** p < 0.001
	LN2-Gal4/UAS-ShakingB^{RNAi}	0.37 ± 0.07	
[10^{-2}]	*UAS-line (control)*	-0.35 ± 0.06	** p < 0.01
	LN2-Gal4/UAS-ShakingB^{RNAi}	0.03 ± 0.09	
[10^{-1}]	*UAS-line (control)*	-0.50 ± 0.04	*** p < 0.001
	LN2-Gal4/UAS-ShakingB^{RNAi}	0.17 ± 0.09	

Table R11. Statistical analysis of 1-HEX dose-response curve (Fig. R10-B) for experimental genotype, *LN2-Gal4/UAS-ShakingB^{RNAi}* and *UAS line* as control.

Then, we evaluated the responses to IAA (**Fig. R11**). The experimental eLNs-attenuated flies perceived the lowest concentration (10^{-3}) more repulsive than control fly groups whereas to the other tested concentrations, any significant differences were observed (**Fig. R11-A**, **Table R12**). Again, experimental eLNs-attenuated flies showed pretty similar OI values among the three tested concentrations as in the case of previously obtained OI values to 1-HEX (**Table R10**). These results could corroborate the relevance of electrical eLNs component to discriminate among odorant concentrations, at least for 1-HEX and IAA.

By contrast, the experimental iLNs-attenuated flies did not produce any significant effect to IAA perception, behaving as a control fly group (**Fig. R11-B**, **Table R13**). As in the case of eLNs-attenuated flies (**Fig. R11-A**), the perception of IAA odorant for iLNs-attenuated flies also shifted to repulsive responses. Thus, our results showed that IAA perception does not seem to be affected by electrical attenuation in this particular subset of iLNs (**Table R13**).

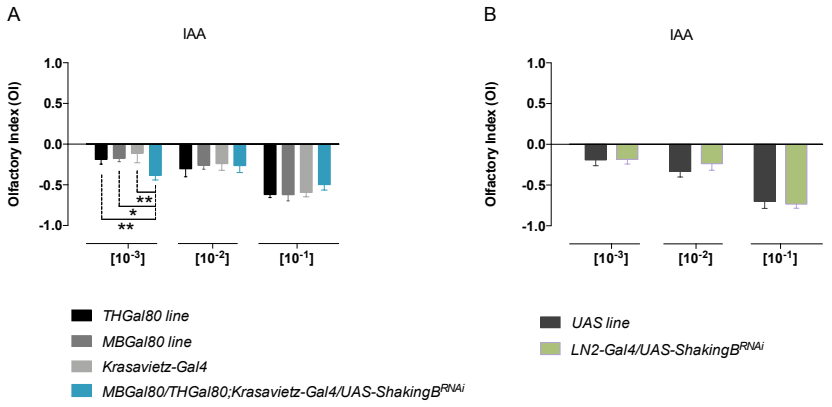

Fig. R11. Attenuation of electrical synapses in LNs modifies olfactory perception. (A-B) Dose-response curves for IAA. **(A)** Dose-response curve for eLNs experimental flies: *MBGal80/THGal80;krasavietz-Gal4/UAS-ShakingB^{RNAi}* (in blue); and controls: 1) *THGal80 line* (in black), 2) *MBGal80 line* (in grey) and 3) *krasavietz-Gal4* (in light grey). **(B)** Dose-response curve for iLNs experimental flies: *LN2-Gal4/UAS-ShakingB^{RNAi}* (in green) and control: *UAS line* (in grey). Each data point represents the average ± SEM. For all genotypes N=350-400 per data point. Statistical t-test results are indicated with: *** p < 0.001, ** p < 0.01, * p < 0.05 for control group comparison.

[IAA]	Genotype	OI value	Statistical Analysis (vs. THGal80)	(vs. MBGal80)	(vs. krasavietz-Gal4)
[10^{-3}]	*THGal80 (control)*	-0.19 ± 0.06			
	MBGal80 (control)	-0.17 ± 0.04			
	krasavietz-Gal4 (control)	-0.11 ± 0.12			
	MBGal80/THGal80; krasavietz-Gal4/ UAS-ShakingB^{RNAi}	-0.38 ± 0.06	** p < 0.01	* p < 0.05	** p < 0.01
[10^{-2}]	*THGal80 (control)*	-0.30 ± 0.10			
	MBGal80 (control)	-0.26 ± 0.05			
	krasavietz-Gal4 (control)	-0.24 ± 0.08			
	MBGal80/THGal80; krasavietz-Gal4/ UAS-ShakingB^{RNAi}	-0.26 ± 0.08	ns	ns	ns
[10^{-1}]	*THGal80 (control)*	-0.62 ± 0.04			
	MBGal80 (control)	-0.62 ± 0.08			
	krasavietz v-Gal4 (control)	-0.59 ± 0.05			
	MBGal80/THGal80; krasavietz -Gal4/ UAS-ShakingB^{RNAi}	-0.50 ± 0.07	ns	ns	ns

Table R12. Statistical analysis of IAA dose-response curve (Fig. R11-A) for experimental genotype: *MBGal80/THGal80;krasavietz-Gal4/UAS-ShakingB^{RNAi}* and as control genotypes: *THGal80, MBGal80* and *krasavietz-Gal4*.

[IAA]	Genotype	OI value	Statistical Analysis (vs. Control)
[10^{-3}]	*UAS-line (control)*	-0.20 ± 0.07	ns
	LN2-Gal4/UAS-ShakingB^{RNAi}	-0.18 ± 0.05	
[10^{-2}]	*UAS-line (control)*	-0.33 ± 0.07	ns
	LN2-Gal4/UAS-ShakingB^{RNAi}	-0.24 ± 0.08	
[10^{-1}]	*UAS-line (control)*	-0.70 ± 0.09	ns
	LN2-Gal4/UAS-ShakingB^{RNAi}	-0.73 ± 0.05	

Table R13. Statistical analysis of IAA dose-response curve (Fig. R11-B) for experimental genotype, *LN2-Gal4/UAS-ShakingB^{RNAi}* and *UAS line* as control.

Finally, the perception of EB also evoked olfactory responses toward repulsion after attenuating electrical synapses in both subsets of neurons: eLNs (**Fig. R12-A**) and iLNs (**Fig. R12-B**). Again, we found concentration-dependent differences between both experimental fly groups. Remarkably, experimental eLNs-attenuated flies detected the intermediate concentration (10^{-2}) significantly more repulsive than control flies (**Fig. R12-A**) whereas in the case of experimental iLNs-attenuated flies, only the highest concentration (10^{-1}) was perceived more negative than control flies (**Fig. R12-B**). By contrast, to the rest of tested concentrations both experimental fly groups behaved as their respective control flies (**Table R14** and **Table R15**).

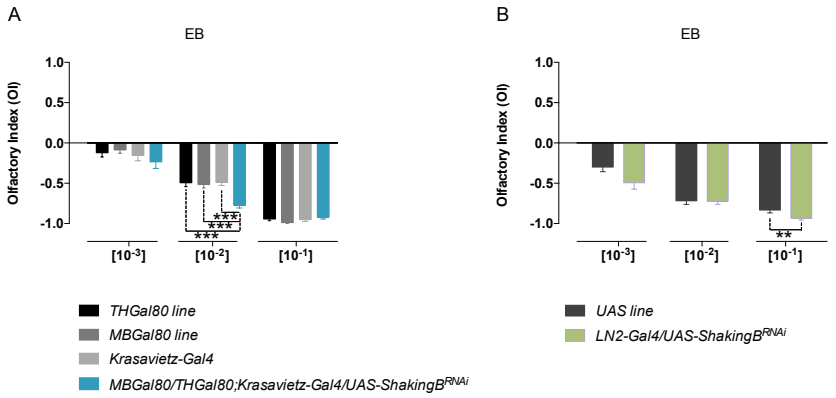

Fig. R12. Attenuation of electrical synapses in LNs modifies olfactory perception. (A-B) Dose-response curves for EB. **(A)** Dose-response curve for eLNs experimental flies: *MBGal80/THGal80;krasavietz-Gal4/UAS-ShakingB^{RNAi}* (in blue); and controls: 1) *THGal80 line* (in black), 2) *MBGal80 line* (in grey) and 3) *krasavietz-Gal4* (in light grey). **(B)** Dose-response curve for iLNs experimental flies: *LN2-Gal4/UAS-ShakingB^{RNAi}* (in green) and control: *UAS line* (in grey). Each data point represents the average ± SEM. For all genotypes N=350-400 per data point. Statistical t-test results are indicated with: *** p < 0.001, ** p < 0.01, * p < 0.05 for control group comparison.

[EB]	Genotype	OI value	Statistical Analysis (vs. THGal80)	(vs. MBGal80)	(vs. krasavietz-Gal4)
[10^{-3}]	*THGal80 (control)*	-0.12 ± 0.05			
	MBGal80 (control)	-0.07 ± 0.04			
	krasavietz-Gal4 (control)	-0.15 ± 0.07			
	MBGal80/THGal80; krasavietz-Gal4/ UAS-ShakingB^{RNAi}	-0.23 ± 0.07	ns	ns	ns
[10^{-2}]	*THGal80 (control)*	-0.51 ± 0.05			
	MBGal80 (control)	-0.48 ± 0.04			
	krasavietz-Gal4 (control)	-0.49 ± 0.05			
	MBGal80/THGal80; krasavietz-Gal4/ UAS-ShakingB^{RNAi}	-0.77 ± 0.03	*** p < 0.001	*** p < 0.001	*** p < 0.001
[10^{-1}]	*THGal80 (control)*	-0.94 ± 0.02			
	MBGal80 (control)	-0.99 ± 0.01			
	krasavietz v-Gal4 (control)	-0.95 ± 0.02			
	MBGal80/THGal80; krasavietz -Gal4/ UAS-ShakingB^{RNAi}	-0.95 ± 0.02	ns	ns	ns

Table R14. Statistical analysis of EB dose-response curve (Fig. R12-A) for experimental genotype: *MBGal80/THGal80;krasavietz-Gal4/UAS-ShakingB^{RNAi}* and as control genotypes: *THGal80*, *MBGal80* and *krasavietz-Gal4*.

[EB]	Genotype	OI value	Statistical Analysis (vs. Control)
[10^{-3}]	*UAS-line (control)*	-0.30 ± 0.06	ns
	LN2-Gal4/UAS-ShakingB^{RNAi}	-0.49 ± 0.08	
[10^{-2}]	*UAS-line (control)*	-0.72 ± 0.04	ns
	LN2-Gal4/UAS-ShakingB^{RNAi}	-0.72 ± 0.04	
[10^{-1}]	*UAS-line (control)*	-0.83 ± 0.03	** p < 0.01
	LN2-Gal4/UAS-ShakingB^{RNAi}	-0.93 ± 0.02	

Table R15. Statistical analysis of EB dose-response curve (Fig. R12-B) for experimental genotype, *LN2-Gal4/UAS-ShakingB^{RNAi}* and *UAS line* as control.

Our data allow us to conclude that olfactory behavior is strongly affected after attenuating the electrical component in LNs. In these neurons, olfactory changes were greater in magnitude than those obtained for PNs. Indeed, we can infer that electrical component of this neuronal population might not only be relevant to code the olfactory information in the AL but also, to discriminate among different odorant concentrations, being particularly relevant in the case of eLNs.

2.5. Electrical synapse restoration in the whole brain and in selected LNs populations rescues normal olfaction

We have previously observed that the attenuation of electrical synapses in the whole brain and in specific olfactory neuronal populations generates changes in olfactory perception. In this experiment, we wondered whether the restoration of electrical synapses is able to restore normal olfactory responses.

Here, we focused our study on three experimental conditions: 1) in the whole brain (*Elav-Gal4*), 2) in selected iLNs (*LN2-Gal4;Gal80^{ts}*, 30-37 iLNs per AL) and 3) in selected eLNs (*krasavietz-Gal4*, 6-8 eLNs per AL). We combined *UAS-ShakingB^{Neural}* construct in a *ShakB^{2}* background by using these three specific Gal4 drivers. Then, we examined their olfactory responses to three concentrations of EB. Here, we maintained the *LN2-Gal4* driver under Gal80^{ts} control, allowing the expression of the corresponding UAS construct only when flies are 7 ± 3 days old. Also, due to the fact that expression pattern of *krasavietz-Gal4* domain contains extrinsic mushroom body (MB) neurons and a subset of dopaminergic neurons, we used a *MBGal80* construct and *THGal80* construct to silence these cells. All genotypes under study followed the same protocol based on Gal4 temporary control by temperature, performing the olfactory behavioral test at 22 days (see Material and Methods for details).

We first analyzed if the restoration of electrical component in the whole brain was able to restore olfactory perception (**Fig. R13**). To this end, the pan-neural *Gal4* driver (*Elav*) was combined to the genetic *ShakB^{2};UAS-shakingB^{neural}* construct. Olfactory responses were compared to control flies (*ShakB^{2};UAS-shakingB^{neural}*, shown in graphs as *UAS-line*) and experimental *Elav-Gal4/UAS-ShakingB^{RNAi}* attenuated flies.

Our data showed that olfactory responses to EB for *ShakB^{2}; Elav-Gal4/UAS-shakingB^{neural}* (shown in graphs as *ShakB^{2};Neural;Elav-Gal4*) were always different to *Elav-Gal4/UAS-ShakingB^{RNAi}* flies (**Fig. R13**). More interestingly, their responses to the highest concentration (10^{-1}) were coincident with control flies (**Table R16**). By contrast, experimental *Elav-Gal4/UAS-ShakingB^{RNAi}* flies evoked more repulsive responses at this concentration, indicating a restoration of the normal olfactory response. In addition, we also observed that OI values to the intermediate concentration (10^{-2}) were more repulsive compared to control (**Fig. R13**, **Table R16**).

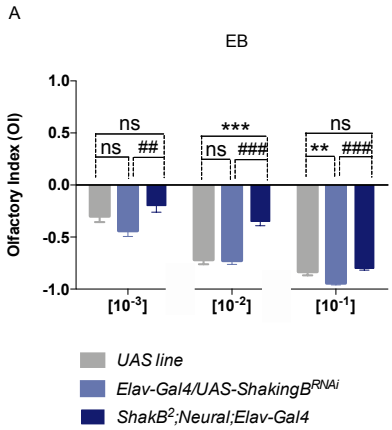

Fig. R13. Restoration of electrical synapses in whole brain leads to normal perception. Dose-response curves to EB for experimental flies: 1) *Elav-Gal4/UAS-ShakingB^{RNAi}* (in light blue) and 2) *ShakB^{2};Neural;Elav-Gal4* (in dark blue); and as a control: *UAS-line* (in grey). Each data point represents the average ± SEM. For all genotypes N=350-400 per data point. Statistical t-test results are indicated with: *** p < 0.001 and ** p < 0.01 for control group comparison and ### p < 0.001 and ## p < 0.01 for experimental group comparison.

[EB]	Genotype	OI value	Statistical Analysis (*vs. control*)	Statistical Analysis (*vs. ShakB^{2};Neural;Elav-Gal4*)
[10^{-3}]	*UAS-line (control)*	-0.08 ± 0.05		
	Elav-Gal4/UAS-ShakingB^{RNAi}	-0.11 ± 0.07	ns	
	ShakB^{2};Neural;Elav-Gal4	0.02 ± 0.07	ns	## p < 0.01
[10^{-2}]	*UAS-line (control)*	-0.36 ± 0.08		
	Elav-Gal4/UAS-ShakingB^{RNAi}	-0.34 ± 0.09	ns	
	ShakB^{2};Neural;Elav-Gal4	-0.03 ± 0.07	*** p < 0.001	### p < 0.001
[10^{-1}]	*UAS-line (control)*	-0.53 ± 0.04		
	Elav-Gal4/UAS-ShakingB^{RNAi}	-0.52 ± 0.05	** p < 0.01	
	ShakB^{2};Neural;Elav-Gal4	-0.20 ± 0.07	ns	### p < 0.001

Table R16. **Statistical Analysis.** Statistical analysis of EB dose-response curve (Fig. R13) for experimental genotypes: *Elav-Gal4/UAS-ShakingB^{RNAi}* and *ShakB^{2};Neural;Elav-Gal4* and as control: *UAS-line*.

Then, we checked the olfactory responses to EB of *ShakB^{2};krasavietz-Gal4/MBGal80/UAS-shakingB^{neural}* flies (shown in graphs as *ShakB^{2};Neural;krasavietz-Gal4*) in order to compare them with experimental *MBGal80/THGal80;krasavietz-Gal4/UAS-ShakingB^{RNAi}* flies (shown in graphs *krasavietz-Gal4/UAS-ShakingB^{RNAi})* and control flies (*krasavietz-Gal4)* (**Fig. R14**).

Again, we observed statistically significant differences among olfactory responses between both experimental fly groups at 10^{-2} and 10^{-1} stimulus concentrations, whereas at 10^{-3} concentration there was not significant changes (**Fig. R14**). Remarkably, the olfactory responses from *ShakB^{2};Neural;krasavietz-Gal4* flies shifted to normal control values (**Table R17**) whereas *MBGal80/THGal80;krasavietz-Gal4/UAS-ShakingB^{RNAi}* flies detected the intermediate concentration (10^{-2}) significantly more repulsive than control flies (**Fig. R14**, **Table R17**).

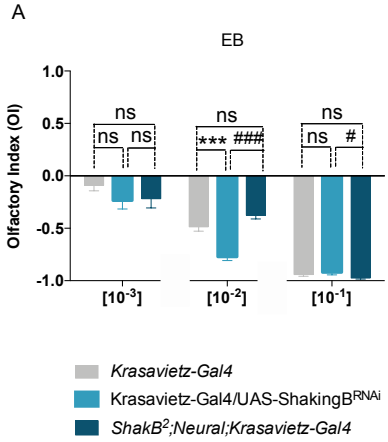

Fig. R14. **Restoration of electrical synapses in whole brain leads to normal perception.** Dose-response curves to EB for experimental flies: 1) *krasavietz-Gal4/UAS-ShakingB^{RNAi}* (in light blue) and 2) *ShakB^{2};Neural;krasavietz-Gal4* (in dark blue); and as a control: *krasavietz-Gal4* (in grey). Each data point represents the average ± SEM. For all genotypes N=350-400 per data point. Statistical t-test results are indicated with: *** $p < 0.001$ for control group comparison and ### $p < 0.001$ and # $p < 0.05$ for experimental group comparison.

[EB]	Genotype	OI value	Statistical Analysis (*vs. control*)	Statistical Analysis (*vs. ShakB^{2};Neural;krasavietz-Gal4*)
[10^{-3}]	*krasavietz-Gal4 (control)*	-0.15 ± 0.07		
	krasavietz-Gal4/UAS-ShakingB^{RNAi}	-0.23 ± 0.07	ns	
	ShakB^{2};Neural;krasavietz-Gal4	-0.10 ± 0.11	ns	ns
[10^{-2}]	*krasavietz-Gal4 (control)*	-0.49 ± 0.05		
	krasavietz-Gal4/UAS-ShakingB^{RNAi}	-0.77 ± 0.03	ns	
	ShakB^{2};Neural;krasavietz-Gal4	-0.38 ± 0.03	*** $p < 0.001$	### $p < 0.001$
[10^{-1}]	*krasavietz-Gal4 (control)*	-0.95 ± 0.02		
	krasavietz-Gal4/UAS-ShakingB^{RNAi}	-0.95 ± 0.02	ns	
	ShakB^{2};Neural;krasavietz-Gal4	-0.97 ± 0.01	ns	# $p < 0.05$

Table R17. **Statistical analysis**. Statistical analysis of EB dose-response curve (Fig. R14) for experimental genotypes: *krasavietz-Gal4/UAS-ShakingB^{RNAi}* and *ShakB^{2};Neural;krasavietz-Gal4* and as control: *krasavietz-Gal4*.

Finally, we also tested the olfactory responses to *ShakB^{2};LN2-Gal4/Gal80^{ts}/UAS-shakingB^{neural}* flies (shown in graphs as *ShakB^{2};Neural;LN2-Gal4;Gal80^{ts}*) flies comparing them to *LN2-Gal4/UAS-ShakingB^{RNAi}* flies and control flies (*LN2-Gal4;Gal80^{ts})* (**Fig. R15**).

The olfactory responses of *ShakB^{2};Neural;LN2-Gal4;Gal80^{ts}* flies were always statistically different from *LN2-Gal4/UAS-ShakingB^{RNAi}* (**Fig. R15**). In these iLNs-attenuated flies, the lowest and intermediate concentration (10^{-3} and 10^{-2}, respectively) were perceived more negative than control flies (**Fig. R15**, **Table R18**). By contrast, after restoration of electrical synapses in iLNs, we did not detect any olfactory responses different from control flies (**Fig. R15**, **Table R18**).

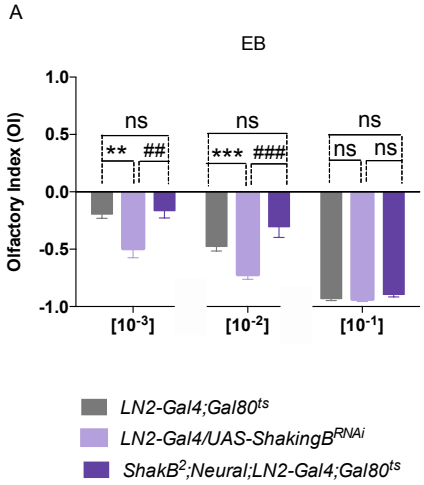

Fig. R15. **Restoration of electrical synapses in whole brain leads to normal perception.** Dose-response curves to EB for experimental flies: 1) LN2-*Gal4/UAS-ShakingB^{RNAi}* (in light purple) and 2) *ShakB^{2};Neural;LN2-Gal4;Gal80^{ts}* (in dark purple); and as a control: *LN2-Gal4;Gal80^{ts}* (in grey). Each data point represents the average ± SEM. For all genotypes N=350-400 per data point. Statistical t-test results are indicated with: *** $p < 0.001$ and ** $p < 0.01$ for control group comparison and ### $p < 0.001$ and ## $p < 0.01$ for experimental group comparison.

[EB]	Genotype	OI value	Statistical Analysis (*vs. control*)	Statistical Analysis (*vs. ShakB^{2};Neural;LN2-Gal4;Gal80^{ts}*)
[10^{-3}]	*LN2-Gal4;Gal80^{ts} (control)*	-0.19 ± 0.04		
	LN2-Gal4/UAS-ShakingB^{RNAi}	-0.18 ± 0.05	** p < 0.01	
	ShakB^{2};Neural;LN2-Gal4;Gal80^{ts}	-0.17 ± 0.06	ns	## p < 0.01
[10^{-2}]	*LN2-Gal4;Gal80^{ts} (control)*	-0.48 ± 0.04		
	LN2-Gal4/UAS-ShakingB^{RNAi}	-0.24 ± 0.08	*** p < 0.001	
	ShakB^{2};Neural;LN2-Gal4;Gal80^{ts}	-0.30 ± 0.09	ns	### p < 0.001
[10^{-1}]	*LN2-Gal4;Gal80^{ts} (control)*	-0.93 ± 0.02		
	LN2-Gal4/UAS-ShakingB^{RNAi}	-0.73 ± 0.05	ns	
	ShakB^{2};Neural;LN2-Gal4;Gal80^{ts}	-0.90 ± 0.02	ns	ns

Table R18. **Statistical Analysis.** Statistical analysis of EB dose-response curve (Fig. R15) for experimental genotypes: *LN2-Gal4/UAS-ShakingB^{RNAi}* and *ShakB^{2};Neural;LN2-Gal4;Gal80^{ts}* and as control: *LN2-Gal4;Gal80^{ts}*.

Taken together, all these data strongly suggest that the restoration of electrical synapses in the whole brain and in selected subsets of local interneurons rescues normal olfactory responses, pointing out the relevant role of electrical synapses in olfactory processing.

CHAPTER 3:

Role of electrical synapses in life expectancy and locomotion in normal and pathological conditions

3.1. Total loss of electrical synapses reduces lifespan and impairs locomotion

3.2. Electrical synapse restoration in the whole brain and in selected LNs populations rescues lifespan

3.3. Electrical synapse restoration in the whole brain and in selected LNs populations preserves normal locomotion

3.4. Aβ42-overexpression in the whole brain and specific LNs increases fly mortality in a ShakB^{2} background

3.5. Aβ42-overexpression in the whole brain and specific LNs increases aggravates ShakB^{2}-dependent locomotor deficits

Drosophila ShakB gene plays a relevant role in the regulation of electrical transmission. Mutations in this gene, such as *ShakB*^{2}, cause a disruption of electrical connectivity in several neural pathways, including the fly giant fiber system (GFS) (Baird et al., 1990; Phelan, 2005). Notably, these mutant flies present defaults in locomotion, a defective flight and impairments in their visual escape behaviors (Pauline Phelan, 2005).

Throughout this Chapter, we addressed whether the restoration of electrical synapses increases the viability of *ShakB*^{2} flies and leads to an improvement in their locomotor activity. On the other hand, previous findings have reported how the overexpression of human variants of Aβ42 peptides in *Drosophila* brain dramatically affects their lifespan and locomotion (López-Arias et al., 2017; Iijima et al., 2004; Doctoral Thesis, Mercedes Arnés, Arnés et al., submitted). Here, we have also wondered whether the absence of electrical synapses in a fly model of Alzheimer's disease is able to generate an aggravation of both phenotypes. To tackle this issue, we carried out the study under three experimental conditions: 1) in the whole brain, 2) in selected iLNs and 3) in selected eLNs. So, we combined *UAS-ShakB*^{Neural} and *UAS-Aβ42(2x)* constructs in a *ShakB*^{2} background using specific Gal4 drivers in order to restore the electrical synapses and/or express Aβ42 peptide in: 1) the whole brain (*Elav-Gal4*), 2) *LN2-Gal4* (30-37 iLNs per AL) and *krasavietz-Gal4* (6-8 eLNs per AL). First, we maintained the *LN2-Gal4* driver under *Gal80*^{ts} control, allowing the expression of the corresponding UAS constructs only when flies are 7 ± 1 days old. Second, due to the fact that expression pattern of *krasavietz-Gal4* domain contains extrinsic mushroom body (MB) neurons, we used a *MBGal80* construct to silence these cells. Due to the high number of constructs to be expressed, we did not have the possibility to use here the *THGal80* repressor in these flies. For this reason, a group of TH-expressing dopaminergic neurons were also present in the expression pattern of krasavietz-Gal4 line in these experiments. Thus, to compare all fly groups, all genotypes under study followed the same protocol based on Gal4 temporary control by temperature (see Material and Methods for details).

To analyze the life expectancy and locomotor activity, both survival and negative geotaxis assays were required (Material and Methods for details). All survival graphs show the percentage of survival (% of survival) *versus* time in days whereas all climbing results indicate the percentage of flies (% of flies) *versus* time in days.

3.1. Total loss of electrical synapses reduces lifespan and impairs locomotion

Since lifespan of *ShakB*^{2} mutant flies had not been analyzed before, we firstly performed a survival analysis. In this experiment, we also checked whether *ShakB*^{2} mutant flies and flies in which *UAS-ShakB*^{Neural} and *UAS-Aβ42(2x)* constructs were inserted in a *ShakB*^{2} background developed a similar behavior in terms of lifespan and locomotion (from now, we will refer to them as *ShakB*^{2}*;Neural* and *ShakB*^{2}*;Aβ42* flies). All experiments were conducted in homozygous *ShakB*^{2} background by using females flies (see Materials and Methods)

Our results showed differences in the median survival values despite of the three tested genotypes carrying the *ShakB*^{2} background (**Fig. R16**). Here, whereas *ShakB*^{2} median survival value was 9.5 days, *ShakB*^{2}*;Neural* flies in turn, showed a significant increase of 26%, extending

the median survival value to 12 days. By contrast, *ShakB²;Aβ42* flies showed a median survival rate of 6 days, 36% significantly shorter than *ShakB²* flies (**Table R19**).

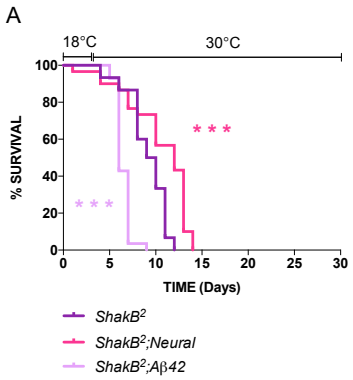

Fig. R16. ***ShakB²* background reduces fly lifespan.** Survival curve for: *ShakB²;Neural* (in pink) and *ShakB²;Aβ42* (in light purple) compared to *ShakB²* mutants (in dark purple). For each genotype, at least 3 experiments were performed with an average of 10 flies/experiment. Statistical analysis with Mantel-Cox Test is shown as *** p < 0.001.

Genotype	n	Median Survival (Days)	Maximum Survival (Days)	Mantel-Cox Test (vs. *ShakB²*)
ShakB²	30	9.5	12	
ShakB²;Neural	30	12 (26%)	14 (16%)	*** p < 0.001
ShakB²;Aβ42	28	6 (36%)	9 (25%)	*** p < 0.001

Table R19. **Statistical analysis of Survival assay.** Change in percentage is shown in brackets respect to *ShakB²*.

Previously data have documented that *ShakB²* mutation leads to abnormalities in locomotor activity preventing flies to control the movement of their legs (Baird et al., 1990). Here, we want to corroborate these data evaluating the climbing activity of these mutant flies. Then, we also asked about the locomotion of the other flies carrying a *ShakB²* background (*ShakB²;Neural* and *ShakB²;Aβ42* flies).

According to previously findings, our results showed that locomotion of *ShakB²* flies is really impaired (**Fig. R17**). Indeed, all genotypes under study developed a similar climbing performance along time, with a proportion of flies drastically decreasing from day 4 of experiment, when the temperature is shifted to 30°C. Indeed, the percentage of flies reaching the 4 cm line never exceeding 50% for none of experimental flies. Statistical analysis showed that the effects in locomotion were not conditioned by genotype and time (**Table R20**), indicating that flies carrying a *ShakB²* background behaved as a *ShakB²* mutant.

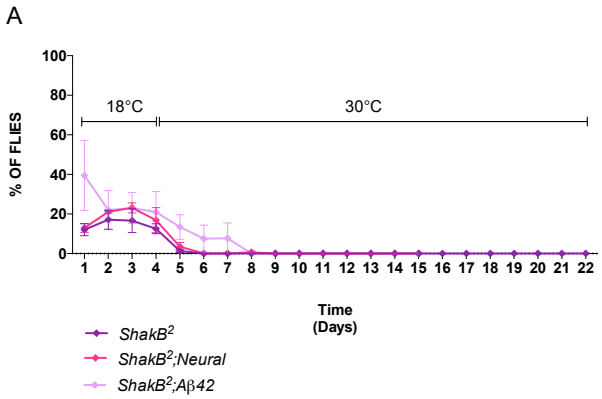

Fig. R17. *ShakB²* background affects locomotor activity. Climbing assay for: *ShakB²* mutants (in dark purple), *ShakB²;Neural* (in pink) and *ShakB²;Aβ42* (in light purple). For each genotype, at least 3 experiments were performed with an average of 10 flies/experiment. Data expressed mean ± SEM and statistical analysis was performed by 2-way ANOVA test.

Genotype	Time	Genotype * Time
F (2,6) = 1.08. **ns** p = 0.388	F (21, 126) = 16.98 *** p < 0.001	F (42, 126) = 1.32 **ns** p = 0.122

Table R20. Statistical analysis Fig. R17.

3.2. Electrical synapse restoration in the whole brain and in selected LNs populations rescues lifespan

To analyze whether lifespan could be improved by restoring electrical synapses, *UAS-ShakB^{Neural}* construct was combined to selected Gal4 drivers in: the whole brain (*Elav-Gal4*) and a certain population of iLNs (*LN2-Gal4*) and eLNs (*Krasavietz-Gal4*).

Initially, we studied the possible restoration of electrical synapses in the whole brain. First, we compared *ShakB²* mutants to control flies (*Elav-Gal4*) (**Fig. R18-A**). As expected, *ShakB²* genotype showed a very significant decrease in lifespan with a median survival value of 9.5 days, 52% shorter than control (20 days) (**Table R21**). Interestingly, survival data obtained for experimental *ShakB²;Neural;Elav-Gal4* flies indicated a highly significant extension in their lifespan, living 136% more than *ShakB²* flies with a median survival rate of 22.5 days (**Fig. R18-B**, **Table R21**). Moreover, these flies reached a median survival value even greater than control, with a 12% increase in lifespan, although this difference was not statistically significant (**Fig. R18-C**, **Table R21**). Taken together, these data allow us to conclude that restoration of electrical connections in the whole brain yields to a rescue of fly life expectancy.

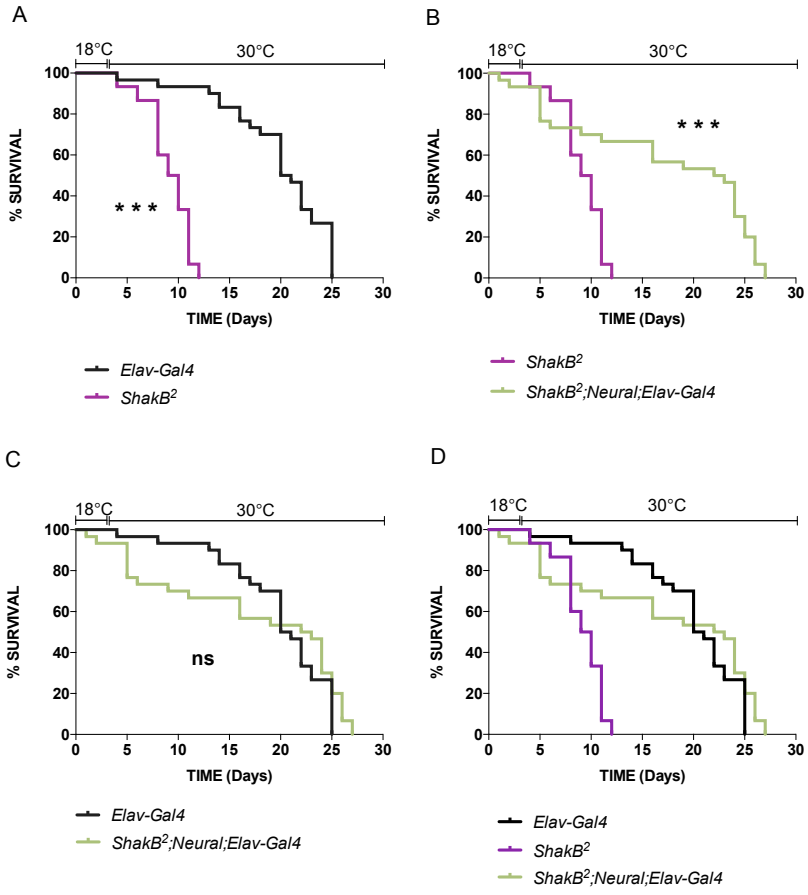

Fig. R18. Recovery of lifespan after restoring electrical synapses in the whole brain. (A-D) Survival curves for the following genotypes: *ShakB²* genotype (in purple) **(A,B,D)** compared to *Elav-Gal4* (control) (in black) **(A)** and *ShakB²;Neural;Elav-Gal4* genotype (in green) **(B,C,D)** compared to *Elav-Gal4* (control) (in black) **(C)** or compared to *ShakB²* **(B)**. **(D)** Survival curve representing survival data in all genotypes. For each genotype, at least 3 experiments were performed with an average of 10 flies/experiment. Statistical analysis with Mantel-Cox Test is shown as *** $p < 0.001$ for comparisons to control (A,C) and compared to *ShakB²* (B).

Genotype	n	Median Survival (Days)	Maximum Survival (Days)	Mantel-Cox Test
***Elav-Gal4* vs Groups**				
Elav-Gal4	30	20	25	
ShakB²	30	9.5 **(52%)**	12 **(52%)**	*** p < 0.001
ShakB²;Neural;Elav-Gal4	30	22.5 **(12%)**	27 **(8%)**	ns
***ShakB²* vs Groups**				
ShakB²	30	9.5	12	
ShakB²;Neural;Elav-Gal4	30	22.5 **(136%)**	27 **(116%)**	*** p < 0.001

Table R21. **Statistical analysis of Survival assay.** Change in percentage is shown in brackets respect to *Elav-Gal4* (control) or *ShakB²* values.

Secondly, we studied the effect on survival after restoring electrical synapses in specific population of iLNs (*LN2-Gal4 driver*). Regarding to previous result obtained, *ShakB²* flies showed a significant reduction of life expectancy compared to control flies (*LN2-Gal4;Gal80^{ts}*) (**Fig. R19-A**). Here, *ShakB²* median survival value was 56% shorter than control flies with 22 days (**Table R22**).

Surprisingly, experimental *ShakB²;Neural;LN2-Gal4;Gal80^{ts}* flies not only showed a significant increase of 142% in median survival rate (23 days) compared to *ShakB²* flies value (**Fig. R19-B**), but also this value was pretty similar to control flies values with 22 days (**Fig. R19-C**,**Table R22**).

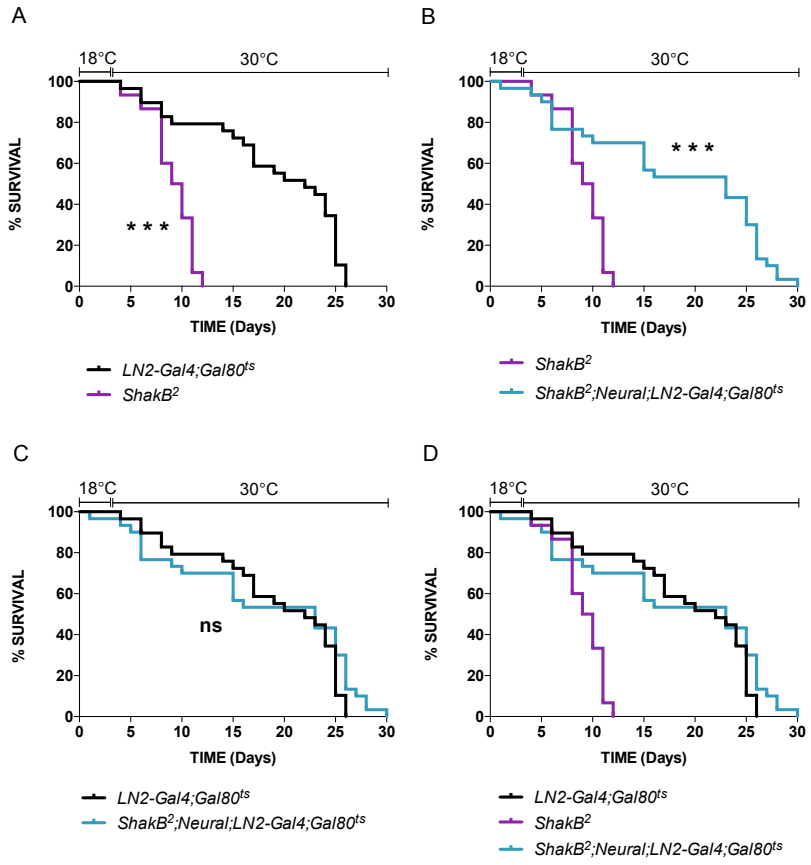

Fig. R19. Recovery of life expectancy after restoring electrical synapses in the subsets of iLNs. (A-D) Survival curves for the following genotypes: *ShakB²* genotype (in purple) **(A,B,D)** compared to *LN2-Gal4;Gal80ᵗˢ* (control) (in black) **(A)** and *ShakB²;Neural;LN2-Gal4;Gal80ᵗˢ* genotype (in green) **(B,C,D)** compared to *LN2-Gal4;Gal80ᵗˢ* (control) (in black) **(C)** or compared to *ShakB²* **(B)**. **(D)** Survival curve representing survival data in all genotypes. For each genotype, at least 3 experiments were performed with an average of 10 flies/experiment. Statistical analysis with Mantel-Cox Test is shown as *** $p < 0.001$ for comparisons to control (A,C) and compared to *ShakB²* (B).

Genotype	n	Median Survival (Days)	Maximum Survival (Days)	Mantel-Cox Test
LN2-Gal4;Gal80^{ts} **vs Groups**				
LN2-Gal4;Gal80^{ts}	29	22	26	
ShakB^{2}	30	9.5 **(56%)**	12 **(54%)**	*** p < 0.001
ShakB^{2};Neural;LN2-Gal4;Gal80^{ts}	30	23 **(4%)**	30 **(15%)**	*** p < 0.001
ShakB^{2} **vs Groups**				
ShakB^{2}	30	9.5	12	
ShakB^{2};Neural;LN2-Gal4;Gal80^{ts}	30	23 **(142%)**	30 **(150%)**	*** p < 0.001

Table R22. **Statistical analysis of Survival assay.** Change in percentage is shown in brackets respect to *LN2-Gal4;Gal80^{ts}* (control) or *ShakB^{2}* values.

Then, we analyzed the data obtained after restoring the electrical synapses in a smaller subset of eLNs (*krasavietz-Gal4* driver) (**Fig. R20**). Here, our results also showed an improvement in fly lifespan. Again, ShakB^{2} flies showed a significant decrease in fly viability living 27% shorter than control flies (*krasavietz-Gal4;MBGal80,* abbreviated as *krasavietz-Gal4*) (13 days) (**Fig. R20-A**, **Table R23**). In this case, experimental *ShakB^{2};Neural;Krasavietz-Gal4;MBGal80* flies (abbreviated as *ShakB^{2};Neural;krasavietz-Gal4*) significantly improved the negative effect of *ShakB^{2}* background, increasing the median survival rate to 11 days, living 15% more than *ShakB^{2}* flies (**Fig. R20-B**, **Table R23**), although this recovery did not reach control survival value. In fact, experimental *ShakB^{2};Neural;krasavietz-Gal4* flies showed a significant decrease in lifespan, living 15% less than control flies with 13 days (**Fig. R20-C**, **Table R23**).

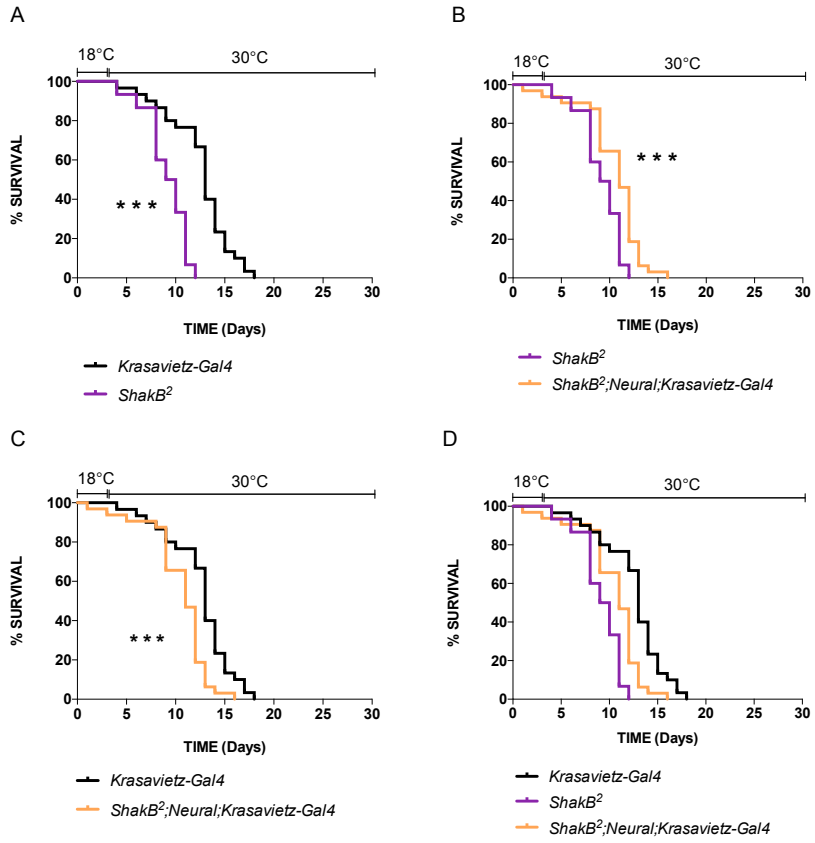

Fig. R20. Recovery of lifespan after restoring electrical synapses in the subsets of eLNs. (A-D) Survival curves for the following genotypes: *ShakB²* genotype (in purple) **(A,B,D)** compared to *krasavietz-Gal4* (control) (in black) **(A)** and *ShakB²;Neural;krasavietz-Gal4* genotype (in green) **(B,C,D)** compared to *krasavietz -Gal4* (control) (in black) **(C)** or compared to *ShakB²* **(B)**. **(D)** Survival curve representing survival data in all genotypes. For each genotype, at least 3 experiments were performed with an average of 10 flies/experiment. Statistical analysis with Mantel-Cox Test is shown as *** $p < 0.001$ for comparisons to control (A,C) and compared to *ShakB²* (B).

Genotype	n	Median Survival (Days)	Maximum Survival (Days)	Mantel-Cox Test
***krasavietz-Gal4* vs Groups**				
krasavietz-Gal4	30	13	18	
ShakB²	30	9.5 **(27%)**	12 **(33%)**	*** p < 0.001
ShakB²;Neural;krasavietz-Gal4	32	11 **(15%)**	16 **(11%)**	*** p < 0.001
***ShakB²* vs Groups**				
ShakB²	30	9.5	12	
ShakB²;Neural;krasavietz-Gal4	32	11 **(15%)**	16 **(33%)**	*** p < 0.001

Table R23. **Statistical analysis of Survival assay.** Change in percentage is shown in brackets respect to *krasavietz-Gal4* (control) or *ShakB²* values.

It is worth comparing the survival curves of three experimental groups of flies (**Fig. R21**). On one hand, electrical synapse restoration in the whole brain surprisingly had the same positive effects in lifespan as the restoration in selected subset of 30-37 iLNs (**Fig. R21-A**). In fact, no significant differences were found between these experimental groups of flies, pointing that these iLNs could be relevant for fly viability (**Table R24**). On the other hand, when the electrical synapse restoration was directed to 6-8 eLNs, the improvement in fly viability was not as effective as in the other two experimental conditions (*Elav-Gal4* and *LN2-Gal4* drivers) (**Fig. R21-B,C**, **Table R24**).

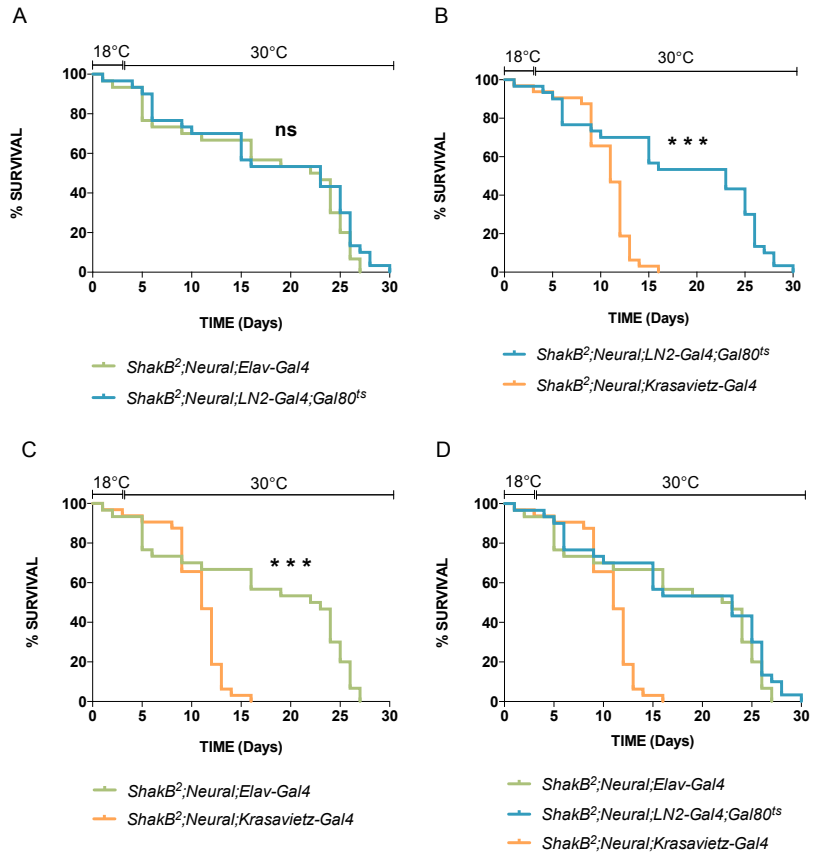

Fig. R21. Comparison of survival curves for experimental flies. Survival curves for following genotypes: *ShakB^2;Neural;Elav-Gal4* genotype (in green) **(A,C,D)**; *ShakB^2;Neural;LN2-Gal4;Gal80^{ts}* genotype (in blue) **(A,B,D)** and *ShakB^2;Neural;krasavietz-Gal4* genotype (in orange) **(B,C,D)**. **(D)** Survival curves representing survival data in all experimental genotypes. For each genotype, at least 3 experiments were performed with an average of 10 flies/experiment. Statistical analysis with Mantel-Cox Test is shown as *** $p < 0.001$ for comparisons to *ShakB^2;Neural;Krasavietz-Gal4* (B,C).

Genotype	n	Median Survival (Days)	Maximum Survival (Days)	Mantel-Cox Test
***ShakB²;Neural;Elav-Gal4* vs Exp**				
ShakB²;Neural;Elav-Gal4	30	22.5	27	
ShakB²;Neural;LN2-Gal4;Gal80ᵗˢ	30	23 (2%)	30 (11%)	ns
ShakB²;Neural;krasavietz-Gal4	32	11 (51%)	16 (40%)	*** p < 0.001
ShakB²;Neural;*krasavietz-Gal4* vs Exp				
ShakB²;Neural;krasavietz-Gal4	33	11	16	
ShakB²;Neural;LN2-Gal4;Gal80ᵗˢ	30	23 (109%)	30 (87%)	*** p < 0.001

Table R24. **Statistical analysis of Survival assay.** Change in percentage is shown in brackets respect to experimental *ShakB²;Neural;Elav-Gal4* or *ShakB²;Neural;krasavietz-Gal4* values.

We can conclude from all these data that the restoration of electrical synapses in a *ShakB²* background, significantly improves the viability of experimental flies allowing them to reach normal lifespan values. Considerably, the number of electrical connections restored and the chemical synapse type (inhibitory or excitatory) of the LNs subsets seems to be crucial for *ShakB²* fly survival. Furthermore, these data point out, for the first time, an unexpected role of electrical connections on fly viability.

3.3. Electrical synapse restoration in the whole brain and in selected LNs populations preserves normal locomotion

Our successful results in survival analysis obtained after selective electrical restoration on *ShakB²* flies, encouraged us to explore whether locomotion deficits observed in *ShakB²* flies (**Fig. R2**) could be also restored using the same experimental procedure. To evaluate locomotor activity, we performed a negative geotaxis assay with the same groups of flies employed in survival assays. In this test, we considered: 1) number of flies that reached the 4 cm line in the given time and 2) number of flies stayed at the bottom of the vial (Material and Methods for details).

In general, we detected an improvement in climbing performance after restoring electrical synapses in all experimental conditions. Indeed, in all experimental fly groups the negative effect of *ShakB²* background in locomotion was reverted, even developing a pretty similar climbing performance to their respective control flies (**Fig. R22**).

First, when we restored the electrical synapses in the whole brain, the statistical analysis showed an interaction between genotype and time, indicating that locomotion is conditioned by both factors: time and genotype (**Table R25**). We detected how experimental *ShakB²;Neural;Elav-Gal4* individuals showed a significant increase in the proportion of flies reaching the 4 cm line compared to the percentage of *ShakB²* flies (**Fig. R22**). Indeed, the proportion of experimental *ShakB²;Neural;Elav-Gal4* flies exceeding the 4cm line were around 80% during the first four days

of experiment, with percentages even higher than control flies (*Elav-Gal4*). In fact, locomotion performed by these experimental flies was strikingly similar to control flies during all the assay and we only detected significant differences at day 1 and day 6 of experiment (**Fig. R22**). However, we observed a reduction in climbing performance of these experimental flies at day 6, whose percentages were under 50%. Probably these deficits in locomotor activity were impaired by the temperature shift as well as flies aging.

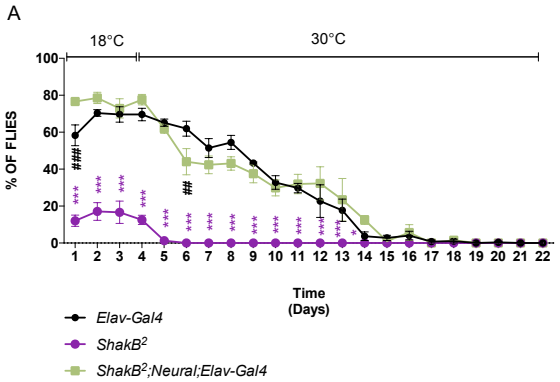

Fig. R22. Restoration of electrical synapses in whole brain improves climbing activity. Climbing curves for experimental genotype: *ShakB^2;Neural;Elav-Gal4* genotype (in green), *ShakB^2* genotype (in purple) and *Elav-Gal4* genotype (control, in black). For each genotype, at least 3 experiments were performed with an average of 10 flies/experiment. Data expressed mean ± SEM and statistical analysis was performed by 2-way ANOVA test and corrected by Tukey´s test method where *** $p < 0.001$; ** $p < 0.01$ for comparisons between *ShakB^2;Neural;Elav-Gal4 versus ShakB^2* and ### $p < 0.001$; ## $p < 0.01$ for comparisons between *Elav-Gal4 versus ShakB^2;Neural;Elav-Gal4.*

Genotype	Time	Genotype * Time
F (2,6) = 136.5 *** p < 0.001	F (21, 126) = 114.0 *** p < 0.001	F (42, 126) = 19.8 *** p < 0.001

Table R25. Statistical analysis Fig. R22.

In turn, when the restoration was directed to iLNs, the statistical analysis also indicated that climbing is affected by genotype and time (**Table R26**). Interestingly, we only detected a significant difference at day 7 in climbing performance developed by experimental *ShakB^2;Neural;LN2-Gal4;Gal80^{ts}* flies compared to control flies (*LN2-Gal4;Gal80^{ts}*) (**Fig. R23**). In addition, the locomotor activity of these experimental flies also showed a higher improvement than ShakB^2 flies, as well as we observed in experimental *ShakB^2;Neural;Elav-Gal4* flies (**Fig. R22**). Notably, these experimental flies started to overexpress the *UAS-ShakB^{Neural}* construct at day 5, when the flies were shifted to 30°C. In this case, the proportion of flies exceeding 4 cm line were maintained over 50% until day 13 (**Fig. R23**).

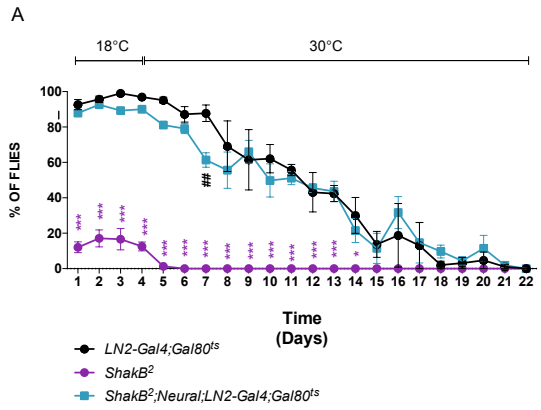

Fig. R23. Restoration of electrical synapses in iLNs leads to recover locomotion. Climbing curves for experimental genotype: *ShakB²;Neural;LN2-Gal4;Gal80ᵗˢ* genotype (in blue), *ShakB²* genotype (in purple) and *LN2-Gal4;Gal80ᵗˢ* genotype (control, in black). For each genotype, at least 3 experiments were performed with an average of 10 flies/experiment. Data expressed mean ± SEM and statistical analysis was performed by 2-way ANOVA test and corrected by Tukey´s test method where *** p < 0.001; * p < 0.05 for comparisons between *ShakB²;Neural;LN2-Gal4;Gal80ᵗˢ versus ShakB²* and ## p < 0.01 for comparisons between *LN2-Gal4;Gal80ᵗˢ versus ShakB²;Neural; LN2-Gal4;Gal80ᵗˢ*.

Genotype	Time	Genotype * Time
F (2,6) = 57.63 *** p < 0.001	F (21, 126) = 76.05 *** p < 0.001	F (42, 126) = 14.68 *** p < 0.001

Table R26. Statistical analysis Fig. R23.

On the other hand, we also detected an interaction between genotype and time after restoring the electrical connections in a subset of 6-8 eLNs (**Table R27**). Thus, experimental *ShakB²;Neural;krasavietz-Gal4* flies showed a significant locomotor improvements compared to *ShakB²* flies during all the experiment (**Fig. R24**). At the beginning of assay, with a temperature fixed to 18°C, the proportion of experimental flies reaching the 4 cm line was similar to their corresponding control flies (*krasavietz-Gal4*). However, when flies were shifted to 30°C, we observed a statistically significant reduction in experimental percentages compared to those from control flies from day 5 to day 8, albeit their climbing activity remained to be better than *ShakB²* flies (**Fig. R24**).

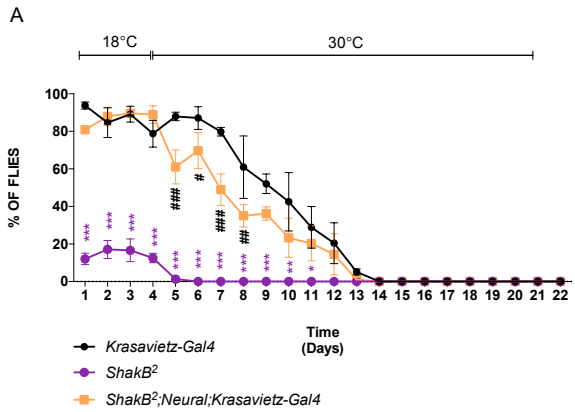

Fig. R24. Restoration of electrical synapses in eLNs improves locomotor activity. Climbing curves for experimental genotype: *ShakB²;Neural;krasavietz-Gal4* genotype (in orange), *ShakB²* genotype (in purple) and *krasavietz-Gal4* genotype (control, in black). For each genotype, at least 3 experiments were performed with an average of 10 flies/experiment. Data expressed mean ± SEM and statistical analysis was performed by 2-way ANOVA test and corrected by Tukey´s test method where *** $p < 0.001$; ** $p < 0.01$ and * $p < 0.05$ for comparisons between *ShakB²;Neural;krasavietz-Gal4 versus ShakB²* and ### $p < 0.001$; ## $p < 0.01$ and # $p < 0.05$ for comparisons between *krasavietz-Gal4 versus ShakB²;Neural;krasavietz-Gal4.*

Genotype	Time	Genotype * Time
F (2,6) = 75.03 *** p < 0.001	F (21, 126) = 87.71 *** p < 0.001	F (42, 126) = 16.96 *** p < 0.001

Table R27. Statistical analysis Fig. R24.

Finally, we compared the climbing performance of our three experimental fly groups. For all genotypes, locomotor defaults became more evident as flies aged. However, the comparison of climbing activity among these three electrical synapse restoration conditions showed significant differences.

Remarkably, the statistical analysis showed an interaction between genotype and time when we compared the experimental groups in which the restoration was directed to the whole brain and a specific subset of 30-37 iLNs (**Fig. R25**, **Table R28**). We observed that these experimental *ShakB²;Neural;LN2-Gal4;Gal80^{ts}* flies exhibited a significantly better locomotion than *ShakB²;Neural;Elav-Gal4* flies with statistically significant differences at punctual days of assay.

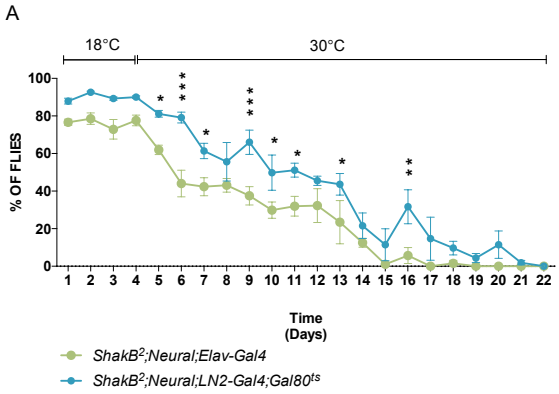

Fig. R25. Comparison of climbing activity among experimental fly groups. Climbing curves for following experimental genotypes: *ShakB²;Neural;Elav-Gal4* genotype (in green) and *ShakB²;Neural;LN2-Gal4;Gal80ᵗˢ* genotype (in blue). For each genotype, at least 3 experiments were performed with an average of 10 flies/experiment. Data expressed mean ± SEM and statistical analysis was performed by 2-way ANOVA test and corrected by Tukey´s test method where significant differences are shown as: *** p < 0.001; ** p < 0.01 and * p < 0.05.

Genotype	Time	Genotype * Time
F (1,4) = 22.55 **ns** p = 0.009	F (21, 84) = 80.75 *** p < 0.001	F (21, 84) = 1.53 ** p < 0.01

Table R28. Statistical analysis Fig. R25.

In turn, when we compared the experimental groups in which the restoration was directed to the two specific subsets of LNs, the statistical analysis showed again an interaction between genotype and time (**Table R29**). Climbing activity developed by *ShakB²;Neural;krasavietz-Gal4* flies was significantly worst compared to experimental *ShakB²;Neural;LN2-Gal4;Gal80ᵗˢ* flies with statistically significant differences from day 8 to day 14 and day 16 (**Fig. R26**).

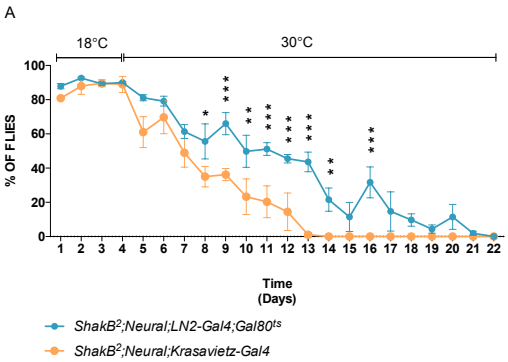

Fig. R26. Comparison of climbing activity among experimental fly groups. Climbing curves for following experimental genotypes: *ShakB²;Neural;LN2-Gal4;Gal80ᵗˢ* genotype (in blue) and *ShakB²;Neural;krasavietz-Gal4* genotype (in orange). For each genotype, at least 3 experiments were performed with an average of 10 flies/experiment. Data expressed mean ± SEM and statistical analysis was performed by 2-way ANOVA test and corrected by Tukey´s test method where significant differences are shown as: *** p < 0.001; ** p < 0.01 and * p < 0.05.

Genotype	Time	Genotype * Time
F (1,4) = 40.70 ** p < 0.01	F (21, 84) = 73.31 *** p < 0.001	F (21, 84) = 2.55 ** p < 0.01

Table R29. **Statistical analysis Fig. R26.**

Finally, the statistical analysis showed and interaction between genotype and time when we compared the experimental flies where the restoration was directed to 6-8 eLNs (*ShakB²;Neural;krasavietz-Gal4* flies) and the experimental *ShakB²;Neural;Elav-Gal4* flies, where the restoration was directed to the whole brain (**Fig. R27**, **Table R30**). Climbing performance developed by these experimental groups was remarkably similar with only significant differences at punctual days of assay, the days 6 and 13.

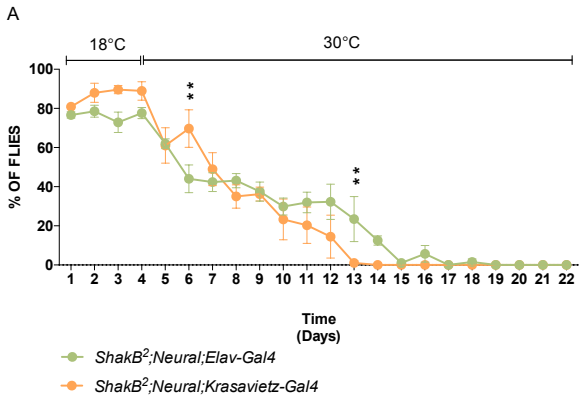

Fig. R27. Comparison of climbing activity among experimental fly groups. Climbing curves for following experimental genotypes: *ShakB²;Neural;Elav-Gal4* genotype (in green) and *ShakB²;Neural;krasavietz-Gal4* genotype (in orange). For each genotype, at least 3 experiments were performed with an average of 10 flies/experiment. Data expressed mean ± SEM and statistical analysis was performed by 2-way ANOVA test and corrected by Tukey´s test method where significant differences are shown as: ** p < 0.01.

Genotype	Time	Genotype * Time
F (1,4) = 0.09 **ns** p = 0.777	F (21, 84) = 83.78 *** p < 0.001	F (21, 84) = 2.49 ** p < 0.01

Table R30. **Statistical analysis Fig. R27.**

Taken all together, our data indicate that the electrical synapse restoration directed to the whole brain as well as to specific subsets of LNs (eLNs or iLNs) leads to an improvement in climbing performance compared to *ShakB²* mutants. Intriguingly, a better locomotion performance was detected when the restoration of electrical connections was directed to the subset of iLNs, suggesting that these olfactory neurons might be also relevant in locomotor activity (see Discussion).

3.4. Aβ42-overexpression in the whole brain and specific LNs increases fly mortality in a ShakB² background

It is well known that Aβ42 expression has a strong negative effect in lifespan, mainly when it is expressed throughout the brain (using *Elav-Gal4* driver) (Iijima et al., 2004; López-Arias et al., 2017; Doctoral Thesis Mercedes Arnés; Arnés et al., submitted). Thus, we aimed here to analyze the effect of electrical synapse loss in a pathological context, using a *Drosophila* model of Alzheimer's disease. To address this issue, an extremely toxic *UAS-Aβ42(2x)* construct was inserted in a *ShakB²* background and combined to the same Gal4 drivers previously employed for electrical synapse restoration.

First, we found that expression of Aβ42 peptide in the whole brain in a *ShakB²* background (experimental *ShakB²;Aβ42;Elav-Gal4* flies), showed a comparable mortality rates to *ShakB²* mutant flies (**Fig. R28-A**). Despite of previously data reported, the combination of Aβ42 toxic effects and the absence of electrical synapses in the brain reduced the median survival value to 8 days for these experimental flies, living 15% less than *ShakB²* flies, with 9.5 days (**Table R31**). In addition, life expectancy was significantly decreased (60%) compared to control flies (*Elav-Gal4*), with a median survival value of 20 days (**Fig. R28-B**, **Table R31**).

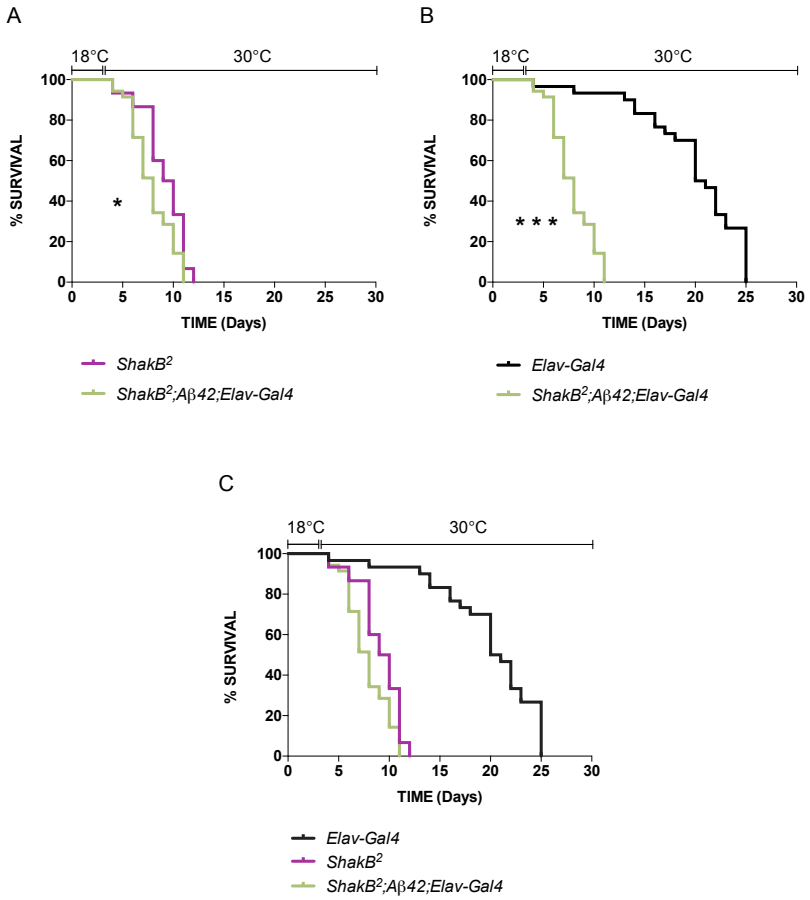

Fig. R28. Lifespan is reduced after Aβ42 expression in the whole brain in *ShakB²* background. (A-C) Survival curves for the following genotypes: *ShakB²;Aβ42;Elav-Gal4* genotype (in green) **(A,B,C)** compared to *ShakB²* genotype (in purple) **(A,C)** or compared to *Elav-Gal4* (control) (in black) **(B,C). (C)** Survival curve representing survival data in all genotypes. For each genotype, at least 3 experiments were performed with an average of 10 flies/experiment. Statistical analysis with Mantel-Cox Test is shown as *** $p < 0.001$ for comparisons to control (B) or * $p<0.05$ for comparisons to ShakB² (A).

Genotype	n	Median Survival (Days)	Maximum Survival (Days)	Mantel-Cox Test
***Elav-Gal4* vs Group**				
Elav-Gal4	30	20	25	
ShakB²;Aβ42;Elav-Gal4	35	8 **(60%)**	11 **(56%)**	*** p < 0.001
***ShakB²* vs Group**				
ShakB²	30	9.5	12	
ShakB²;Aβ42;Elav-Gal4	35	8 **(15%)**	11 **(8%)**	* p < 0.05

Table R31. **Statistical analysis of Survival assay.** Change in percentage is shown in brackets respect to *Elav-Gal4* (control) or *ShakB²* values.

Then, we carried out the Aβ42 overexpression in iLNs in a *ShakB²* background (**Fig. R29**). We detected a significant reduction of fly lifespan in these experimental *ShakB²;Aβ42;LN2-Gal4* flies, with a median survival value of 7 days, living 26% less than *ShakB²* flies (**Fig. R29-A**, **Table R32**). Further, we also found a strong decrease in experimental *ShakB²;Aβ42;LN2-Gal4* flies lifespan respect to control flies (*LN2-Gal4*), living 68% less than control, with a median survival rate to 22 days (**Fig. R29-B**, **Table R32**).

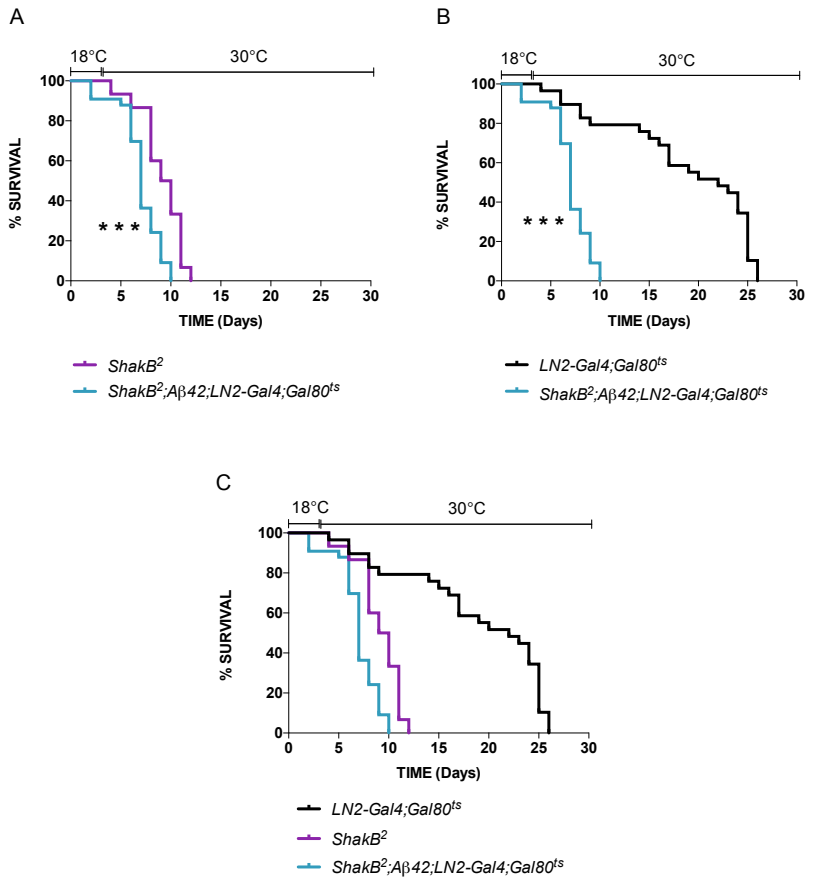

Fig. R29. Expression of Aβ42 in iLNs in absence of electrical synapses reduces the life expectancy. (A-C) Survival curves for the following genotypes: *ShakB²;Aβ42;LN2-Gal4;Gal80ᵗˢ* genotype (in blue) **(A,B,C)** compared to *ShakB²* genotype (in purple) **(A,C)** or compared to *LN2-Gal4;Gal80ᵗˢ* (control) (in black) **(B,C). (C)** Survival curve representing survival data in all genotypes. For each genotype, at least 3 experiments were performed with an average of 10 flies/experiment. Statistical analysis with Mantel-Cox Test is shown as *** $p < 0.001$ for comparisons to control (B) and for comparisons to *ShakB²* (A).

Genotype	n	Median Survival (Days)	Maximum Survival (Days)	Mantel-Cox Test
***LN2-Gal4;Gal80^{ts}* vs Group**				
LN2-Gal4;Gal80^{ts}	29	22	26	
ShakB^{2};Aβ42;LN2-Gal4	33	7 **(68%)**	10 **(61%)**	*** p < 0.001
***ShakB^{2}* vs Group**				
ShakB^{2}	30	9.5	12	
ShakB^{2};Aβ42;LN2-Gal4;Gal80^{ts}	33	7 **(26%)**	10 **(16%)**	*** p < 0.001

Table R32. **Statistical analysis of Survival assay.** Change in percentage is shown in brackets respect to *LN2-Gal4;Gal80^{ts}* (control) or *ShakB^{2}* values.

Next, the toxic effect of Aβ42 peptide expressed in 6-8 eLNs on lifespan was not statistically different compared to *ShakB^{2}* (**Fig. R30-A**, **Table R33**), probably due to the high number of deaths of experimental *ShakB^{2};Aβ42;krasavietz-Gal4;MBGal80* flies (abbreviated as *ShakB^{2};Aβ42;krasavietz-Gal4*) practically since the beginning of assay. Interestingly, these experimental flies had the same median survival rate (7 days) as experimental *ShakB^{2};Aβ42;LN2-Gal4* flies (**Table R33** and **Table R32**). In turn, experimental *ShakB^{2};Aβ42;krasavietz-Gal4* flies showed a significant 46% reduction in their lifespan respect to control flies (*krasavietz-Gal4*) (**Fig. R30-B**, **Table R33**).

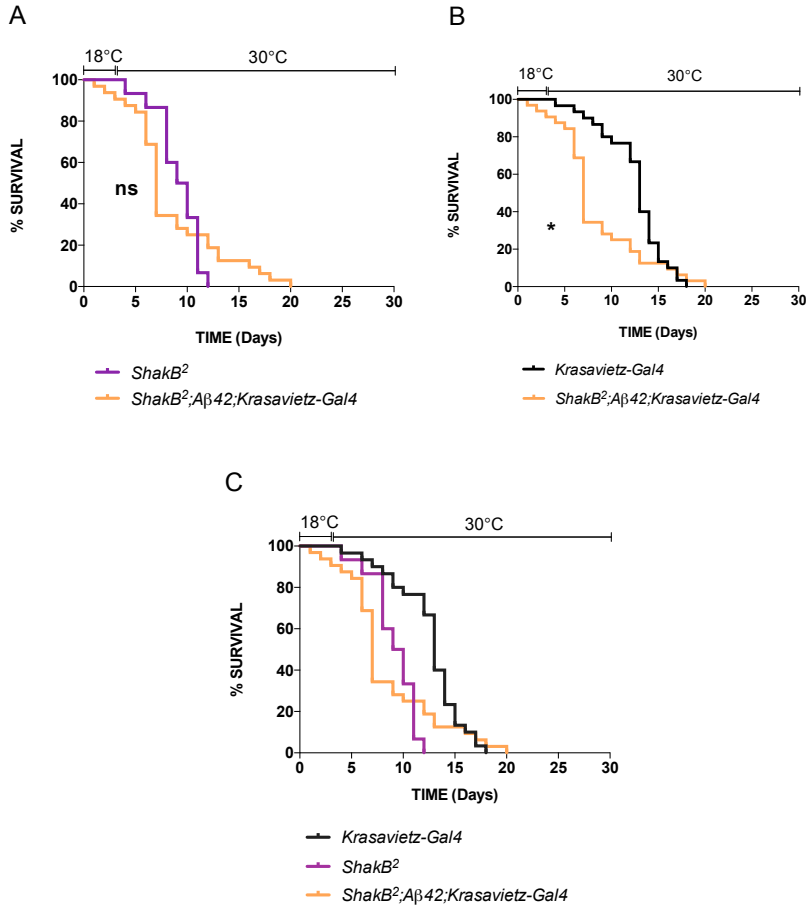

Fig. R30. Lifespan is not affected after expressing Aβ42 in eLNs in absence of electrical synapses. (A-C) Survival curves for the following genotypes: *ShakB²;Aβ42;krasavietz-Gal4* genotype (in orange) **(A,B,C)** compared to *ShakB²* genotype (in purple) **(A,C)** or compared to k*rasavietz-Gal4* (control) (in black) **(B,C). (C)** Survival curve representing survival data in all genotypes. For each genotype, at least 3 experiments were performed with an average of 10 flies/experiment. Statistical analysis with Mantel-Cox Test is shown as * $p < 0.05$ for comparisons to control (B) or ns for comparisons to *ShakB²* (A).

Genotype	n	Median Survival (Days)	Maximum Survival (Days)	Mantel-Cox Test
***krasavietz-Gal4* vs Group**				
krasavietz-Gal4	30	13	18	
ShakB²;Aβ42;krasavietz-Gal4	32	7 (46%)	20 (11%)	* p < 0.05
***ShakB²* vs Group**				
ShakB²	30	9.5	12	
ShakB²;Aβ42;krasavietz -Gal4	32	7 (26%)	20 (66%)	ns

Table R33. **Statistical analysis of Survival assay.** Change in percentage is shown in brackets respect to *krasavietz-Gal4* (control) or *ShakB²* values.

Finally, we compared the survival curves of all experimental fly groups (**Fig. R31**). Considering that all experimental genotypes have a *ShakB²* background, we observed that Aβ42-induced negative effect is remarkably similar in the three conditions under study, independently of Aβ42 expression in the whole brain or in a smaller subset of iLNs or eLNs. We did not find any significant differences among them (**Table R34**).

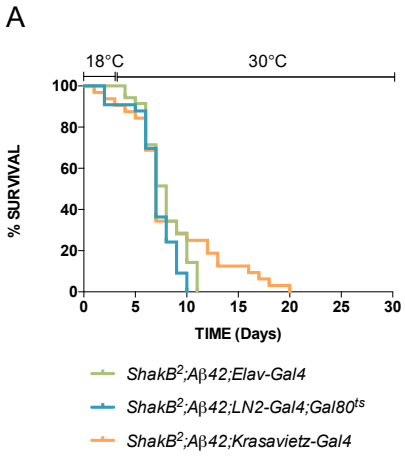

Fig. R31. Comparison of survival curves for experimental flies. Survival curves for the following genotypes: *ShakB²;Aβ42;Elav-Gal4* genotype (in green) and *ShakB²; Aβ42;LN2-Gal4;Gal80ts* genotype (in blue) compared to *ShakB²;Aβ42;krasavietz-Gal4* genotype (in orange). For each genotype, at least 3 experiments were performed with an average of 10 flies/experiment. Statistical analysis with Mantel-Cox Test.

Genotype	n	Median Survival (Days)	Maximum Survival (Days)	Mantel-Cox Test
***ShakB²;Aβ42;Elav-Gal4* vs Exp**				
ShakB²;Aβ42;Elav-Gal4	30	8	11	
ShakB²;Aβ42;LN2 -Gal4;Gal80ᵗˢ	33	7 **(12%)**	10 **(9%)**	ns
ShakB²; Aβ42;krasavietz-Gal4	32	7 **(12%)**	20 **(81%)**	ns
***ShakB²;Aβ42;krasavietz-Gal4* vs Exp**				
ShakB²;Aβ42;krasavietz -Gal4	32	7	20	
ShakB²;Aβ42;LN2 -Gal4;Gal80ᵗˢ	33	7	10 **(50%)**	ns

Table R34. **Statistical analysis of Survival assay.** Change in percentage is shown in brackets respect to *ShakB²;Aβ42;Elav-Gal4* or *ShakB²;Aβ42;krasavietz-Gal4* values.

Taken together, these data lead us to conclude that expression of an extremely toxic variant of human Aβ42 peptide in a *ShakB²* background dramatically affects the viability of flies, even when it is expressed in a reduced subset of olfactory LNs, being especially toxic to iLNs population.

3.5. Aβ42-overexpression in the whole brain and specific LNs increases aggravates ShakB²-dependent locomotor deficits

Locomotor activity impairment represents one of the most frequent affectations in patients suffering from neurodegenerative diseases as AD and PD (Iijima et al., 2004; Iijima et al., 2008; Feany & Bender, 2000). Conversely, locomotion is extremely impaired in *Drosophila* after human Aβ42 peptide expression in fly brain in an aged-dependent manner (Iijima et al., 2004; López-Arias et al., 2017; Doctoral Thesis Mercedes Arnés; Arnés et al., submitted). As previously mentioned, the absence of electrical synapses in *Drosophila* also produces locomotor defaults in *ShakB²* flies (Chapter 3.2). Hence, we wondered whether locomotion is also impaired after expressing human Aβ42 peptide in a *ShakB²* background.

We have analyzed the three experimental fly groups employed in survival assays to evaluate their locomotor activity in a climbing test. In all three experimental conditions, the statistical analysis showed that there is an interaction between genotype and time, indicating that locomotion is conditioned by both factors (**Table R35-R37**).

Our results indicated that the expression of Aβ42 in a context of no electrical synapses (*ShakB²* background) produced a reduction in climbing performance in all experimental fly groups (**Fig. R32-R34**). This negative effect in climbing performance depends on the temperature shift to 30°C. None of genotypes showed any sign of locomotor deficits at 18°C, reaching percentages around 80-90% similar to control flies (**Fig. R32-R34**). In fact, at the beginning of the assay, experimental *ShakB²;Aβ42;Elav-Gal4* flies reached even higher percentages than their respective control flies (*Elav-Gal4*) (**Fig. R32**). Remarkably, all experimental fly groups developed a better climbing activity than *ShakB²* mutants during all the assay, indicating that the presence

of Aβ42 in absence of electrical synapses does not seem to aggravate the locomotion phenotype (**Fig. R32-R34**).

However, when we examined the locomotion of experimental *ShakB²;Aβ42;Elav-Gal4* flies, the locomotor defaults started at day 5 of experiment, just one day after the temperature shift with percentages lower than 50% (**Fig. R32**). This fact could be correlated to the fast accumulation and aggregation of Aβ42 peptide since the beginning of assay.

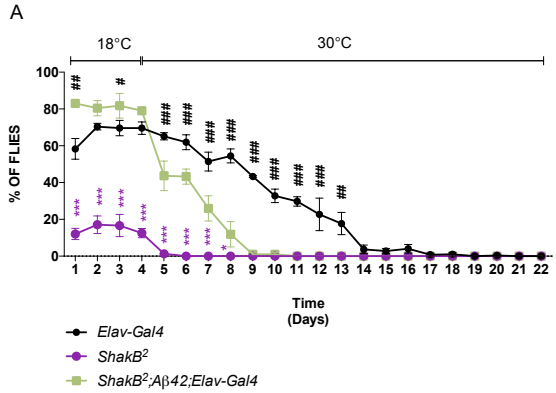

Fig. R32. Locomotion activity is aggravated by Aβ42 expression in whole brain. Climbing curves for the experimental genotypes: *ShakB²;Aβ42;Elav-Gal4* genotype (in green), *ShakB²* genotype (in purple) and *Elav-Gal4* genotype (control, in black). For each genotype, at least 3 experiments were performed with an average of 10 flies/experiment. Data expressed mean ± SEM and statistical analysis was performed by 2-way ANOVA test and corrected by Tukey´s test method where significant differences are shown as: *** $p < 0.001$ and * $p < 0.05$ for comparisons between *ShakB²;Aβ42;Elav-Gal4* and *ShakB²* and ### $p < 0.001$; ## $p < 0.01$ and # $p < 0.5$ for comparisons between *Elav-Gal4* and *ShakB²;Aβ42;Elav-Gal4*.

Genotype	Time	Genotype * Time
F (2,9) = 105.8 *** p < 0.001	F (21, 189) = 105.1 *** p < 0.001	F (42, 189) = 22.8 *** p < 0.001

Table R35. Statistical analysis Fig. R32.

Interestingly, this fast reduction in climbing performance was even more drastic when the expression of Aβ42 was directed to 30-37 iLNs (experimental *ShakB²;Aβ42;LN2-Gal4;Gal80ᵗˢ* flies) (**Fig. R33**). Here, due to the use of temperature-dependent Gal80 repressor factor, Aβ42 expression driven by *LN2-Gal4* started at day 4 of experiment, and locomotor deficits were only detected two days after the expression, at day 6, where percentages decrease lower than 50% compared to those obtained for control flies (*LN2-Gal4;Gal80ᵗˢ*) (**Fig. R33**).

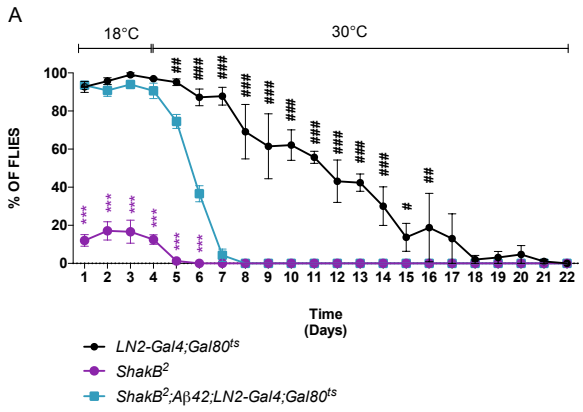

Fig. R33. Climbing is affected by Aβ42 expression in iLNs. Climbing curves for the experimental genotypes: *ShakB²;Aβ42;LN2-Gal4;Gal80ᵗˢ* genotype (in blue), *ShakB²* genotype (in purple) and *LN2-Gal4;Gal80ᵗˢ* genotype (control, in black). For each genotype, at least 3 experiments were performed with an average of 10 flies/experiment. Data expressed mean ± SEM and statistical analysis was performed by 2-way ANOVA test and corrected by Tukey´s test method where significant differences are shown as: *** $p < 0.001$ for comparisons between *ShakB²;Aβ42;LN2-Gal4;Gal80ᵗˢ* and *ShakB²* and ### $p < 0.001$; ## $p < 0.01$ and # $p < 0.5$ for comparisons between *LN2-Gal4;Gal80ᵗˢ* and *ShakB²;Aβ42;LN2-Gal4;Gal80ᵗˢ*.

Genotype	Time	Genotype * Time
F (2,8) = 72.38 **ns** p = 0.777	F (21, 168) = 163.9 *** p < 0.001	F (42, 168) = 42.55 *** p < 0.001

Table R36. Statistical analysis Fig. R33.

On the other hand, the appearance of locomotor defaults, with a proportion of flies exceeding the 4 cm line lower than 50%, was delayed until day 7 of experiment when Aβ42 expression was directed to a subset of 6-8 eLNs, the experimental *ShakB²;Aβ42;krasavietz-Gal4;MBGal80* flies (abbreviated as *ShakB²;Aβ42;krasavietz-Gal4*) whereas control flies (*krasavietz-Gal4*) maintained more in time their climbing activity (**Fig. R34**). In all experimental conditions, the percentage of flies that were not able to climb was progressively increasing as the flies aged.

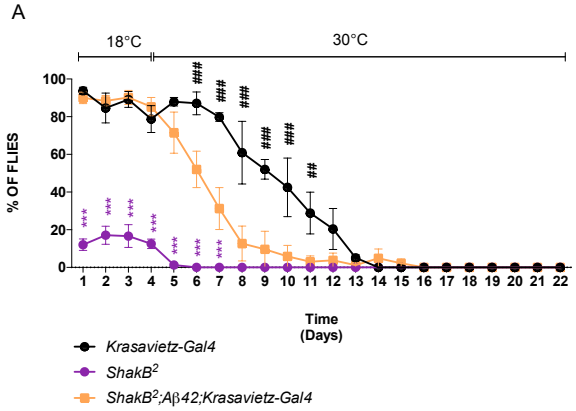

Fig. R34. Locomotion activity is aggravated by Aβ42 expression in eLNs. Climbing curves for the following genotypes: *ShakB²;Aβ42;krasavietz-Gal4* genotype (in orange), *ShakB²* genotype (in purple) and *krasavietz-Gal4* (control, in black). For each genotype, at least 3 experiments were performed with an average of 10 flies/experiment. Data expressed mean ± SEM and statistical analysis was performed by 2-way ANOVA test and corrected by Tukey´s test method where significant differences are shown as: *** $p < 0.001$ for comparisons between *ShakB²;Aβ42;krasavietz-Gal4* and *ShakB²* and ### $p < 0.001$ and ## $p < 0.01$ for comparisons between *krasavietz-Gal4* and *ShakB²;Aβ42;krasavietz-Gal4*.

Genotype	Time	Genotype * Time
F (2,10) = 19.37 *** p < 0.001	F (21, 210) = 64.64 *** p < 0.001	F (42, 210) = 13.20 *** p < 0.001

Table R37. Statistical analysis Fig. R34.

Finally, the comparison of climbing activity in all experimental groups showed an interaction between genotype and time, indicating that locomotion is affected by both factors (**Fig. R35**, **Table R38**). All experimental fly groups performed a similar climbing activity with significant differences at punctual days of assay. However, it is worth pointing that flies expressing Aβ42 in a subset of 6-8 eLNs exhibited a locomotion performance remarkably similar to those in flies in which the Aβ42 expression was directed to the whole brain (*ShakB²;Aβ42;Elav-Gal4* flies), with only significant difference at day 5 of experiment.

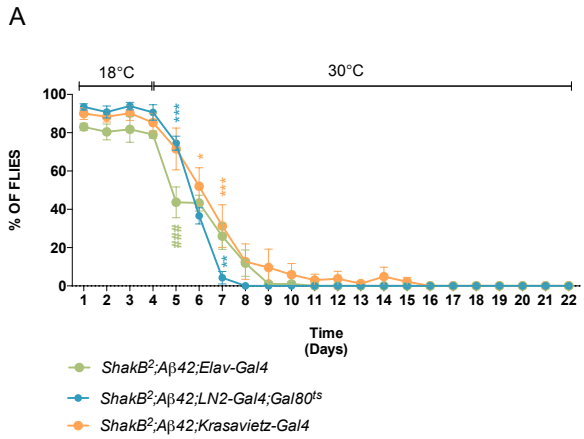

Fig. R35. Comparison of climbing performance for experimental flies. Climbing assay for the following genotypes: *ShakB²;Aß42;Elav-Gal4* genotype (in green) and *ShakB²;Aß42;LN2-Gal4;Gal80ᵗˢ* genotype (in blue) and *ShakB²;Aß42;krasavietz-Gal4* genotype (in orange). For each genotype, at least 3 experiments were performed with an average of 10 flies/experiment. Data expressed mean ± SEM and statistical analysis was performed by 2-way ANOVA test and corrected by Tukey´s test method where significant differences are shown as: *** $p < 0.001$, ** $p < 0.01$ and * $p < 0.05$ for comparisons between *ShakB²;Aß42;LN2-Gal4;Gal80ᵗˢ* versus *ShakB²;Aß42;Elav-Gal4* (asterisks in blue) and *ShakB²;Aß42;Elav-Gal4* (asterisks in orange). ### $p < 0.001$ for comparisons between *ShakB²;Aß42;Elav-Gal4 versus ShakB²;Aß42;krasavietz-Gal4*.

Genotype	Time	Genotype * Time
F (2,15) = 1.19 **ns** p = 0.0002	F (21, 315) = 255.2 *** p < 0.001	F (42, 315) = 2.12 *** p < 0.001

Table R38. Statistical analysis Fig. R35.

To conclude, our data highlight the toxic effects of Aβ42 in a deficient electrical synapse background. Interestingly, despite of the absence of statistical differences among experimental fly groups, the subset of iLNs within the *LN2-Gal4* domain and carrying the *Gal80ᵗˢ* repressor seems to be more sensitive to toxic effect of Aβ42 peptide than the other two experimental conditions. These differences in phenotype might be explained by the toxicity and time of accumulation of Aβ42 peptide. Indeed, the neuronal population type and number of neurons affected by amyloid peptide seems to be relevant to develop a normal climbing activity. Moreover, the temperature shift of our protocol could allow a faster peptide aggregation and accumulation, which would be impairing a normal locomotion.

CHAPTER 4:

Analysis of PI3K-dependent olfactory restoration after Aβ42-induced olfactory deficits

4.1. Aβ42 accumulation in olfactory neurons

4.2. PI3K yields to a restoration of Aβ42-induced olfactory deficits in a selective subset of iLNs

4.3. PI3K also restores the Aβ42-induced olfactory deficits in eLNs

Alzheimer´s disease is characterized by synapse loss and extensive neuronal death. In addition, an increasing number of scientific studies reveal the existence of olfactory dysfunctions at early stages of brain illnesses such as multiple sclerosis, Alzheimer´s diseases, Parkinson´s disease, schizophrenia and depression (Strous and Schoenfeld, 2012; William et al., 2009). Recent findings have also demonstrated the existence of Aβ42-dependent synaptotoxicity in *Drosophila* brain (López-Arias et al., 2017; Doctoral Thesis Mercedes Arnés, Arnés et al., submitted). Simultaneously, other scientific works have identified olfactory learning impairments in flies overexpressing Aβ42 peptide (Iijima et al., 2008). However, no data have been obtained characterizing Aβ42-dependent effects on odor processing and discrimination.

In this chapter, we set out to evaluate whether Aβ42 overexpression in selected subsets of LNs impairs olfaction in flies. We also wondered if the previously synaptogenic and neuroprotective effects of PI3K are able to restore a normal olfactory perception. To address this issue, we performed olfactory behavioral tests for EB odorant in a range of 10^{-3} to 10^{-1} (v/v) concentrations.

4.1. Aβ42 accumulation in olfactory neurons

Firstly, we set out to analyze the Aβ42 accumulation over time in olfactory neurons by immunohistochemistry, using the 6E10 antibody in 22 days-old fly brains of *LN2-Gal4* and *GH298-Gal4* lines. This antibody recognizes the N-terminus of the amyloid peptide, an epitope not found in the Amyloid Precursor (APLP) *Drosophila* protein. For this reason, we did not obtain any signal in control brains.

However, we did not find a clear 6E10 signal in the AL of any of these two lines, probably due to the few numbers of Aβ42-expressing olfactory neurons in both domains. In parallel, our collaborators at the Cajal Institute (Mercedes Arnés, Sergio Casas-Tintó in the laboratory of Alberto Ferrús) also examined 6E10 immunopositive puncta to detect Aβ42-overexpressing in the whole adult brain by using the *elav-Gal4* driver and the *UAS-Aβ42(2X)* construct. In this case, a clear 6E10 positive signal was detected in brains from Aβ42-overexpressing flies, a signal that was absent in control or PI3K-overexpressing brains (**Fig. R36**). Interestingly, this positive signal was increased in intensity and extent in PI3K+Aβ42 brains (Doctoral Thesis Mercedes Arnés, Arnés et al., submitted).

In conclusion, the use of the *UAS-Aβ42(2X)* construct and other different constructs expressing the amyloid peptide allows to accumulate the peptide over time in our own experiments in concordance with previously shown in several publications (López-Arias et al., 2017; Iijima et al., 2004).

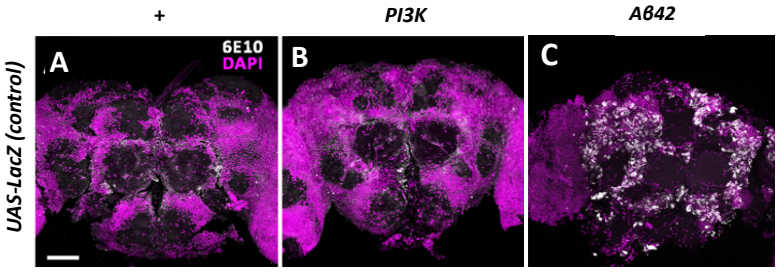

Fig. R36. Expression of PI3K increases Aβ42 levels. (A-C) Confocal image examples of Aβ (in white) immunostainings visualizing adult brains expressing: **(A)** UAS-LacZ (control), **(B)** *UAS-PI3K^{CAAX}*, **(C)** *UAS-Aβ42(2x)* with *elav-Gal4/Tub-Gal80^{ts}*. Scale bar 50 μm. Figure obtained from Arnés et al., submitted manuscript.

Additionally, we generated single-neuron mosaics by using of FRT/FLP recombination (Nellen et al., 1997) to determine the possible morphological effects of PI3K and Aβ42 overexpression in iLNs of the *GH298* domain (**Fig. R37**). As previously shown in larval motor neurons and large-field neurons of the ellipsoidal body (Martin-Pena et al., 2006) as well as in PNs and MB neurons (Acebes et al., 2012), PI3K overexpression also induces a thicker diameter and a profuse branching in the axonal projections of iLNs of *GH298* domain (**Fig. R37-B**) compared to control (**Fig. R37-A**). By contrast, a *GH298* neuron reduces its branching and exhibits axon morphological changes when Aβ42 is overexpressed (**Fig. R37-C**).

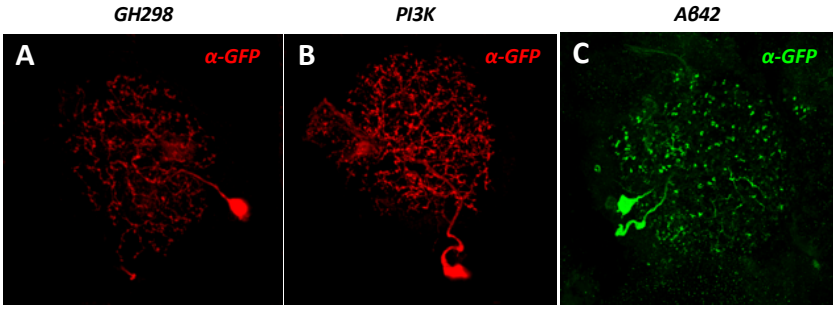

Fig. R37. Single iLN of *GH298* domain and the morphological effects of expressing PI3K and Aβ42. (A-C) Confocal image examples of a single inhibitory local interneuron of GH298 domain visualized by GFP expressing: **(A)** GH298-Gal4 (control), **(B)** *UAS-PI3K^{CAAX}*, **(C)** *UAS-Aβ42(2x)* with *GH298-Gal4*.

4.2. PI3K yields to a restoration of Aβ42-induced olfactory deficits in a selective subset of iLNs

To analyze olfactory dysfunctions elicited by Aβ42 peptide, we have overexpressed two copies of human amyloid Aβ42 peptide (*UAS-Aβ42(2x)* construct) within the *LN2-Gal4* driver (30-37 iLNs per AL). Additionally, we have overexpressed a constitutively active form of PI3K (*UAS-PI3K^{CAAX}* construct) in order to analyze the possible restoration of olfactory deficits.

In order to restrain the Aβ42 expression to adult stages where olfactory deficits could be more evident, we employed the Gal80^{ts} construct to activate the expression of selected genes only in adulthood in the *LN2* domain. All fly groups were grown at 18°C and maintained 6 days after hatching. At day 7 of experiment (7 ± 3 flies age), flies were shifted to 30°C for 15 days to allow the expression of Gal4. Olfactory behavioral test was performed at day 22 of experiment (22 ± 3 flies age) (see Material and Methods for details).

First, we analyzed the olfactory behavior of flies expressing PI3K within *LN2-Gal4* domain (*LN2-Gal4;Gal80^{ts};UAS-PI3K^{CAAX}* flies, shown in graphs as *PI3K*). These flies evoked repulsive responses fully coincident with those from control flies (*LN2-Gal4;Gal80^{ts}*) throughout the whole range of EB stimulus concentrations (**Fig.R38-A**, **Table R39**).

However, we detected olfactory changes in perception of EB for Aβ42-expressing flies (*LN2-Gal4;Gal80^{ts};UAS-Aβ42(2x*), shown in graphs as Aβ42*)* respect to control flies (*LN2-Gal4;Gal80^{ts}*) (**Fig. R38-B**). In fact, these flies yielded even more repulsive olfactory responses than control to the lowest and intermediate stimulus concentration (10^{-3} and 10^{-2}, respectively), albeit only statistically significant differences were found to 10^{-2} concentration. Indeed, it is worth pointing that the strength of repulsive reaction is still proportional to odorant stimulus, indicating that Aβ42 effects do not prevent the discrimination among different EB concentrations (**Table R39**).

In turn, the simultaneous combination of PI3K with Aβ42 peptide within LN2 domain (*LN2-Gal4;Gal80^{ts};UAS-PI3K^{CAAX};UAS-Aβ42(2x)* flies, shown in graphs as *PI3K+Aβ42*) also evoked repulsive responses (**Fig. R38-C**). We detected a significant difference to the intermediate concentration (10^{-2}) compared to control flies, although with a lower magnitude than observed in Aβ42-expressing flies (**Table R39**). Additionally, when we compared Aβ42 and *PI3K+Aβ42*-expressing flies, we did not find differences in their olfactory responses at any tested EB concentrations (**Fig. R38-D**, **Table R39**).

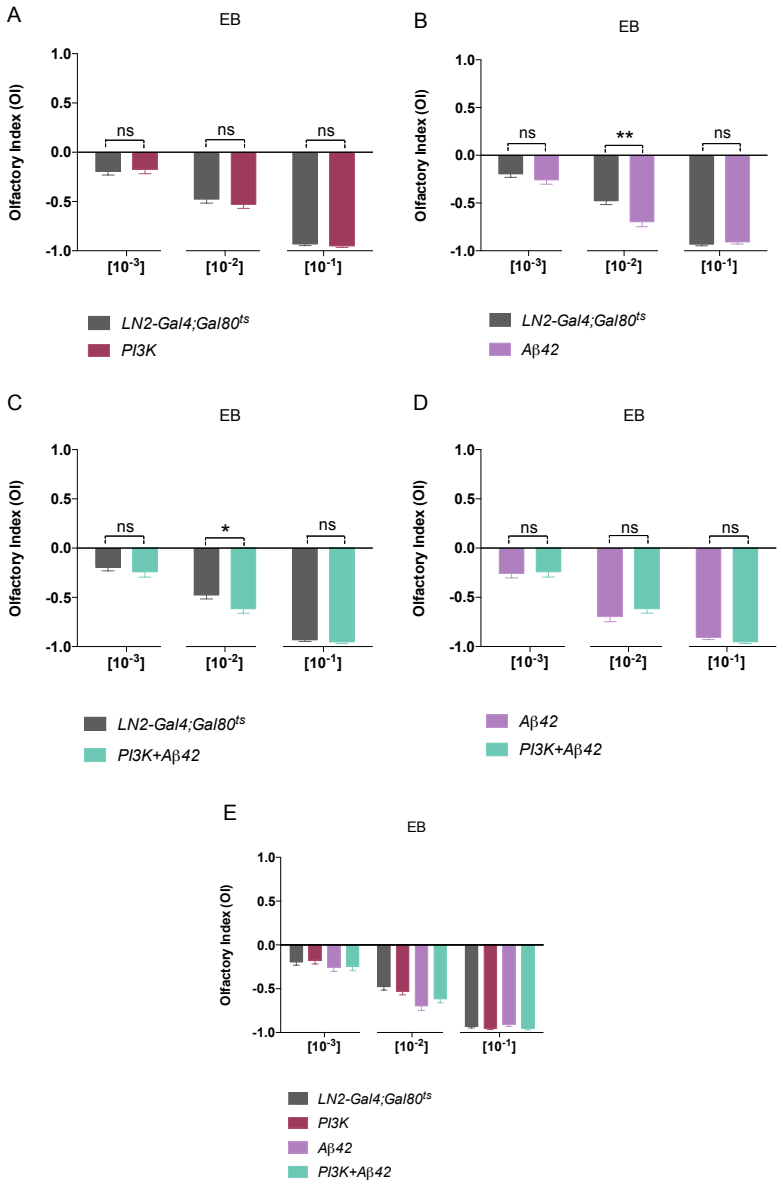

Fig. R38. Expression of PI3K in iLNs partially ameliorates olfactory dysfunctions induced by Aβ42. (A-E) Dose-response curves to EB for the following genotypes: **(A,E)** *PI3K* (in red); **(B,D,E)** *Aβ42* (in purple) and **(C,D,E)** *PI3K+Aβ42* (in blue) compared to *LN2-Gal4;Gal80^{ts}* (control, in grey) or compared to *Aβ42* genotype **(D),** expressing the corresponding UAS constructs with *LN2-Gal4;Gal80^{ts}*. **(E)** Dose-response curve representing olfactory perception for all genotypes. Each data point represents the average ± SEM. For all genotypes N=350-400 per data point. Statistical t-test results are shown as: ** $p < 0.01$ and * $p < 0.05$ or ns.

[EB]	Genotype	OI value	Statistical Analysis (*vs. control*)	(*vs. Aβ42*)
[10^{-3}]	*LN2-Gal4;Gal80^{ts} (control)*	-0.20 ± 0.04		
	PI3K	-0.17 ± 0.05	ns	
	Aβ42	-0.26 ± 0.05	ns	
	PI3K+Aβ42	-0.24 ± 0.05	ns	ns
[10^{-2}]	*LN2-Gal4;Gal80^{ts} (control)*	-0.48 ± 0.04		
	PI3K	-0.53 ± 0.04	ns	
	Aβ42	-0.70 ± 0.05	** p < 0.01	
	PI3K+Aβ42	-0.62 ± 0.05	* p < 0.05	ns
[10^{-1}]	*LN2-Gal4;Gal80^{ts} (control)*	-0.93 ± 0.02		
	PI3K	-0.95 ± 0.01	ns	
	Aβ42	-0.91 ± 0.02	ns	
	PI3K+Aβ42	-0.95 ± 0.02	ns	ns

Table R39. **Statistical analysis for dose-response curve for EB (Fig. R38).** Statistical Unpaired t-test with Welch´s correction is shown as: ** p < 0.01, * p < 0.05 and ns compared to control or compared to *Aβ42*.

Taken together, these data indicate that PI3K expression within *LN2-Gal4* domain partially ameliorates the negative effect elicited by Aβ42 peptide to 10^{-2} concentration of EB, yielding to less negative OI value than Aβ42 flies even though the restoration of normal olfactory responses is not produced. Plausibly, the strictly period of activation of *LN2-Gal4* driver during adulthood did not provide a sufficient PI3K expression to achieve a total rescue of Aβ42-induced olfactory dysfunctions in this particular subset of *LN2* iLNs (see Discussion).

We then decided to apply another strategy. Instead of restricting the overexpression to adulthood, we tried to express Aβ42 peptide during all fly development using another Gal4 driver. In this case, we have employed the *GH298-Gal4* line which is expressed in 30-32 iLNs per AL. Here, we have employed again the *UAS-Aβ42(2x)* construct and a different non-constitutively active form of PI3K, *UAS-PI3K* construct. In this experiment, all fly groups were grown at 25°C and maintained at the same temperature after hatching. Olfactory behavioral test to EB odorant was performed on flies with 5- to 7-days old (see Materials and Methods for details).

First, we detected that PI3K-expressing flies (*GH298-Gal4;UAS-PI3K* flies, shown in graphs as PI3K) yielded olfactory responses fully coincident to control flies (*GH298-Gal4*) throughout the whole range of concentrations (**Fig. R39-A**, **Table R40**).

Remarkably, we found drastic changes in olfactory perception to Aβ42-expressing flies (*GH298-Gal4;UAS-Aβ42(2x)* flies, shown in graph as Aβ42) respect to control individuals (**Fig. R39-B**). In fact, these Aβ42 flies evoked strongly olfactory responses toward repulsion to the lowest and

intermediate odorant stimulus concentration (10^{-3} and 10^{-2} respectively) compared to control flies (**Table R40**). Again, the strength of repulsive reactions of these Aβ42 flies was proportional to odorant stimulus, noting that Aβ42 expression in *GH298* domain do not prevent the discrimination among odorant-concentrations, at least for EB.

Then, we combined the expression of PI3K and Aβ42 peptide under the control of *GH298-Gal4* driver (*GH298-Gal4;UAS-PI3K;UAS-Aβ42(2x)* flies, shown in graph as PI3K+Aβ42). Interestingly, we detected that these experimental flies showed similar and non-statistically different, olfactory responses to control flies along the whole range of concentrations (**Fig. R39-C**, **Table R40**). By contrast, statistically significant differences were found to 10^{-3} and 10^{-2} concentrations when we compared Aβ42 and PI3K+Aβ42-expressing flies, pointing to restoration of normal olfactory values (**Fig. R39-D**, **Table R40**).

Conversely, we did not find any significant olfactory change to the highest concentration (10^{-1}) for any experimental fly groups (**Table R40**).

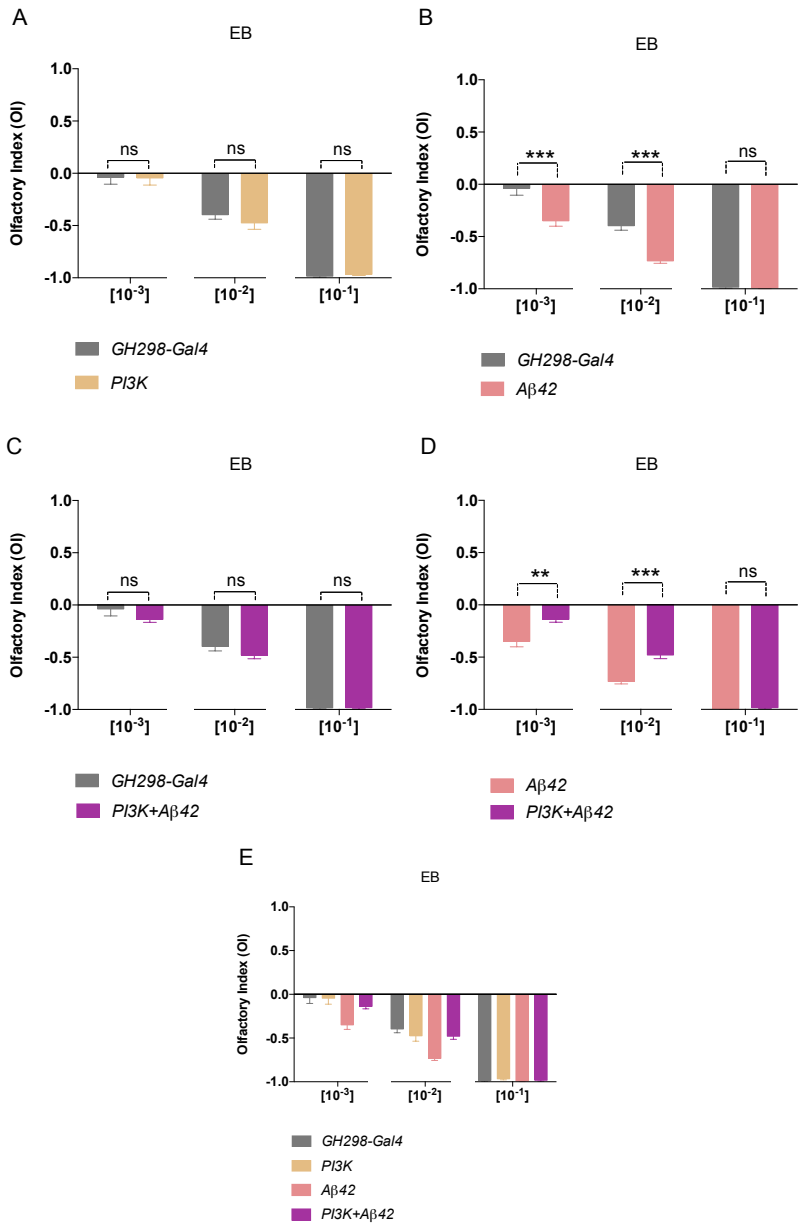

Fig. R39. Expression of PI3K in iLNs restores olfactory dysfunctions induced by Aβ42. (A-E) Dose-response curves to EB for the following genotypes: **(A,E)** *PI3K* (in yellow); **(B,D,E)** *Aβ42* (in pink) and **(C,D,E)** *PI3K+Aβ42* (in purple) compared to *GH298-Gal4* (control, in grey) or compared to *Aβ42* genotype **(D),** expressing the corresponding UAS constructs with *GH298-Gal4*. **(E)** Dose-response curve representing olfactory perception for all genotypes. Each data point represents the average ± SEM. For all genotypes N=350-400 per data point. Statistical t-test results are shown as: *** p < 0.001 and ** p < 0.01.

[EB]	Genotype	OI value	Statistical Analysis (*vs. control*)	Statistical Analysis (*vs. Aβ42*)
[10^{-3}]	*GH298-Gal4 (control)*	-0.04 ± 0.07		
	PI3K	-0.04 ± 0.07	ns	
	Aβ42	-0.35 ± 0.05	*** p < 0.001	
	PI3K+Aβ42	-0.14 ± 0.03	ns	** p < 0.01
[10^{-2}]	*GH298-Gal4 (control)*	-0.40 ± 0.07		
	PI3K	-0.47 ± 0.06	ns	
	Aβ42	-0.73 ± 0.02	*** p < 0.001	
	PI3K+Aβ42	-0.48 ± 0.04	ns	*** p < 0.001
[10^{-1}]	*GH298-Gal4 (control)*	-0.98 ± 0.01		
	PI3K	-0.97 ± 0.01	ns	
	Aβ42	-0.98 ± 0.01	ns	
	PI3K+Aβ42	-0.98 ± 0.01	ns	ns

Table R40. **Statistical analysis for dose-response curve for EB (Fig. R39).** Statistical unpaired t-test with Welch´s correction is shown as: *** p < 0.001, ** p < 0.001 and ns compared to control or compared to *Aβ42*.

Taken all together, our results indicate that a non-constitutively active PI3K expression in the subset of iLNs within *GH298-Gal4* domain is able to counteract the negative effect elicited by Aβ42, restoring normal olfactory values to 10^{-3} and 10^{-2} concentrations. Since both genetic drivers employed in these experiments are chronically active, we hypothesize that, at least for *LN2* and *GH298* subsets of iLNs, time accumulation is needed to generate a sufficient PI3K expression in order to achieve a complete rescue of Aβ42-elicited olfactory defaults (see Discussion).

4.2. PI3K also restores the Aβ42-induced olfactory deficits in eLNs

Then, we further investigated the Aβ42-induced effects in olfactory perception after overexpressing the amyloid peptide in a population of 6-8 eLNs (*krasavietz-Gal4* domain). Due to the fact that the expression pattern of *krasavietz* domain belongs to extrinsic mushroom body neurons, we made use of a *MBGal80* construct to silence these cells. As in chapter 3, we did not have the possibility to use the *THGal80* construct in *krasavietz* domain. In this experiment we also employed the *UAS-Aβ42(2x)* construct and the constitutively active form of PI3K by using *UAS-PI3K^{CAAX}* construct, to maintain the same protocol and conditions previously employed with *LN2-Gal4* driver.

All fly groups were grown at 18°C and maintained 6 days after hatching and shifted to 30°C for 15 days to allow the expression of Gal4. However, we detected a high degree of mortality in experimental flies after being shifted to 30°C, making this experiment inviable in these conditions. For this reason, we decided to modify our initial protocol maintaining the flies at 18°C and performing the behavioral test at day 22 of experiment (22 ± 3 flies age) (Material and Methods for details).

Again, we first analyzed the olfactory responses obtained from PI3K-expressing flies (*MBGal80;krasavietz-Gal4;UAS-PI3K^{CAAX}* flies, shown in graphs as PI3K) (**Fig. R40-A**). The olfactory responses to EB for these flies were slightly, albeit non-statistically significant, more repulsive than control flies (*krasavietz-Gal4*) (**Table R41**).

Then, we evaluated the olfactory perception of Aβ42-expressing flies (*MBGal80;krasavietz-Gal4;UAS-Aβ42(2x)* flies, shown in graphs as Aβ42) (**Fig. R40-B**). Interestingly, the olfactory responses shifted to repulsion to 10^{-3} and 10^{-2} stimulus concentration whereas the highest concentration (10^{-1}), yielded to less repulsive OI value. All olfactory responses were statistically significant compared to control flies (**Table R41**).

Finally, we simultaneously combined PI3K and Aβ42 in the *krasavietz* domain (*MBGal80; krasavietz-Gal4;UAS-PI3K^{CAAX};UAS-Aβ42(2x)* flies, shown in graphs as PI3K+Aβ42). These flies showed similar olfactory responses compared to control flies to the lowest and highest concentrations (10^{-3} and 10^{-1}, respectively) (**Fig. R40-C**). In addition, we also found a statistically significant change to 10^{-2} concentration showing an OI value more positive than control flies (**Fig. R40-C**, **Table R41**). The restoration of OI values detected in PI3K+Aβ42-expressing flies were highly statistically significant to 10^{-3} and 10^{-2} concentrations respect to Aβ42-expressing flies (**Fig. R40-D**, **Table R41**).

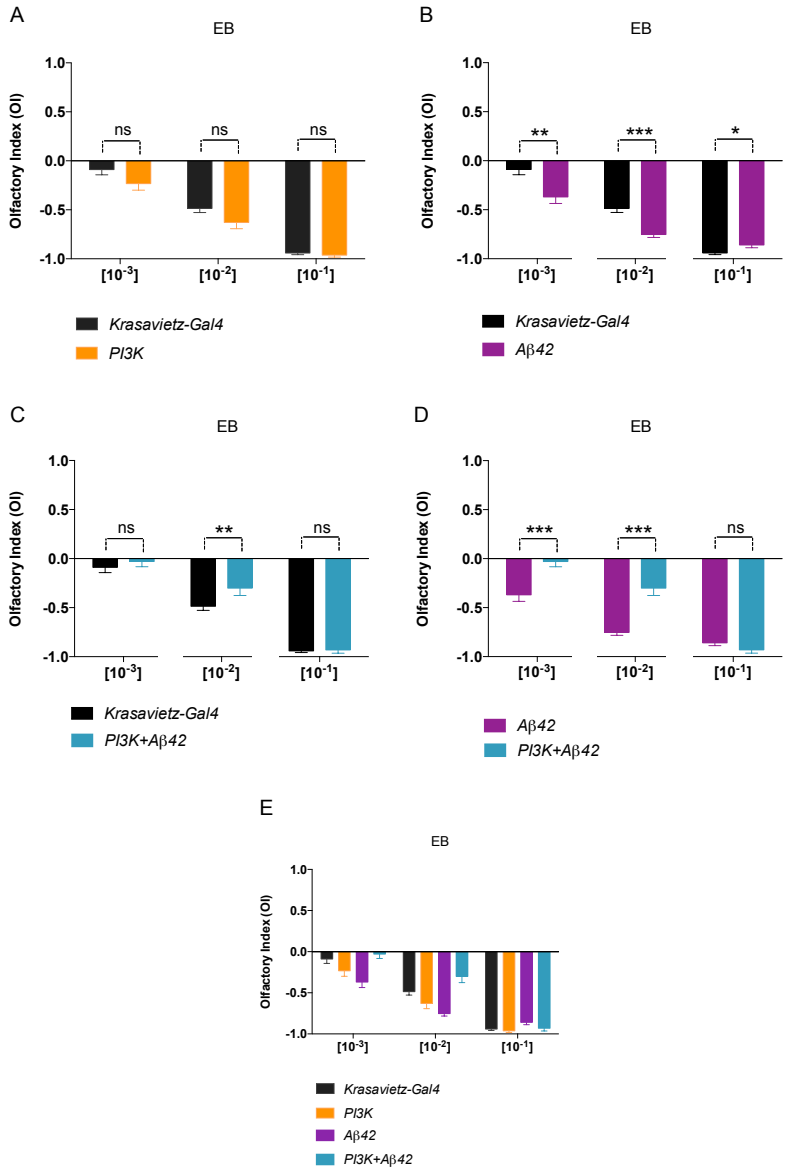

Fig. R40. Expression of PI3K in eLNs improves olfactory deficits induced by Aβ42. (A-E) Dose-response curves to EB for the following genotypes: **(A,E)** *PI3K* (in orange); **(B,D,E)** *Aβ42* (in purple) and **(C,D,E)** *PI3K+Aβ42* (in blue) compared to *krasavietz-Gal4* (control, in black) or compared to *Aβ42* genotype **(D),** expressing the corresponding UAS constructs with *krasavietz-Gal4*. **(E)** Dose-response curve representing olfactory perception for all genotypes. Each data point represents the average ± SEM. For all genotypes N=350-400 per data point. Statistical t-test results are shown as: *** $p < 0.001$, ** $p < 0.01$, * $p < 0.05$ or ns.

[EB]	Genotype	OI value	Statistical Analysis (*vs. control*)	Statistical Analysis (*vs. Aβ42*)
$[10^{-3}]$	*krasavietz-Gal4 (control)*	-0.09 ± 0.05		
	PI3K	-0.23 ± 0.07	ns	
	Aβ42	-0.37 ± 0.07	** p < 0.01	*** p < 0.001
	PI3K+Aβ42	-0.03 ± 0.05	ns	
$[10^{-2}]$	*krasavietz-Gal4 (control)*	-0.48 ± 0.04		
	PI3K	-0.63 ± 0.06	ns	
	Aβ42	-0.70 ± 0.03	*** p < 0.001	
	PI3K+Aβ42	-0.30 ± 0.07	** p < 0.01	*** p < 0.001
$[10^{-1}]$	*krasavietz-Gal4 (control)*	-0.94 ± 0.02		
	PI3K	-0.96 ± 0.02	ns	
	Aβ42	-0.86 ± 0.03	* p < 0.05	
	PI3K+Aβ42	-0.93 ± 0.03	ns	ns

Table R41. Statistical analysis for dose-response curve for EB (Fig. R40). Statistical unpaired t-test with Welch´s correction is shown as: *** p < 0.001; ** p < 0.01, * p < 0.05 and ns compared to control or compared to *Aβ42*.

Altogether, our results demonstrate that PI3K overexpression within *Krasavietz* domain is able to counteract the negative effect of Aβ42 in this subset of eLNs, restoring normal olfaction values, at least for two of the three tested concentrations.

From all these set of data, we can conclude that, intriguingly, the effects on fly olfactory perception elicited by Aβ42 overexpression in inhibitory and excitatory LNs are globally the same: changes towards more repulsive values. However, the resulting behavioral changes are still consistent with odorant concentration, meaning that the stimulus dosage-dependence of the behavioral responses is still preserved. We have also demonstrated that PI3K expression is able to restore normal olfactory responses counteracting Aβ42-elicited olfactory changes.

CHAPTER 5:

Analysis of PI3K-dependent synapse restoration on lifespan and locomotion in an Aβ42-induced neurodegeneration

5.1. PI3K expression in specific eLNs partially ameliorates Aβ42-induced lifespan reduction

5.2. Aβ42 does not affect locomotor activity when expressed in eLNs

5.3. Expression of PI3K in specific iLNs improves lifespan of Aβ42-expressing flies

5.4. Aβ42-induced locomotion defaults are improved by PI3K overexpression in iLNs

Dysfunctions in locomotion activity and reduction in life expectancy have been previously characterized in *Drosophila* models of Alzheimer´s disease (Iijima et al., 2004; Iijima et al., 2008; Casas-Tinto et al., 2011; López-Arias et al., 2017). Expression of an extremely toxic construct (*UAS- Aβ42(2x)*), consisting in two tandem copies of human amyloid Aβ42 peptide fused to a secretion signal, leads to stronger neurotoxic phenotypes and an extensive neuronal death (Casas-Tinto et al., 2011). Additionally, recent data have demonstrated the synaptogenic and neuroprotective actions of PI3K in an Aβ42-induced neurodegeneration model (using the same *UAS- Aβ42(2x)*) by restoring the negative effects on locomotion and lifespan (Doctoral Thesis, Mercedes Arnés, Arnés et al., submitted).

In this chapter, we have employed the same *UAS-Aβ42(2x)* construct to generate Aβ42-induced neurodegeneration in two particular subsets of olfactory LNs, using the *krasavietz-Gal4* and *LN2-Gal4* drivers. As pointed out in chapter 4, olfactory deficits were found after Aβ42 selectively expression in inhibitory and excitatory populations of LNs. However, we also detected a reduced viability and locomotion defaults in these flies. These unexpected findings encouraged us to explore in depth both phenotypes. Additionally, we also aimed to investigate whether PI3K expression in both populations of LNs could also ameliorate the life expectancy reduction and the locomotor deficits of these flies.

5.1. PI3K expression in specific eLNs partially ameliorates Aβ42-induced lifespan reduction

Firstly, we wondered whether fly viability is affected when Aβ42 expression is directed to the subset of 6-8 eLNs (*krasavietz-Gal4* domain). In this experiment, we also analyzed if fly lifespan could be ameliorated by PI3K overexpression. Again, we did not silence here the expression of TH-expressing neurons, but we made use of the *MBGal80* construct to silence the expression on MB neurons in this Gal4 line. Although this Gal80 factor is not temperature dependent, we also applied the temperature protocol shift employed in previous experiments (Chapters 2, 3 and 4) in order to maintain the same experimental conditions and allow data comparisons among all experimental fly groups.

Our results indicate that, flies overexpressing PI3K alone (*MBGal80;krasavietz-Gal4;UAS-PI3K^{CAAX}* flies, shown in graphs as PI3K) maintained the same extension in life expectancy as control flies (*krasavietz-Gal4*) (**Fig. R41-A**). In fact, the median survival rate for both fly groups were 13 days (**Table R42**). Conversely, Aβ42-expressing flies (*MBGal80;krasavietz-Gal4/UAS-Aβ42(2x)* flies, shown in graphs as Aβ42) showed a significant reduction in lifespan compared to control flies with a median survival rate to 11 days, living 15% less than control flies with 13 days (**Fig. R41-B**,**Table R42**).

However, the simultaneously expression of PI3K and Aβ42 within *Krasavietz-Gal4* domain (*MBGal80;krasavietz-Gal4;UAS-PI3K^{CAAX};UAS-Aβ42(2x)* flies, shown in graphs as PI3K+Aβ42) slightly improved the negative effects on lifespan elicited by Aβ42 (**Fig. R41-D**). Although PI3K+Aβ42 flies extended the median survival rate to 12 days (9% increase) compared to Aβ42-

expressing flies, this difference was not statistically significant (**Table R42**). However, this subtle improvement detected in PI3K+ Aβ42 flies did not reach the control median survival value, with 7% decrease in lifespan (**Fig. R41-C**, **Table R42**).

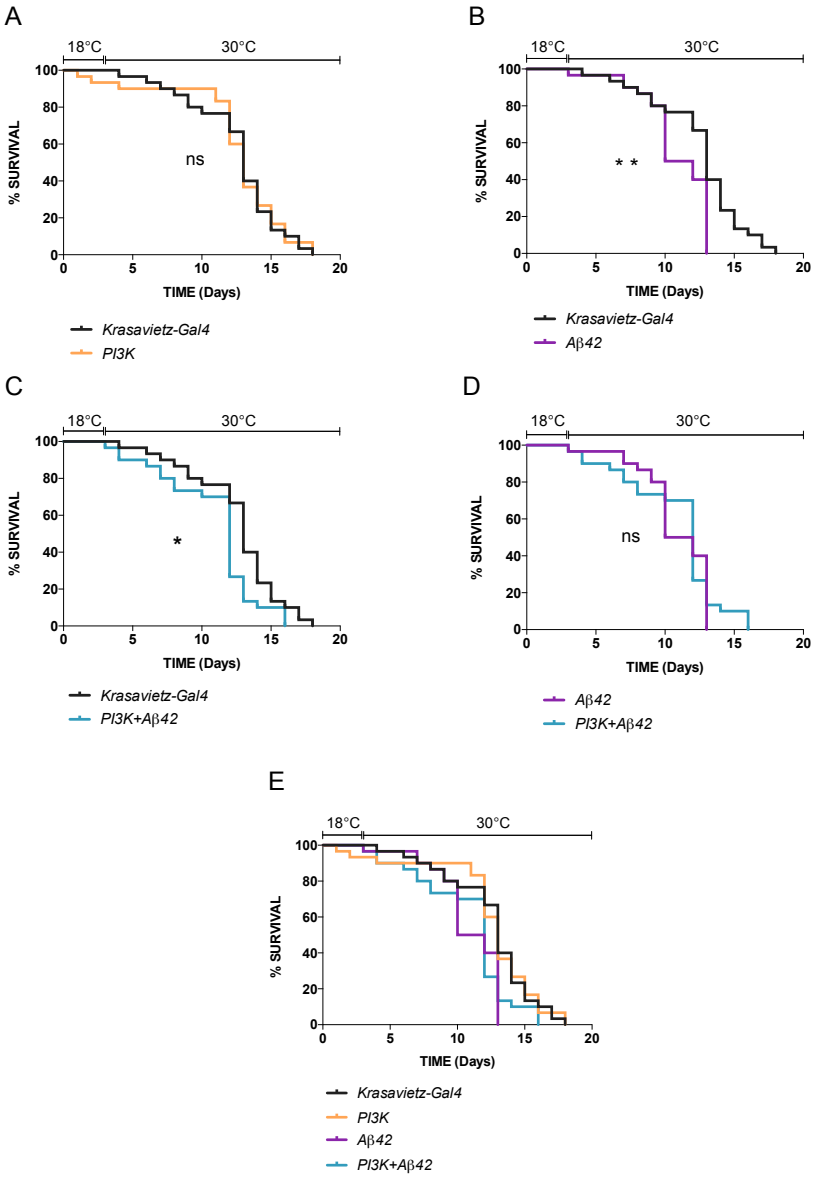

Fig. R41. PI3K expression in eLNs slightly improves Aβ42 flies lifespan. (A-E) Survival curves for the following genotypes: *PI3K* (in orange) **(A,E)**; *Aβ42* (in purple) **(B,D,E)**; and *PI3K+Aβ42* (in blue) **(C,D,E)** compared to *krasavietz-Gal4* (control, in black) **(A-C)** or compared to *Aβ42* genotype **(D)** expressing the corresponding UAS constructs with *krasavietz-Gal4*. **(E)** Survival curve representing survival data in all genotypes. Statistical analysis with Mantel-Cox Test is shown as ** $p < 0.01$; * $p < 0.05$; and ns for comparisons to control (A-C); and ns for comparisons to *Aβ42* genotype (D).

Genotype	n	Median Survival (Days)	Maximum Survival (Days)	Mantel-Cox Test
***krasavietz-Gal4* vs Groups**				
krasavietz-Gal4	30	13	18	
PI3K	30	13	18	ns
Aβ42	30	11 **(15%)**	13 **(27%)**	** p < 0.01
PI3K+Aβ42	30	12 **(7%)**	16 **(11%)**	* p < 0.05
Aβ42 vs PI3K+Aβ42				
Aβ42	30	11	13	
PI3K+Aβ42	30	12 (9%)	16 (23%)	ns

Table R42. **Statistical analysis of Survival assay.** Change in percentage is shown in brackets respect to *krasavietz-Gal4* (control) or *Aβ42* values.

Taken together, our results indicate that PI3K overexpression in a reduced subset of eLNs was not enough to totally ameliorate Aβ42-induced negative effects on lifespan, suggesting that probably the number of eLNs expressing PI3K were not enough to achieve a reversion of the negative effect elicited by the Aβ42 peptide.

5.2. Aβ42 does not affect locomotor activity when expressed in eLNs

In this experiment, we also wonder whether Aβ42-elicited locomotion deficits could be restored by PI3K expression within the *krasavietz* domain, employing the same flies previously mentioned. To address this issue, we examined the climbing performance of these flies evaluating the number of flies reaching the 4 cm threshold line in the given time (Materials and Methods for details).

Firstly, we observed that the affectations in climbing performance became evident as flies aged in all genotypes under study (**Fig. R42-E**). Secondly, we analyzed the locomotion of PI3K-expressing flies compared to control flies (*krasavietz-Gal4*) (**Fig. R42-A**). Statistical analysis showed that there is no interaction between genotype and time, indicating that PI3K-expressing flies behave similar to control (**Table R43**). In fact, the development of climbing activity is pretty similar between them, with percentages around 80% of flies climbing above the line at the beginning of assay. Surprisingly, whereas locomotion defaults in control and Aβ42-expressing flies (**Fig. R42-B**) appeared at day 9 of experiment with a proportion of flies lower than 50%, PI3K-expressing flies (**Fig. R42-A**) maintaining a normal climbing performance delaying these deficits until day 12 of experiment.

In turn, Aβ42-expressing flies did not either show changes in their locomotor activity when compared with control flies (**Fig. R42-B**). Indeed, their aggravation in climbing activity over time was similar to control flies and was not exacerbated by Aβ42-expression.

In concordance with this finding, when PI3K expression is combined to Aβ42 peptide, we did not detect major changes in climbing activity compared to control (**Fig. R42-C**) neither with Aβ42-expressing flies (**Fig. R42-D**).

The statistical analysis showed that there is no interaction between genotype and time when we compared Aβ42-expressing flies, PI3K+Aβ42-expressing flies and control flies (*krasavietz-Gal4*) (**Table R43**).

Taken together, these results indicated an absence of major Aβ42-induced climbing deficits when Aβ42 expression was selectively directed to the populations of eLNs driven by the *krasavietz* domain.

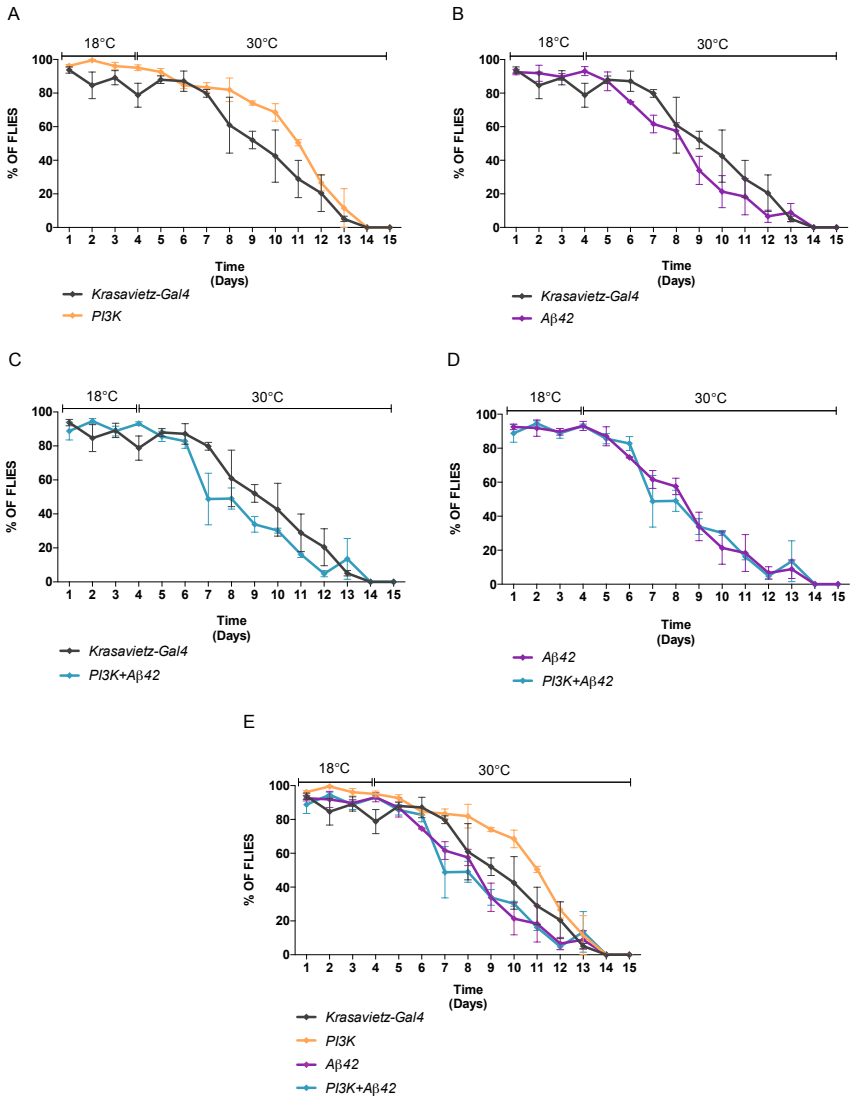

Fig. R42. PI3K expression develop the same locomotion activity as Aβ42 flies. (A-E) Climbing assay for the following genotypes: *PI3K* (in orange) **(A,E)**; *Aβ42* (in purple) **(B,D,E)**; and *PI3K+Aβ42* (in blue) **(C,D,E)** compared to *krasavietz-Gal4* (control, in black) **(A-C,E)** or compared to *Aβ42* genotype **(D)** expressing the corresponding UAS constructs with *krasavietz-Gal4*. **(E)** Climbing assay representing locomotion data in all genotypes. For each genotype, at least 3 experiments were performed with an average of 10 flies/experiment. Data expressed mean ± SEM and statistical analysis was performed by 2-way ANOVA test to analyze the effect of age, genotype and their interaction.

Fig.	Genotype	Time	Genotype * Time
R42-A	F (1,4) = 3.91 **ns** p = 0.119	F (14, 56) = 83.85 *** p < 0.001	F (14, 56) = 1.45 **ns** p = 0.160
*R42-B-D	F (2,6) = 0.66 **ns** p = 0.549	F (14, 84) = 126.30 *** p < 0.001	F (28, 84) = 1.48 **ns** p = 0.087

Table R43. **Statistical analysis Fig. R42-A and Fig. R42-B-D.** * 2-way ANOVA performed with data from *Aβ42, PI3K+ Aβ42* and control genotypes**.**

5.3. Expression of PI3K in specific iLNs improves lifespan of Aβ42-expressing flies

In this experiment, we have focused on *LN2-Gal4* domains carrying the *Gal80^{ts}* factor to drive Gal4 expression into 30-37 iLNs at later stages of development. First, we analyzed whether fly life expectancy is reduced after overexpressing Aβ42 peptide in this neuronal population. Second, we wondered whether lifespan reduction could be restored by PI3K expression.

Interestingly, PI3K-expressing flies (*LN2-Gal4;Gal80^{ts};UAS-PI3K^{CAAX}* flies, shown in graphs as PI3K) showed a reduction in lifespan compared to control flies (*LN2-Gal4;Gal80^{ts}*) (**Fig. R43-A**) with a median survival rate to 14.5 days, living 34% less than control flies with 22 days (**Table R44**).

In turn, the lifespan of Aβ42-expressing flies (*LN2-Gal4;Gal80^{ts};UAS-Aβ42(2x)* flies, shown in graph as Aβ42) is strongly reduced compared to control flies with a median survival value to 13 days, 40% shorter than control flies (**Fig. R43-B**, **Table R44**).

Finally, the combination of PI3K and Aβ42 (*LN2-Gal4;Gal80^{ts};UAS-PI3K^{CAAX};UAS-Aβ42(2x)* flies, shown in graph as PI3K+Aβ42) produces a statistically significant improvement of the negative lifespan effect elicited by Aβ42. These flies extended the medial survival rate to 16 days, living 18% more than Aβ42 flies (**Fig. R43-D**, **Table R44**). However, this extension in lifespan was still lower than control values (**Fig. R43-C**, **Table R44**).

Altogether, our results indicate that PI3K expression in this population of olfactory iLNs is able to ameliorate fly lifespan in presence of Aβ42 peptide.

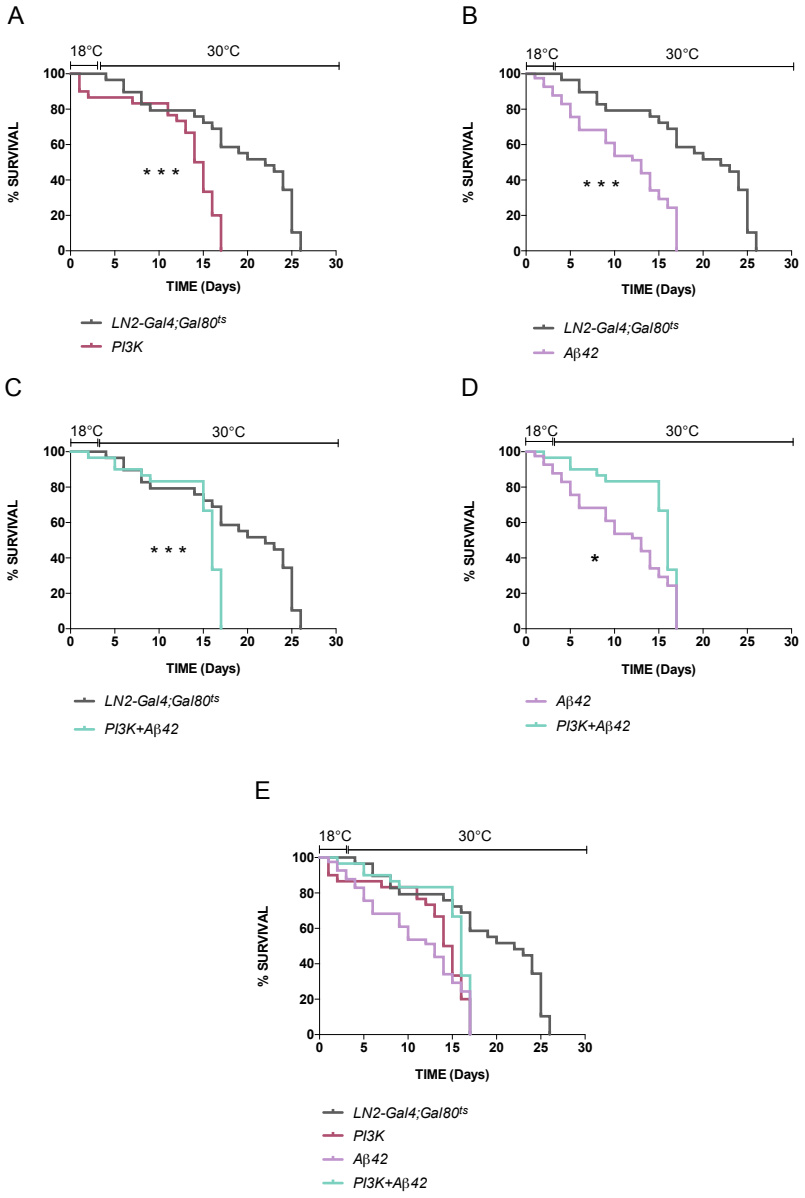

Fig. R43. PI3K expression in specific iLNs increases the lifespan of Aβ42 flies. (A-E) Survival curves for the following genotypes: *PI3K* (in red) **(A,E)**; *Aβ42* (in purple) **(B,D,E)**; and *PI3K+Aβ42* (in blue) **(C,D,E)** compared to *LN2-Gal4;Gal80^{ts}* (control, in grey) **(A-C,E)** or compared to *Aβ42* genotype **(D)** expressing the corresponding UAS constructs with *LN2-Gal4;Gal80^{ts}*. **(E)** Survival curve representing survival data in all genotypes. Statistical analysis with Mantel-Cox Test is shown as *** $p < 0.001$ for comparisons to control (A-C); and * $p < 0.05$ for comparisons to *Aβ42* genotype (D).

Genotype	n	Median Survival (Days)	Maximum Survival (Days)	Mantel-Cox Test
***LN2-Gal4;Gal80^{ts}* vs Groups**				
LN2-Gal4;Gal80^{ts}	29	22	26	
PI3K	30	14.5 **(34%)**	17 **(34%)**	*** p < 0.001
Aβ42	41	13 **(40%)**	17 **(34%)**	*** p < 0.001
PI3K+ Aβ42	30	16 **(27%)**	17 **(34%)**	*** p < 0.001
Aβ42 vs PI3K+ Aβ42				
Aβ42	41	13	17	
PI3K+ Aβ42	30	16 **(18%)**	17	* p < 0.05

Table R44. **Statistical analysis of Survival assay.** Change in percentage is shown in brackets respect to *LN2-Gal4;Gal80^{ts}* (control) or *Aβ42* values.

5.4. Aβ42-induced locomotion defaults are improved by PI3K overexpression in iLNs

This improvement in fly survival urged us to evaluate whether beneficial effects of PI3K could also ameliorate the locomotor defaults elicited by expressing Aβ42 peptide in this population of iLNs. To address this issue, we performed the climbing assay using the same flies previously mentioned and applying the Gal4 temperature-dependent activation protocol (Materials and Methods for details).

First, we analyzed the climbing performance of PI3K-expressing flies compared to control flies (*LN2-Gal4;Gal80^{ts}*). The statistical analysis showed that there is interaction between genotype and time (**Table R45**), indicating the effect of PI3K alone leads to improve the locomotor activity. In fact, during the first part of assay, these PI3K-expressing flies developed a climbing performance similar to control flies, with high percentages of flies reaching the line around 90% (**Fig. R44-A**). However, we detected differences in their climbing activity after 10 days. Locomotion deficits appeared at day 12 of experiment for control flies with percentages under 50% whereas locomotor activity is maintained in time until day 15 for PI3K-expressing flies where percentages decreased to 50%.

Noticeably, the expression of Aβ42 within *LN2* domain elicited a reduction in climbing performance at day 13 of experiment decreasing the percentage of flies that were able to climb under 50% (**Fig. R44-B**). This reduction was aggravated in time, just 3 days after, at day 16 of experiment, where the proportion of flies was lower than 20%.

Finally, the simultaneous combination of PI3K and Aβ42 peptide delayed the appearance of locomotor deficits until day 17 of experiment where the proportion of flies that climbed above the line decreased to 20% (**Fig. R44-D**). In fact, this recovery of climbing activity is observed from day 13 to day 16 in these flies PI3K+Aβ42-expressing flies compared to Aβ42-expressing flies. In addition, these flies maintained their climbing activity better than control flies, with significant differences from day 11 to day 16 (**Fig. R44-C**).

The statistical analysis also showed an interaction between genotype and time when we compared Aβ42-expressing flies, PI3K+Aβ42-expressing flies and control flies (*LN2-Gal4;Gal80^{ts}*). This interaction indicates that development of climbing activity is affected by genotype and time. In fact, as flies aged, climbing defaults became more evident in all genotypes under study (**Fig. R44-E**). However, negative effects of Aβ42 caused a fast reduction of locomotion which was aggravated in time. Interestingly, we only appreciated signs of locomotor defaults in PI3K+Aβ42 flies the latest days of assays probably due to the flies aged, pointing that expression of PI3K in this population of iLNs delays Aβ42-induced locomotion deficits and gets a recovery of climbing activity.

Taken together, our results indicate that synaptogenic effects of PI3K lead to restore the locomotion deficits elicited by Aβ42 expression within LN2-Gal4 domain.

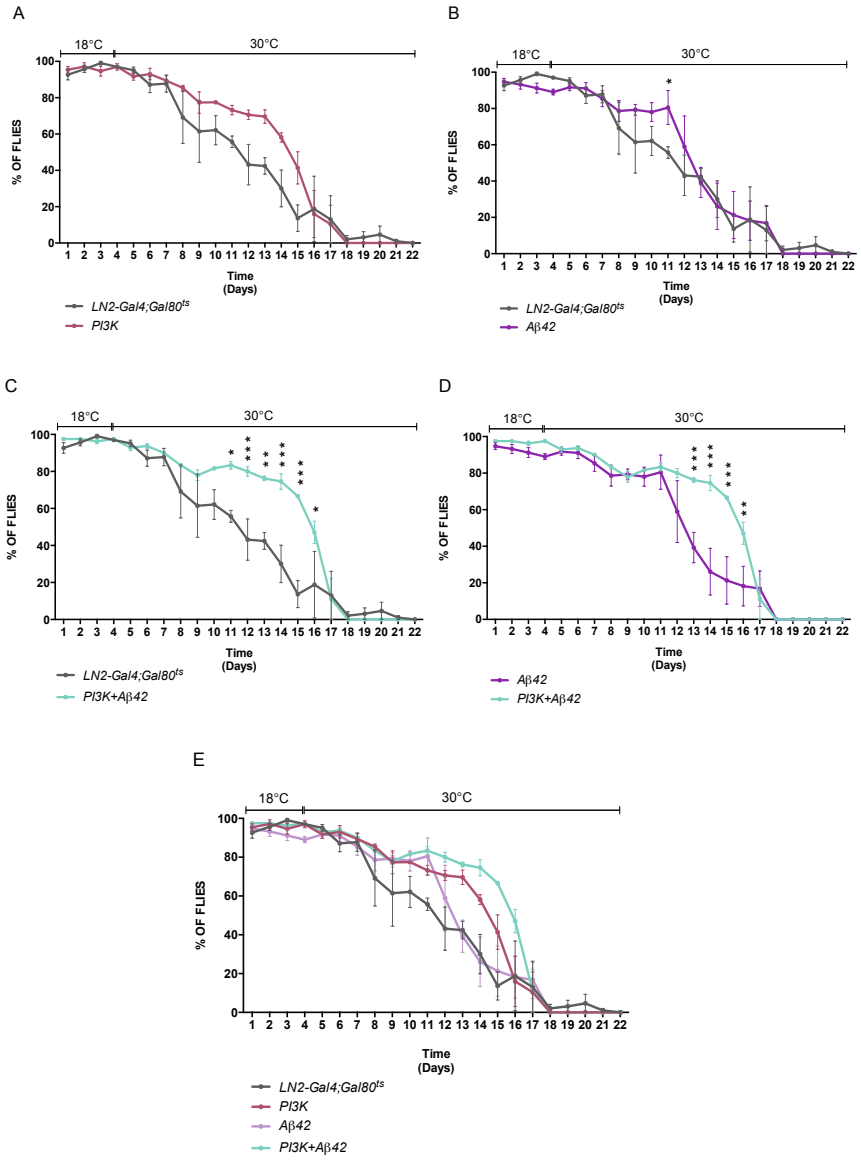

Fig. R44. Restoration of electrical synapses produces a recovery in locomotion. (A-D) Climbing assay for the following genotypes: *PI3K* (in red) **(A,E)**; *Aβ42* (in purple) **(B,D,E)**; and *PI3K+Aβ42* (in blue) **(C,D,E)** compared to *LN2-Gal4;Gal80^{ts}* (control, in grey) **(A-C)** or compared to *Aβ42* genotype **(D)** expressing the corresponding UAS constructs with *LN2-Gal4;Gal80^{ts}*. **(E)** Climbing assay representing locomotion data in all genotypes. For each genotype, at least 3 experiments were performed with an average of 10 flies/experiment. Data expressed mean ± SEM and statistical analysis was performed by 2-way ANOVA test and corrected by Tukey´s test method where significant differences are shown as: *** $p < 0.001$; ** $p < 0.01$ and * $p < 0.05$.

Fig.	Genotype	Time	Genotype * Time
Fig. R44-A	F (1,4) = 1.73 **ns** p = 0.258	F (21, 84) = 98.68 *** p < 0.001	F (21, 84) = 2.47 ** p < 0.01
*Fig. R44-B-D	F (2,7) = 2.31 **ns** p = 0.169	F (21, 47) = 139.10 *** p < 0.001	F (42, 147) = 3.38 *** p < 0.001

Table R45. **Statistical analysis Fig. R44-A and Fig. R44-B-D.*** 2-way ANOVA performed with data from *Aβ42, PI3K+ Aβ42* and control genotypes.

As a conclusion, previous data have reported the beneficial actions of PI3K allowing to get an improvement in life expectancy and locomotor activity in an Aβ42-induced neurodegeneration model (Doctoral Thesis, Mercedes Arnés, Arnés et al., submitted manuscript). Here we have demonstrated how the expression of Aβ42 peptide is able to decrease the fly viability and impair the locomotion when is expressed in smaller subsets of olfactory neurons. Indeed, we have also evidenced how the synaptogenic effects of PI3K are able to restore both phenotypes depending on the chemical nature of neuronal population and number of neurons in which PI3K is expressed.

DISCUSSION

1. Role of electrical synapses in olfactory processing of *Drosophila*

1.1. Loss of electrical synapses modifies olfactory processing
1.2. Selective electrical synapses attenuation alters olfactory responses
1.3. Selective electrical synapse restoration yields to normal olfactory response

2. Role of electrical synapses in life expectancy and locomotion

3. Role of electrical synapses in an Aβ42-induced neurodegeneration model

PI3K-dependent protective effect in an Aβ42-induced neurodegeneration model

5. Perspectives

This thesis aims to characterize the behavioural consequences of synapse restoration in a *Drosophila* model of neurodegeneration. First, we have characterized the role and function of electrical synapses in olfactory processing of *Drosophila melanogaster*. We have identified how the absence of electrical connections in the brain but also their selective attenuation in certain neuronal populations of olfactory pathway, yields to acute behavioral changes in terms of odorant specificity and discrimination among stimulus concentrations (Chapter 2). Besides, we have also demonstrated that their selective electrical synapse rescue is able to restore normal olfactory responses (Chapter 2). In addition to their role in olfaction, this thesis also evidences that electrical synapses play a relevant role in life expectancy and locomotion. Interestingly, the strong reduction in life expectancy and the severe deficits in locomotor activity observed in gap-junction defective *ShakB*^{2} mutants were completely restored when electrical synapses were recovered in the whole brain and in specific LN populations (Chapter 3). We have also described that electrical synapse loss in an Aβ42-induced neurodegeneration model strongly aggravates both phenotypes. This affectation occurs in the whole brain, but it is especially significant in a specific subset of olfactory iLNs, revealing an unexpected role of these neurons in normal locomotor activity (Chapter 3). Furthermore, this thesis has also demonstrated the beneficial PI3K-induced synaptogenic and neuroprotective effects on olfaction, life expectancy and locomotion, by increasing the number of chemical synapses in specific subsets of LNs (Chapters 4 and 5). Our data highlight that electrical and chemical synapses are both required to develop adequate olfactory and locomotor behaviors as well as to get a normal life expectancy.

1. Role of electrical synapses in olfactory processing of *Drosophila*

Electrical and chemical synapses are known to be present in many organisms and brain structures but the properties and distribution of these two types of transmission are still emerging (Pereda, 2014). Recently, many efforts have been directed on understanding the electrical signal propagation, their relevance in the neural circuit and how the interaction with chemical synapses is achieved.

1.1. Loss of electrical synapses modifies olfactory processing

Previous works developed by Wilson´s laboratory have revealed the presence of electrical connections among *Drosophila* central olfactory neurons (Wilson, 2013; Yaksi & Wilson, 2010). Using electrophysiological recordings, they have shown that gap-junction defective mutant *ShakB*^{2} had not electrical synapses among neuronal populations of olfactory pathway (iLNs-eLNs, eLNs-PNs and PNs-PNs), strongly suggesting that these *ShakB*^{2} mutants could be anosmic flies.

Here we show that, even though perception of *ShakB*^{2} individuals differs from normal flies, it is not totally abnormal. Indeed, these flies are able to develop a dose-response curve to all tested odorants, highlighting that the sense of smell is not affected in these flies and hence, demonstrating that they are not anosmic flies. By contrast, olfactory responses are consistent according to the functional group present in the odorant molecule, turning out to attraction from 10^{-3} and 10^{-2} concentration of 1-HEX (an alcohol) and shifting several of their responses to

repulsion to IAA (10^{-2} and 10^{-1}). In similar odorants sharing the ether functional group, IAA and EB, responses are also different: repulsion to IAA and attraction to 10^{-1} of EB, indicating that these mutant flies have not lost the sensitivity to differentiate between odorants with very similar chemical nature, at least for those tested here. Noticeably, the ability to discriminate among stimulus concentration remains unaltered at least for two of the three tested odorants (10^{-3} of IAA and 10^{-3} and 10^{-2} of EB). These results seem to point out the relevance of electrical component to discriminate high odorant concentrations, taking advantage of fast transmission offered by electrical synapses, probably to prevent the system from saturation. However, why the absence of total electrical synapses in the brain does not alter *ShakB*^{2} mutant responses to the lowest tested concentrations of these two odorants? In this point, further olfactory experiments at lower range of concentrations would be necessary to explore the possible role of electrical synapses to discriminate among odorant concentrations.

On the other hand, our results seem to indicate that the absence of electrical synapses does not seem to interfere with the development and functionality of chemical synapses. In fact, previous work from Wilson's group and later confirmed in our own laboratory has demonstrated that the integrity of chemical synapses in the AL (by nc82 staining) is essentially normal (**Fig. D1**). Most likely, the lack of electrical synapses might be compensated by the function of chemical synapses providing olfactory information and sending it to higher brain centers such as MB and LH. Even though there are remarkable changes in olfactory responses due to the absence of electrical synapses, neither recognition nor processing of odorants at central level in AL is abolished.

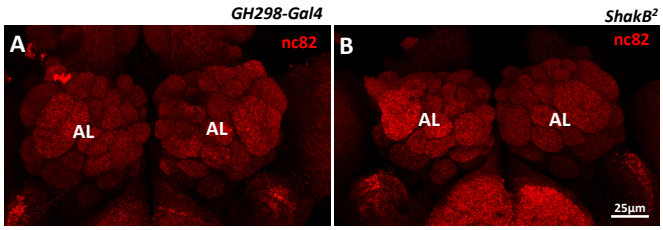

Fig. D1. Antennal lobe morphology. Each panel shows the structure of AL from GH298 domain (control) **(A)** and ShakB^{2} (mutant) **(B)** labeled with nc82 monoclonal antibody to reveal AL synapses**.** Scale bar A-B, (in B), 25 µm.

1.2. Selective electrical synapses attenuation alters olfactory responses

In this work, we also show that the genetic attenuation of electrical synapses prevents the development of normal odorant-specific and concentration-dependent responses. Interestingly, the attenuation in the whole brain yields to olfactory changes lower in magnitude than *ShakB*^{2} mutant responses. These results help us to reinforce the idea of the existence of a compensatory mechanism in which chemical synapses could supply the reduction of electrical connections to process the odor information and determine an olfactory response. According to a published evidence (Pereda, 2014), our data supports the close interaction between both synaptic types revealing that any disruptions among them can yield to behavioral alterations. In turn, selective

electrical synapse attenuation in specific subsets of olfactory PNs and LNs might be modifying two relevant processes within the AL: lateral excitation and lateral inhibition and consequently, affecting transference of olfactory information outside the AL.

Previous studies demonstrated that lateral excitation allows to detect subtle stimuli whereas overall level of inhibition in the AL increases with rising stimulus intensity (Olsen et al., 2010; Silbering & Galizia, 2007; Silbering et al., 2008). The attenuation of electrical connections in LNs would be affecting two types of connections: a) eLNs-iLNs in the same glomerulus, connected mainly by chemical connections and b) PNs-eLNs, with a strong electrical component, although eLNs also present a small chemical component (Yaksi & Wilson, 2010). In turn, electrical affectation in eLNs could generate an alteration of lateral inhibition mediated by iLNs, connected to PNs and eLNs through chemical synapses. Additionally, alterations in lateral inhibition might result in less sensitive PNs to their ORNs inputs, preventing PNs to encode changes in stimulus concentrations (Wilson, 2013). Plausibly, both lateral excitation and inhibition processes will be compromised by electrical synapse attenuation of LNs.

In addition to the involvement of lateral excitation and inhibition among LNs, the abovementioned attenuation of the strong electrical communication between PNs could explain the different odorant-specific and concentration-dependent olfactory responses to 1-HEX, IAA and EB detected in *MZ19* (12-15 PNs) and *GH146* (83-90 PNs) flies. Here, it would be also interesting to check further whether PNs from *MZ19* domain are included into PNs from *GH146* domain or if they belong to two separated subsets of PN populations. It is known that *MZ19* neurons project to DA1, VA1 and DC3 glomerulus (Berdnik et al., 2008; Jefferis, 2003). Due to the greater number of PNs from *GH146* domain, it is possible that some of these PNs project to the same glomeruli from those targeted by *MZ19* domain neurons (Wong et al., 2002). Our behavioral data have revealed striking differences in their responses to the same odorant, suggesting that they could belong to two separated populations. Besides PNs-PNs electrical synapses, there are also electrical connections between eLNs and PNs. For this reason, we cannot discard the possibility that olfactory differences observed in these PNs domains are caused by disturbances in eLNs olfactory processing. Indeed, a reduction in lateral excitation would be reducing the direct excitation of PNs and the indirect inhibition of iLNs (Yaksi & Wilson, 2010). This imbalance would be affecting the transfer of information to posterior brain areas and probably conditioning the fly behavioral response.

The coexistence of excitatory and inhibitory LNs in the same glomerulus has a joint functional role in the elaboration of olfactory perception and the maintenance of excitation and inhibition levels (Yaksi & Wilson, 2010). This could explain why, in our study, olfactory changes produced by attenuation in LNs are greater in magnitude than in PNs. We detected that independently of the subset of LNs attenuated (6-8 eLNs and 30-37 iLNs, *krasavietz* and *LN2* domain, respectively) the 1-HEX odorant leads to strong changes in perception whereas we found differences to the other tested odorants (IAA and EB). The electrical attenuation directed to iLNs only produces changes to 10^{-1} concentration to EB whereas IAA is perceived without alterations. By contrast, the attenuation in eLNs yields to changes to 10^{-3} and 10^{-2} to IAA and EB, respectively. Our data strongly indicate that olfactory changes depend on the neuronal population affected and the odorant concentration.

Additionally, we observed that both attenuated-flies have difficulties to discriminate odorant concentrations of 1-HEX and IAA. This could be related to the affectation of both phenomenon of lateral excitation and lateral inhibition. As a consequence, the communication to PNs is also altered which could be modifying the information transferred to LH to discriminate properly odorant concentrations. Notably, we did not observe olfactory changes to any EB concentration in neither of two subsets of LNs, despite of EB is chemically similar to IAA. This fact points the odorant-specificity of electrical connections.

Finally, even though eLNs-iLNs interaction is predominantly chemical, they are also interconnected by an electrical component (Yaksi & Wilson, 2010). Our results highlight the relevance of this electrical connection to detect odorant stimulus concentration, especially in the subset of eLNs. In this line, the electrical component of eLNs seems to be involved in coding olfactory information, corroborating previous study reporting that eLNs are crucial to lateral excitation, helping to maintain a state of basal activity within the AL (Yaksi & Wilson, 2010).

Further experiments will be necessary to explore in-depth the specific weight of one synapse type *versus* the other in the olfactory neuronal network. In example, previous studies have demonstrated that PI3K-dependent synaptic changes alter the excitation/inhibition ratio of chemical synapses within the AL leading to drastic modifications in olfactory perception and olfactory habituation (Acebes et al., 2011; Acebes et al., 2012). It will be worthy to design an experiment in which both electrical and chemical connections are altered. For instance, we propose to employ an increase (by PI3K expression) and a decrease of chemical synapses (by using a dominant negative form of PI3K) in a context of electrical synapse attenuation by interference RNA. This experiment, among others, might be of great help to continue deciphering the role of each synaptic type in olfactory processing.

1.3. Selective electrical synapse restoration yields to normal olfactory response

Previous work in Wilson´s laboratory, using an electrophysiological approach, has reported the restoration of lateral excitation phenomenon after restoring the electrical connections by *UAS-ShakingB*^{Neural} construct in *ShakB*^{2} mutants (Yaksi & Wilson, 2010). In this work, for the first time, we have found a restoration of normal olfactory responses after rescuing electrical synapses in the whole brain, but also in particular subsets of olfactory neurons.

This result points a more crucial than expected role of electrical synapses in *Drosophila* olfactory processing. Probably, this is also suggesting that a proper balance between electrical and chemical synapses is required to develop a normal response and once this balance is perturbed (attenuation of electrical synapses), the odorant codification in the AL is not adequate. These results highlight the closely interaction between both synaptic types (Pereda, 2014) and how any change trying to restore their relation is able to maintain, at least in this case, a normal olfactory behavior. On the other hand, it is noteworthy that, even in the case of electrical synapse restoration in the whole brain, we never elicited out of range responses, indicating the reliability of the restoration and the accuracy of the olfactory system.

However, with our set of data only available for EB odorant, we cannot assure that this rescue is a general trait for all odorant´s repertoire. For this reason, a more extended battery of odorants will be necessary to a further in-depth analysis of our findings.

2.Role of electrical synapses in life expectancy and locomotion

Electrical synapses are a typical feature of escape circuits in vertebrates and invertebrates. Innexins proteins form gap-junction structures in invertebrates, being *ShakB* innenxin the most thoroughly studied as a critical component of the giant fiber system (GFS) (Phelan et al., 2008; Phelan et al., 1996). Electrical synapses in GFS are establishing connections through chemical synapses with two types of neurons: peripherally synapses interneuron (PSI) and tergotrochanteral motor neuron (TTMn) (Tanouye & Wyman, 1980; Allen et al., 2006). Thus, the $ShakB^{2}$ mutation disrupts the electrical connections in the giant fiber escape pathway, optic lobe and auditory neurons from Johnston´s Organ (JO) in the antenna, producing a strongly affectation in visual escape behaviors and a defective flight (Lehnert et al., 2003; Curtin et al., 2002; Phelan et al., 1996; Sun & Wyman, 1996; Thomas & Wyman, 1984). In addition, there are also evidences that $ShakB^{2}$ can acts as a seizure suppressor in epilepsy (Song and Tanouye, 2006).

The lifespan and locomotor activity restoration were achieved for all our experimental conditions (*Elav-Gal4, LN2-Gal4* and *Krasavietz-Gal4*) by using the *UAS-*$ShakB^{neural}$ construct, demonstrating the relevance of electrical synapses in both features. A crucial finding of this work is that, we identified a subset of 30-37 iLNs eliciting the same degree of restoration than the one performed in the whole brain, even reaching climbing values and viability scores of healthy flies. Indeed, the number and nature of neuronal populations in which the electrical restoration has been produced seems to be relevant for the rescue of locomotion and life expectancy. It is also necessary to point out that we are able to generate these behavioral effects in a $ShakB^{2}$ background.

This unexpected role on locomotion from iLNs of the *LN2* domain prompted us to search for relationships between central and descending motor neurons. It is known that the control of rhythm generation, which is localized in ventral nerve cord (VNC) and the circuit that integrate sensory information and initiate movements, are anatomically separated (Hsu & Bhandawat, 2016). Both circuits are connected via a diverse population of descending neurons (DNs) which are originated in the brain, projecting to thoracic motor centers and maintaining or modulating locomotion and other behaviors (Hsu & Bhandawat, 2016).

Albeit the descending motor control remains poorly unknown in *Drosophila*, previous information obtained from different insects have pointed out the relevance of lateral accessory lobe (LAL) in locomotion, indicating that the descending pathway through LAL is likely to be common across insects. LAL is a neuropil highly associated with central complex (CX) that facilitates the communication between CX and motor centers (Namiki & Kanzaki, 2016). Besides, LAL has been proposed as a center to receive inputs from CX and select the activity of descending output (Wolff & Strausfeld, 2015). Several works have reported a diversity of responses in neurons innervating the LAL in different species such as: flight activity in locusts (Homberg,

1994), walking activity in crickets and moths (Kanzaki et al., 1994; Zorović & Hedwig, 2013) and driving backwards walking in flies (Bidaye et al., 2014). More future studies will be necessary to find out if these around 30-37 iLNs of the *LN2* domain could be involved in locomotion by involving connections to DNs via LAL, but our results might be also understood as a consequence of an interaction between these or other putative motor and descending neurons.

Our data also highlight, for the first time, an unexpected role of electrical connections on fly viability. Whereas *ShakB*^{2} flies showed a significant decrease in lifespan under our experimental procedures, we were able to elicit normal fly lifespan values after electrical restoration. Even though longevity is an extremely complex trait to evaluate (Highfill et al., 2016), our results may suggest that electrical connections could have a potential role on fly lifespan. This finding opens a new field of research that is, in this moment, out of the scope of this thesis. Future experiments during development and adulthood in *Drosophila* and other animal models (i.e. rodents) will be mandatory to assess the specific role of electrical connections in life expectancy.

3. Role of electrical synapses in an Aβ42-induced neurodegeneration model

AD neurotoxicity has been studied in several Aβ42-expressing *Drosophila* models. These models have been based on the fusion of different expression strategies and signal peptides resulting in different toxicity (Fernandez-Funez et al., 2015). In several studies, Aβ42-induced affectations were identified in *Drosophila* neurons indicating that the accumulation of pathogenic Aβ42 peptide produces dysfunctions in neuronal activity and degeneration (Iijima et al., 2004; Iijima et al., 2008; López-Arias et al., 2017; Doctoral Thesis Mercedes Arnés; Arnés et al., submitted). It is well known that one of the main hallmarks in AD is synapse loss and their correlation with cognitive decline. In multiple studies in *Drosophila*, some of neurodegenerative phenotypes have been characterized by locomotion and survival assays (Fernandez-Funez et al., 2015; Fang et al., 2012; Iijima et al., 2004; Iijima et al., 2008; López-Arias et al., 2017). For instance, expression of Aβ42 peptide in larval motor neurons reduces the neurotransmitter release in neuromuscular junction (NMJ) (Chiang et al., 2009). Other studies in adult flies revealed a progressive failure of transmission in the giant fiber system (GFS) induced by Aβ42 expression (Lin et al., 2014; Zhao et al., 2010) leading to a locomotor dysfunction. On the other hand, it is well known that *ShakB*^{2} mutation disrupts the electrical connections in GFS demonstrating severe behavioral deficits in locomotion (Phelan et al., 1996; Sun & Wyman, 1996; Krishnan et al., 1993). However, to date, little is known about the relevance of electrical synapses in AD and how they are affected by Aβ42 expression. Some studies using electroencephalography (EEG) have reported information about topography and neuronal connectivity, showing how Aβ42-induced neuronal loss reduced the brain functional connectivity and hence, it has an influence on EEG signal recordings (Jelic, 2005; Jelic & Kowalski, 2009). Here, for the first time, our data indicate that the lack of electrical synapses generates a strong detrimental effect on locomotion and a reduction of fly viability in an Aβ42-induced neurodegeneration model.

Moreover, in absence of electrical synapses, our results indicate that driving Aβ42 expression in a subset of iLNs has a greater affectation in longevity and locomotion than the Aβ42 expression in the whole brain. Indeed, GABAergic neurons seem to be more sensitive to Aβ and it could

inhibit the excitation circuit suppressing the synaptic transmission (Palop & Mucke, 2010). A reduction in GABAergic synaptic transmission may trigger to synapse loss and a disruption of cognitive functions (Kamenetz et al., 2003; Walsh et al., 2002).

Concerning excitatory neurons, Aβ42 has been involved in abnormal changes in excitatory neuronal circuits (Palop et al., 2007). Moreover, an Aβ42-dependent depression of excitatory cholinergic transmission results in cognitive deficits which have been observed in AD fly models (Fang et al., 2012). Being acetylcholine the main excitatory neurotransmitter in the fly CNS, we have tested the influence of Aβ42 in an excitatory circuit. Our data indicate that the selectively expression of Aβ42 peptide in a smaller subset of 6-8 eLNs, does not seem to affect either locomotion or lifespan even without having electrical synapses. This could be explained due to the reduced number of neurons that were affected by Aβ42 peptide. In this line, we would propose to extend our study to a larger population of eLNs in order to explore whether the behavioral effects would be worsening and/or similar to the other two experimental conditions.

In summary, the toxicity of Aβ42 probably depends on their accumulation at each synapse, the number of neurons and the vulnerability of each synaptic type. It is plausible that Aβ42 peptide affects in *Drosophila* excitatory and inhibitory synapses producing complex imbalances in circuit and network activity. More studies about electrical transmission and their relationship with Aβ42 would be necessary to determine the mechanisms by which locomotion and lifespan are notably affected.

4. PI3K-dependent protective effect in an Aβ42-induced neurodegeneration model

PI3K is a member of crucial signaling pathway with several physiological and developmental functions such as regulation of cell proliferation and metabolism, control of cellular remodeling and migration and synapse plasticity in neurons (Angel Acebes & Morales, 2012; Knafo & Esteban, 2012). Results gathered from several studies in *Drosophila* suggest that Aβ-induced synaptic deficit, cell loss, locomotor decline and a reduction in lifespan which may be caused by different mechanisms that could have requirements for PI3K signaling.

Additionally, synaptogenic actions of PI3K have been demonstrated in studies developed in *Drosophila*, increasing the number of functional synapses in larval motor neurons and adult brain PNs (Jordan-Alvarez et al., 2012; Martin-Pena et al., 2006). Posteriorly, studies in mice and human cells also corroborated this PI3K-dependent synaptogenic effect (Cuesto et al., 2011; Enriquez-Barreto et al., 2014). Recently, several studies have also shown the beneficial effects of PI3K on locomotion and life expectancy in fly models overexpressing Aβ42 in the whole brain (López-Arias et al., 2017; Doctoral Thesis, Mercedes Arnés, Arnés et al., submitted). On the other hand, there are increasing evidences indicating that olfactory deficits are among the first symptoms of neurodegenerative diseases and other disorders (Strous and Schoenfeld, 2006; William et al., 2009; Doty, 2009; Lees et al., 2009). In fact, olfactory learning defaults in flies expressing Aβ42 peptide in the whole brain (Iijima et al., 2004; Iijima et al., 2008) and in the structure of MBs (Martín-Peña et al., 2018), have been reported in the last years.

In most of the mentioned works, the analysis of behavioral defects has been studied in fly models overexpressing Aβ42 in the whole brain. For this reason, in this thesis, we focused our study on specific subsets of LNs to analyze whether the well-known beneficial PI3K effects are able to improve the Aβ42-elicited behavioral defects on olfaction, locomotion and lifespan.

Our results directly show olfactory dysfunctions induced by Aβ42 expression in both subsets of LNs albeit we found differences depending on the number of neurons and synapse type affected. The subset of 6-8 eLNs from *Krasavietz* domain seems to be more sensitive to Aβ42 expression than the subsets of iLNs from *LN2* and *GH298* domains. One previous work using an electrophysiological approach has reported that Aβ42 peptide produced a depression of cholinergic synaptic transmission in a population of PNs (Fang et al., 2012), which would be preventing a correct odorant information transference. This could suggest a potential link between cholinergic transmission in behavioral neural circuit and the neurotoxicity of Aβ42 peptide, affecting the normal odorant processing within the AL. By contrast, in the case of iLNs, we found that depending on the time accumulation of Aβ42 and PI3K expression, the restoration of normal olfactory values can be produced in both subsets of iLNs. A subtle improvement was just detected to 10^{-2} concentration in the subset of 30-37 iLNs from *LN2* domain whereas in the population of 30-32 iLNs from *GH298* domain, this recovery was achieved to 10^{-3} and 10^{-2} concentrations. These differences between both populations of iLNs could be related to the vulnerability of neurons against Aβ42 exposition (Palop & Mucke, 2010) or differences in the time of Aβ42 accumulation. Remarkably, our data also corroborate the neuroprotective effects of PI3K to recover the normal olfactory perception revealing that its beneficial actions are independently of the synaptic nature of the transmission.

On the other hand, it has been reported the negative consequences on locomotion induced by Aβ42 expression in whole brain and in motor neurons (Doctoral Thesis Mercedes Arnés; López-Arias et al., 2017; Iijima et al., 2004; Iijima et al., 2008). Our studies directed to the population of LNs provide further support to these findings. First, our data also correlates the negative effects of Aβ42 when is expressed in iLNs. Second, PI3K overexpression in this iLNs positively affected fly locomotion, being consistent with previous data reported in larvae (Martin-Pena et al., 2006) and in adult brain (Doctoral Thesis Mercedes Arnés, Arnés et al., submitted). Third, the simultaneously expression of PI3K and Aβ42 in the subset of iLNs elicits a partial recovery of locomotor activity that was also found when the simultaneously expression was directed to the whole brain (Doctoral Thesis Mercedes Arnés, Arnés et al., submitted). Again, our finding urged us to explore the plausible role of this iLNs to develop a normal locomotion. By contrast, neither the expression of Aβ42 nor PI3K in the subset of 6-8 eLNs had influence on locomotion. At this point, it is worth mentioning that, in this set of experiments, we cannot rule out the possible contribution of a few subset of dopaminergic neurons included in the expression pattern of *krasavietz* domain. Perhaps, their contribution might be helping to prevent the damage induced by Aβ42. On the other hand, these results lead us to consider two different aspects: the damage caused by Aβ42 in this particular subset is not enough to prevent a normal climbing activity or, the connection between this subset of eLNs from *krasavietz* domain and the population of descending neurons to control mobility is weak or even non-existent. More experiments in a large population of eLNs would be necessary to explore this effect.

Concerning the effect on lifespan, our data show that PI3K expression in iLNs delays the negative effects on fly viability elicited by Aβ42 producing a partial rescue. Interestingly, similar result was obtained in a recent study developed in whole fly brain (Doctoral Thesis Mercedes Arnés, Arnés et al., submitted). This finding points out the possible relevance of this iLNs on fly viability. Again, the combination of PI3K and Aβ42 in eLNs did not have any effect on survival. Due to the fact that longevity is a highly complex trait, which may be notably sensitive to unbalanced conditions, our finding could be correlated to a previous study indicating that fly lifespan is remarkably dependent on toxic amyloid peptide accumulation (López-Arias et al., 2017). In line with another study (Doctoral Thesis Mercedes Arnés, Arnés et al., submitted), our data corroborate that PI3K expression alone extends the lifespan in the case of iLNs, but not in a restricted group of eLNs. This could be explained by a difference in the levels of PI3K pathway activation. Our data are also consistent with the necessity to examine the PI3K effects at different levels in order to evaluate the behavioral consequences of therapeutic approaches.

Finally, we detected that toxicity of Aβ seems to affect population of LNs in a specific and differential manner by an unknown mechanism. Our data support the hypothesis that there are neuronal and non-neuronal cell types more susceptible than others to Aβ toxicity (Arnés et al., 2017; Arnés et al., submitted) which are translated to behavioral consequences.

In summary, using an Aβ42-induced neurodegeneration model in *Drosophila* we demonstrate *in vivo* that PI3K is able to counteract the Aβ42 toxic effects on behavior and lifespan. Our study shows that among the relevant cell types addressed in our study, iLNs play a relevant role in the restoration of Aβ42-induced negative behavioral effects on locomotion and life expectancy. Concerning olfaction, the time of expression of PI3K is relevant to get a total recovery of olfactory defaults elicited by Aβ42, albeit its beneficial effects are independent of nature of synaptic transmission. Furthermore, our results also support that PI3K can be potentially considered as a preventive factor to ameliorate the neurodegenerative features caused by AD.

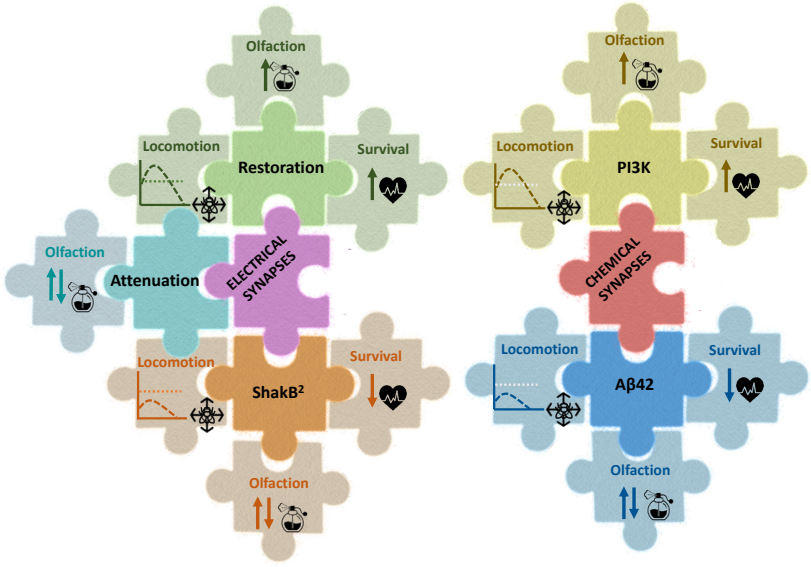

Fig. D2. Schematic cartoon summarizing the results described in this thesis.

5. Perspectives

The results of this work indicate the relevance of electrical synapses in olfactory processing, opening some questions for consideration: Are electrical connections necessary to discriminate among lower odorant concentrations? Why electrical connections seem to be more relevant to one olfactory neuronal population than others? What relationship exists between electrical synapses and odorant specificity?

Interestingly, the restoration of electrical synapses yields to normal olfactory responses, considering that any imbalance in the ratio of electrical and chemical synapses could be altering the transference and codification of olfactory information. In this line, we are convinced that modifying this balanced relationship could help to unravel the specific role of each synaptic type in the olfactory circuit. In the future, more experiments extending the battery of odorants could address this issue and decipher the specific weight of one synapse type *versus* the other.

Since electrical transmission seems to play an important role in locomotion and lifespan, especially in the subset of inhibitory LNs, there are new questions unanswered: what possible mechanisms could be involved between local interneurons and locomotion? Hence, further experiments exploring the possible connections between inhibitory LNs and motor neurons could asses the specific role of electrical connections in locomotion.

It is worth considering that the lack of electrical synapses and the affectation of chemical synapses by Aβ42 expression, strongly reduce the fly activity and lifespan. Noticeably, the population of inhibitory LNs seems to be more sensitive to Aβ42 peptide than excitatory LNs. Here we ask, how could Aβ42-induced toxicity act on electrical synapses? Under which underlying mechanisms? Our findings demonstrate the beneficial actions of PI3K in a neurodegeneration model of AD. Independently of the nature of neuronal population studied, PI3K expression is able to ameliorate the negative behavioral consequences elicited by Aβ42 expression. However, time of expression of PI3K seems to be relevant to achieve a greater degree of recovery on olfaction, locomotion and lifespan.

In conclusion, due to the close interaction between electrical and chemical synapses, a balanced ratio between both synaptic transmission types is crucial to produce an appropriate information transference. Due to the positive actions of PI3K, their beneficial effects will be also analyzed in other pathological animal models in our laboratory to ameliorate the detrimental behavioral consequences and reduced life expectancy caused by neurodegenerative diseases.

CONCLUSIONS

1. Total absence of electrical synapses does not alter odorant detection, smell processing and odorant discrimination ability.

2. Selective attenuation of electrical connections induces changes in olfactory perception depending on the number of electrical connections attenuated, odorant chemical nature and concentration.

3. Restoration of electrical synapses in the whole fly brain and in selected subsets of LNs leads to a lifespan recovery and preserves a normal climbing activity.

4. Aβ42-expression in the whole brain and in specific population of LNs drastically reduces the viability of flies and aggravates *ShakB*^{2}-dependent locomotor defaults.

5. Aβ42-induced olfactory deficits are restored by PI3K expression in selective subsets of inhibitory and excitatory LNs.

6. PI3K expression in specific subsets of inhibitory and excitatory LNs yields to get a partial lifespan rescue of Aβ42 flies.

7. Aβ42-induced climbing reduction is ameliorated by PI3K expression in inhibitory LNs.

CONCLUSIONES

1. La ausencia total de sinapsis eléctricas no impide la detección de olores, su procesamiento a nivel central, ni la capacidad para discriminar entre ellos.

2. La atenuación selectiva de sinapsis eléctricas provoca cambios en la percepción olfativa dependiendo del número de conexiones eléctricas atenuadas, la naturaleza química del olor y su concentración.

3. La recuperación de sinapsis eléctricas en todo el cerebro y en conjuntos específicos de interneuronas locales, conduce a una recuperación de la esperanza de vida y al mantenimiento de una actividad locomotora normal.

4. La expresión de Aβ42 en todo el cerebro y en poblaciones específicas de interneuronas locales en un fondo genético *ShakB*^{2}, reduce de forma drástica la viabilidad de las moscas y agrava los déficits locomotores.

5. Los déficits olfativos causados por el péptido Aβ42, son restaurados tras la expresión de PI3K en poblaciones específicas de interneuronas locales inhibitorias y excitatorias.

6. La expresión de PI3K en poblaciones específicas de interneuronas locales, inhibitorias y excitatorias, conduce a un rescate parcial de la esperanza de vida en las moscas que expresan Aβ42.

7. La reducción en la actividad locomotora provocada por la expresión del péptido Aβ42 se ve mejorada tras la expresión de PI3K en un conjunto de interneuronas locales inhibitorias.

REFERENCES

Acebes, A., Martin-Pena, A., Chevalier, V., & Ferrus, A. (2011). Synapse Loss in Olfactory Local Interneurons Modifies Perception. *Journal of Neuroscience*, *31*(8), 2734–2745.

Acebes, A, & Ferrús, A. (2001). Increasing the number of synapses modifies olfactory perception in Drosophila. *The Journal of Neuroscience : The Official Journal of the Society for Neuroscience*, *21*(16), 6264–6273.

Acebes, Angel, Devaud, J.-M., Arnés, M., & Ferrús, A. (2012). Central adaptation to odorants depends on PI3K levels in local interneurons of the antennal lobe. *The Journal of Neuroscience : The Official Journal of the Society for Neuroscience*, *32*(2), 417–422.

Acebes, Angel, & Morales, M. (2012). At a PI3K crossroads: Lessons from flies and rodents. *Reviews in the Neurosciences*, *23*(1), 29–37.

Aging, Alzheimer's Disease, and Hearing Impairment: Highlighting Relevant Issues and Calling for Additional Research." *American Journal of Audiology*, 16(1), pp. 2–3

Arnés, M., Casas-Tintó, S., Malmendal, A., & Ferrús, A. (2017). Amyloid β42 peptide is toxic to non-neural cells in Drosophila yielding a characteristic metabolite profile and the effect can be suppressed by PI3K. *Biology Open*, *6*(11), 1664–1671.

Arumugam, H., Liu, X., Colombo, P. J., Corriveau, R. A., & Belousov, A. B. (2005). NMDA receptors regulate developmental gap junction uncoupling via CREB signaling. *Nature Neuroscience*, *8*(12), 1720–1726.

Attems, J., & Jellinger, K. A. (2006). Hippocampal sclerosis in Alzheimer disease and other dementias. *Neurology*, 66(5), 775–775.

Baird, D. H., Schalet, A. P., & Wyman, R. J. (1990). The Passover locus in Drosophila melanogaster: complex complementation and different effects on the giant fiber neural pathway. *Genetics*, *126*(4), 1045–1059.

Baker, R., & Llinás, R. (1971). Electrotonic coupling between neurones in the rat mesencephalic nucleus. *The Journal of Physiology*, *212*(1), 45–63.

Bekinschtein, P., Katche, C., Slipczuk, L. N., Igaz, L. M., Cammarota, M., Izquierdo, I., & Medina, J. H. (2007). mTOR signaling in the hippocampus is necessary for memory formation. *Neurobiology of Learning and Memory*, *87*(2), 303–307.

Belousov, A. B., & Fontes, J. D. (2013). Neuronal gap junctions: making and breaking connections during development and injury. *Trends in Neurosciences*, *36*(4), 227–236.

Berdnik, D. (2006). Wiring Stability of the Adult Drosophila Olfactory Circuit after Lesion. *Journal of Neuroscience*, *26*(13), 3367–3376.

Berdnik, Daniela, Fan, A. P., Potter, C. J., & Luo, L. (2008). MicroRNA Processing Pathway Regulates Olfactory Neuron Morphogenesis. *Current Biology*, *18*(22), 1754–1759.

Bhandawat, V., Olsen, S. R., Gouwens, N. W., Schlief, M. L., & Wilson, R. I. (2007). Sensory processing in the Drosophila antennal lobe increases reliability and separability of ensemble odor representations. *Nature Neuroscience*, *10*(11), 1474–1482.

Bidaye SS, Machacek C, Wu Y, Dickson BJ (2014) Neuronal control of Drosophila walking direction. *Science* 344:97–101.

Bittman, K., Owens, D. F., Kriegstein, A. R., & LoTurco, J. J. (1997). Cell coupling and uncoupling in the ventricular zone of developing neocortex. *The Journal of Neuroscience : The Official Journal of the Society for Neuroscience*, *17*(18), 7037–7044.

Blagburn, J. M., Alexopoulos, H., Davies, J. A., & Bacon, J. P. (1999). *Null Mutation in*. *458*(June 1998), 449–458.

Brand, A. H., & Perrimon, N. (1993). Targeted gene expression as a means of altering cell fates and generating dominant phenotypes. *Development (Cambridge, England)*, *118*(2), 401–415.

Buzsáki, G., & Wang, X.-J. (2012). Mechanisms of gamma oscillations. *Annual Review of Neuroscience*, *35*, 203–225.

Cacace AT. (2007). Aging, Alzheimer's disease, and hearing impairment: highlighting relevant issues and calling for additional research. *Am J Audiol*. Jun;16(1):2-3.

Camicioli R, Moore MM, Sexton G, Howieson DB, Kaye JA. (1999). Age-related brain changes associated with motor function in healthy older people. *J Am Geriatr Soc*. Mar;47(3):330-4.

Casas-Tinto, S., Zhang, Y., Sanchez-Garcia, J., Gomez-Velazquez, M., Rincon-Limas, D. E., & Fernandez-Funez, P. (2011). The ER stress factor XBP1s prevents amyloid-beta neurotoxicity. *Human Molecular Genetics*, *20*(11), 2144–2160.

Caughey, B., & Lansbury, P. T. (2003). PROTOFIBRILS, PORES, FIBRILS, AND NEURODEGENERATION: Separating the Responsible Protein Aggregates from The Innocent Bystanders. *Annual Review of Neuroscience*, *26*(1), 267–298.

Chuang, C. F., VanHoven, M. K., Fetter, R. D., Verselis, V. K., & Bargmann, C. I. (2007). An Innexin-Dependent Cell Network Establishes Left-Right Neuronal Asymmetry in C. elegans. *Cell*, *129*(4), 787–799.

Corbett N.J., Hooper N.M. (2018) Soluble Amyloid Precursor Protein α: Friend or Foe?. In: Chattopadhyay K., Basu S. (eds) Biochemical and Biophysical Roles of Cell Surface Molecules. Advances in Experimental Medicine and Biology, vol 1112.

Crowther, D. C., Kinghorn, K. J., Miranda, E., Page, R., Curry, J. A., Duthie, F. A. I., … Lomas, D. A. (2005). Intraneuronal Aβ, non-amyloid aggregates and neurodegeneration in a Drosophila model of Alzheimer's disease. *Neuroscience*, *132*(1), 123–135.

Cuesto, G., Enriquez-Barreto, L., Carames, C., Cantarero, M., Gasull, X., Sandi, C., … Morales, M. (2011). Phosphoinositide-3-Kinase Activation Controls Synaptogenesis and Spinogenesis in Hippocampal Neurons. *Journal of Neuroscience*, *31*(8), 2721–2733.

Cuesto, Germán, Jordán-Álvarez, S., Enriquez-Barreto, L., Ferrús, A., Morales, M., & Acebes, Á. (2015). GSK3β inhibition promotes synaptogenesis in Drosophila and mammalian neurons. *PloS One*, *10*(3), e0118475–e0118475.

Curtin, K. D., Zhang, Z., & Wyman, R. J. (2002). Gap junction proteins expressed during development are required for adult neural function in the Drosophila optic lamina. *The Journal of Neuroscience : The Official Journal of the Society for Neuroscience*, *22*(16), 7088–7096.

De Strooper, B., Vassar, R., & Golde, T. (2010). The secretases: enzymes with therapeutic potential in Alzheimer disease. *Nature Reviews. Neurology*, *6*(2), 99–107.

DeVries, S. H., Qi, X., Smith, R., Makous, W., & Sterling, P. (2002). Electrical coupling between mammalian cones. *Current Biology*, *12*(22), 1900–1907.

Doty, R. L. (2009). The Olfactory System and Its Disorders. *Semin Neurol*, *29*(01), 74–81.

Dudek FE, Snow RW, Taylor CP (1986). Role of electrical interactions in synchronization of epileptiform bursts. *Adv Neurol*. 44:593–617.

Edwards, D. H., Heitler, W. J., & Krasne, F. B. (1999). Fifty years of a command neuron: The neurobiology of escape behavior in the crayfish. *Trends in Neurosciences*, *22*(4), 153–161.

Enriquez-Barreto, L., Cuesto, G., Dominguez, N., Gavilán, E., Ruano, D., Sandi, C., … Morales, M. (2014). Learning improvement after PI3K activation correlates with de novo formation of functional small spines. In *Frontiers in molecular neuroscience* (Vol. 6).

Esparza, T. J., Zhao, H., Cirrito, J. R., Cairns, N. J., Bateman, R. J., Holtzman, D. M., & Brody, D. L. (2013). Amyloid-β oligomerization in Alzheimer dementia versus high-pathology controls. *Annals of Neurology*, *73*(1), 104–119.

Faber, DS.; Pereda, AE. (2011). Physiology of the Mauthner Cell3: Function. *Encycl Fish Physiol From Genome to Environ*. Vol. 1. Elsevier Inc. p. 73-79.

Fang, L., Duan, J., Ran, D., Fan, Z., Yan, Y., Huang, N., … Zhu, Y. (2012). Amyloid-β depresses excitatory cholinergic synaptic transmission in Drosophila. *Neuroscience Bulletin*, *28*(5), 585–594.

Fatt P. Biophysics of junctional transmission. *Physiol Rev*. 1954; 34:674–710.

Feany, M. B., & Bender, W. W. (2000). A Drosophila model of Parkinson's disease. *Nature*, *404*(6776), 394–398.

Fernandez-Funez, P., de Mena, L., & Rincon-Limas, D. E. (2015). Modeling the complex pathology of Alzheimer's disease in Drosophila. *Experimental Neurology*, *274*(Pt A), 58–71. https://doi.org/10.1016/j.expneurol.2015.05.013

Flores, J., Axel, R., Wong, A. M., Vosshall, L. B., & Wang, J. W. (2004). Two-Photon Calcium Imaging Reveals an Odor-Evoked Map of Activity in the Fly Brain. *Cell*, *112*(2), 271–282.

FURSHPAN, E. J., & POTTER, D. D. (1957). Mechanism of Nerve-Impulse Transmission at a Crayfish Synapse. *Nature*, *180*(4581), 342–343.

Goodenough, D. A., & Paul, D. L. (2009). Gap junctions. *Cold Spring Harbor Perspectives in Biology*, *1*(1), a002576–a002576.

Goure, W. F., Krafft, G. A., Jerecic, J., & Hefti, F. (2014). Targeting the proper amyloid-beta neuronal toxins: a path forward for Alzheimer's disease immunotherapeutics. *Alzheimer's Research & Therapy*, *6*(4), 42.

Grabe, V., & Sachse, S. (2018). Fundamental principles of the olfactory code. *BioSystems*, *164*, 94–101.

Greeve, I. (2004). Age-Dependent Neurodegeneration and Alzheimer-Amyloid Plaque Formation in Transgenic Drosophila. *Journal of Neuroscience*, *24*(16), 3899–3906.

Haider, B. (2007). The War of the Soups and the Sparks: The Discovery of Neurotransmitters and the Dispute Over How Nerves Communicate. *The Yale Journal of Biology and Medicine*, *80*(3), 138–139.

Hallem, E. A., & Carlson, J. R. (2006). Coding of Odors by a Receptor Repertoire. *Cell*, *125*(1), 143–160.

Hammond C, Bergman H, Brown P. (2007). Pathological synchronization in Parkinson's disease: networks, models and treatments. *Trends Neurosci*. 30:357–64.

Hamzei-Sichani, F., Davidson, K. G. V., Yasumura, T., Janssen, W. G. M., Wearne, S. L., Hof, P. R., … Rash, J. E. (2012). Mixed Electrical–Chemical Synapses in Adult Rat Hippocampus are Primarily Glutamatergic and Coupled by Connexin-36. *Frontiers in Neuroanatomy*, *6*(May), 1–26.

Hardy JA, Higgings GA. (1992). Alzheimer´s disease: the amyloid cascade hypthesis. Sciencie. April 10;256(5054);184-5.

Heisenberg, M. (2003). Mushroom body memoir: From maps to models. *Nature Reviews Neuroscience*, *4*(4), 266–275.

Hempelmann A, Heils A, Sander T. (2006). Confirmatory evidence for an association of the connexin-36 gene with juvenile myoclonic epilepsy. *Epilepsy Res*. 71:223–8.

Herberholz, J., Antonsen, B. L., & Edwards, D. H. (2002). A lateral excitatory network in the escape circuit of crayfish. *The Journal of Neuroscience : The Official Journal of the Society for Neuroscience*, *22*(20), 9078–9085.

Hirth, F. (2010). Drosophila melanogaster in the study of human neurodegeneration. *CNS & Neurological Disorders Drug Targets*, *9*(4), 504–523.

Homberg, U. (1994). Flight-correlated activity changes in neurons of lateral accessory lobes in the brain of the locust Schistocerca gregaria. In *Journal of Comparative Physiology* (Vol. 175).

Homyk T Jr, Szidonya J, Suzuki DT. (1980). Behavioral mutants of Drosophila melanogaster. III Isolation and mapping of mutations by direct visual observations of behavioral phenotypes. Gen Genet. 1980;177(4):553-65.

Hong, J. G., Kim, D. H., Lee, C. H., Park, S. J., Kim, J. M., Cai, M., … Ryu, J. H. (2012). GSK-3β activity in the hippocampus is required for memory retrieval. *Neurobiology of Learning and Memory*, *98*(2), 122–129.

Hooper, C., Killick, R., & Lovestone, S. (2008). The GSK3 hypothesis of Alzheimer's disease. *Journal of Neurochemistry*, *104*(6), 1433–1439.

Hormuzdi, S. G., Pais, I., LeBeau, F. E. N., Towers, S. K., Rozov, A., Buhl, E. H., … Monyer, H. (2001). Impaired electrical signaling disrupts gamma frequency oscillations in connexin 36-deficient mice. *Neuron*, *31*(3), 487–495.

Hsu, C. T., & Bhandawat, V. (2016). Organization of descending neurons in Drosophila melanogaster. *Scientific Reports*, *6*, 20259.

Huang, J. K., Ma, P. L., Ji, S. Y., Zhao, X. L., Tan, J. X., Sun, X. J., & Huang, F. De. (2013). Age-dependent alterations in the presynaptic active zone in a Drosophila model of Alzheimer's Disease. *Neurobiology of Disease*, *51*, 161–167. Iijima, K., Chiang, H.-C., Hearn, S. A., Hakker, I., Gatt, A., Shenton, C., … Zhong, Y. (2008). Abeta42 mutants with different aggregation profiles induce distinct pathologies in Drosophila. *PloS One*, *3*(2), e1703–e1703.

Iijima, K., Liu, H.-P., Chiang, A.-S., Hearn, S. A., Konsolaki, M., & Zhong, Y. (2004). Dissecting the pathological effects of human Abeta40 and Abeta42 in Drosophila: a potential model for Alzheimer's disease. *Proceedings of the National Academy of Sciences of the United States of America*, *101*(17), 6623–6628.

Jefferis, G. S. X. E. (2003). Developmental origin of wiring specificity in the olfactory system of Drosophila. *Development*, *131*(1), 117–130.

Jelic, V., & Kowalski, J. (2009). Evidence-Based Evaluation of Diagnostic Accuracy of Resting EEG in Dementia and Mild Cognitive Impairment. *Clinical EEG and Neuroscience*, *40*(2), 129–142.

Jordan-Alvarez, S., Fouquet, W., Sigrist, S. J., & Acebes, A. (2012). Presynaptic PI3K activity triggers the formation of glutamate receptors at neuromuscular terminals of Drosophila. *Journal of Cell Science*, *125*(15), 3621–3629.

Kamenetz, F., Tomita, T., Hsieh, H., Seabrook, G., Borchelt, D., Iwatsubo, T., … Point, W. (2003). APP Processing and Synaptic Function State University of New York at Stony Brook. *Neuron*, *37*, 925–937.

Kandler, K., & Katz, L. C. (1995). Neuronal coupling and uncoupling in the developing nervous system. *Current Opinion in Neurobiology*, *5*(1), 98–105.

Kanzaki, R., Ikeda, A., & Shibuya, T. (1994). Morphological and Physiological Properties of Pheromone-Triggered Flipflopping Descending Interneurons of the Male Silkmoth Bombyx Mori. In *Journal of Comparative Physiology A* (Vol. 175).

Kazama, H., & Wilson, R. I. (2008a). Homeostatic matching and nonlinear amplification at identified central synapses. *Neuron*, *58*(3), 401–413.

Kazama, H., & Wilson, R. I. (2008b). Homeostatic Matching and Nonlinear Amplification at Identified Central Synapses. *Neuron*, *59*(1), 183.

Knafo, S., & Esteban, J. A. (2012). Common pathways for growth and for plasticity. *Current Opinion in Neurobiology*, *22*(3), 405–411.

Krishnan, S. N., Frei, E., Swain, G. P., & Wyman, R. J. (1993). Passover: A gene required for synaptic connectivity in the giant fiber system of Drosophila. *Cell*, *73*(5), 967–977.

Lee, T., & Luo, L. (2001). Mosaic analysis with a repressible cell marker (MARCM) for Drosophila neural development. *Trends in Neurosciences*, *24*(5), 251–254.

Lehnert, B. P., Baker, A. E., Gaudry, Q., Chiang, A.-S., & Wilson, R. I. (2013). Distinct roles of TRP channels in auditory transduction and amplification in Drosophila. *Neuron*, *77*(1), 115–128.

Liang, L., Li, Y., Potter, C. J., Yizhar, O., Deisseroth, K., Tsien, R. W., & Luo, L. (2013). GABAergic projection neurons route selective olfactory inputs to specific higher-order neurons. *Neuron*, *79*(5), 917–931.

Linda, B., & Richard Axel. (1991). A Novel Multigene Family May Encode Odrant Receptors: A Molecular Basis for Odor Recognition. *Cell*, *65*, 175–187.

Llinas, R., Baker, R., & Sotelo, C. (1974). Electrotonic coupling between neurons in cat inferior olive. *Journal of Neurophysiology*, *37*(3), 560–571.

López-Arias, B., Turiégano, E., Monedero, I., Canal, I., & Torroja, L. (2017). Presynaptic Aβ40 prevents synapse addition in the adult Drosophila neuromuscular junction. *PLoS ONE*, *12*(5), 1–22.

Luo, S. X., Axel, R., & Abbott, L. F. (2010). Generating sparse and selective third-order responses in the olfactory system of the fly. *Proceedings of the National Academy of Sciences of the*

United States of America, *107*(23), 10713–10718.
Maher, B. J., McGinley, M. J., & Westbrook, G. L. (2009). Experience-dependent maturation of the glomerular microcircuit. *Proceedings of the National Academy of Sciences*, *106*(39),
Marin-Burgin, A. (2005). Sequential Development of Electrical and Chemical Synaptic Connections Generates a Specific Behavioral Circuit in the Leech. *Journal of Neuroscience*, *25*(10), 2478–2489.
Marin-Burgin A, Eisenhart FJ, Kristan WB, French KA (2006). Embryonic electrical connections appear to pre-figure a behavioral circuit in the leech CNS. *J Comp Physiol A Neuroethol Sens Neural Behav Physiol*. 192:123–33.
Martin-Pena, A., Acebes, A., Rodriguez, J.-R., Sorribes, A., de Polavieja, G. G., Fernandez-Funez, P., & Ferrus, A. (2006). Age-Independent Synaptogenesis by Phosphoinositide 3 Kinase. *Journal of Neuroscience*, *26*(40), 10199–10208.
Martin-Peña, A., Rincon-Limas, D. E., & Fernandez-Funez, P. (2017). Anti-Aβ single-chain variable fragment antibodies restore memory acquisition in a Drosophila model of Alzheimer's disease. *Scientific Reports*, *7*(1), 11268.
Martín-Peña, A., Rincón-Limas, D. E., & Fernandez-Fúnez, P. (2018). Engineered Hsp70 chaperones prevent Aβ42-induced memory impairments in a Drosophila model of Alzheimer's disease. *Scientific Reports*, *8*(1), 1–14.
MARTIN, A. R., & PILAR, G. (1963). DUAL MODE OF SYNAPTIC TRANSMISSION IN THE AVIAN CILIARY GANGLION. *The Journal of Physiology*, *168*(2), 443–463.
Mas C (2004). Association of the connexin36 gene with juvenile myoclonic epilepsy. *J Med Genet*. 41:e93.
Masse, N. Y., Turner, G. C., & Jefferis, G. S. X. E. (2009). Olfactory Information Processing in Drosophila. *Current Biology*, *19*(16), R700–R713.
Mehta A, et al. (2017) Homology Requirements and Competition between Gene Conversion and Break-Induced Replication during Double-Strand Break Repair. *Mol. Cell* 65(3):515-526.e3
Mhatre, S. D., Satyasi, V., Killen, M., Paddock, B. E., Moir, R. D., Saunders, A. J., & Marenda, D. R. (2014). Synaptic abnormalities in a Drosophila model of Alzheimer's disease. *Disease Models & Mechanisms*, *7*(3), 373–385.
Moghaddam, B. (2003). *Moghaddam - 2003 - Bringing Order to the Glutamate Chaos in Schizophrenia*. *40*, 881–884.
Moghaddam, B., & Javitt, D. (2012). From revolution to evolution: the glutamate hypothesis of schizophrenia and its implication for treatment. *Neuropsychopharmacology : Official Publication of the American College of Neuropsychopharmacology*, *37*(1), 4–15.
Molinuevo, J. L., Minguillon, C., Rami, L., & Gispert, J. D. (2018). The Rationale behind the New Alzheimer's Disease Conceptualization: Lessons Learned during the Last Decades. *Journal of Alzheimer's Disease*, *62*(3), 1067–1077.
Montoro, R. J., & Yuste, R. (2004). Gap junctions in developing neocortex: A review. *Brain Research Reviews*, *47*(1–3), 216–226.
Moreth, J., Mavoungou, C., & Schindowski, K. (2013). Passive anti-amyloid immunotherapy in Alzheimer's disease: What are the most promising targets? *Immunity & Ageing : I & A*, *10*(1), 18.
Musumeci, G., Sciarretta, C., Rodriguez-Moreno, A., Al Banchaabouchi, M., Negrete-Diaz, V., Costanzi, M., … Minichiello, L. (2009). TrkB Modulates Fear Learning and Amygdalar Synaptic Plasticity by Specific Docking Sites. *Journal of Neuroscience*, *29*(32), 10131–10143.
Namiki, S., & Kanzaki, R. (2016). Comparative neuroanatomy of the lateral accessory lobe in the insect brain. *Frontiers in Physiology*, *7*(JUN), 1–14.
Nellen, D., Burke, R., Struhl, G., & Basler, K. (1997). *Cell 1996*. *85*, 1–12.
Ng, M., Roorda, R. D., Lima, S. Q., Zemelman, B. V, Morcillo, P., & Miesenböck, G. (2002). Transmission of olfactory information between three populations of neurons in the antennal lobe of the fly. *Neuron*, *36*(3), 463–474.

Nieoullon, A. (2002). Dopamine and the regulation of cognition and attention. *Progress in Neurobiology*, *67*(1), 53–83.

Niimura, Y. (2012). Olfactory receptor multigene family in vertebrates: from the viewpoint of evolutionary genomics. *Current Genomics*, *13*(2), 103–114.

Okada, R., Awasaki, T., & Ito, K. (2009). Gamma-aminobutyric acid (GABA)-mediated neural connections in the Drosophila antennal lobe. *Journal of Comparative Neurology*, *514*(1), 74–91.

Olsen, S. R., Bhandawat, V., & Wilson, R. I. (2007). Excitatory interactions between olfactory processing channels in the Drosophila antennal lobe. *Neuron*, *54*(1), 89–103.

Olsen, S. R., Bhandawat, V., & Wilson, R. I. (2010). Divisive normalization in olfactory population codes. *Neuron*, *66*(2), 287–299. https://doi.org/10.1016/j.neuron.2010.04.009

Olsen, S. R., & Wilson, R. I. (2008). Cracking neural circuits in a tiny brain: new approaches for understanding the neural circuitry of Drosophila. *Trends in Neurosciences*, *31*(10), 512–520.

Palop, J. J., Chin, J., Roberson, E. D., Wang, J., Thwin, M. T., Bien-Ly, N., … Mucke, L. (2007). Aberrant Excitatory Neuronal Activity and Compensatory Remodeling of Inhibitory Hippocampal Circuits in Mouse Models of Alzheimer's Disease. *Neuron*, *55*(5), 697–711.

Palop, J. J., & Mucke, L. (2010). Amyloid-beta-induced neuronal dysfunction in Alzheimer's disease: from synapses toward neural networks. *Nature Neuroscience*, *13*(7), 812–818.

Park, W.-M., Wang, Y., Park, S., Denisova, J. V, Fontes, J. D., & Belousov, A. B. (2011). Interplay of chemical neurotransmitters regulates developmental increase in electrical synapses. *The Journal of Neuroscience : The Official Journal of the Society for Neuroscience*, *31*(16), 5909–5920.

Penn AA, Wong RO, Shatz CJ. (1994). Neuronal coupling in the developing mammalian retina. *J Neurosci*. 14:3805–3815.

Penzes, P., Buonanno, A., Passafaro, M., Sala, C., & Sweet, R. A. (2013). Developmental vulnerability of synapses and circuits associated with neuropsychiatric disorders. *Journal of Neurochemistry*, *126*(2), 165–182.

Pereda, A. E. (2014). Electrical synapses and their functional interactions with chemical synapses. *Nature Reviews. Neuroscience*, *15*(4), 250–263.

Pereda, A. E., Rash, J. E., Nagy, J. I., & Bennett, M. V. L. (2004). Dynamics of electrical transmission at club endings on the Mauthner cells. *Brain Research Reviews*, *47*(1–3), 227–244.

Pézier, A. P., Jezzini, S. H., Bacon, J. P., & Blagburn, J. M. (2016). Shaking B Mediates Synaptic Coupling between Auditory Sensory Neurons and the Giant Fiber of Drosophila melanogaster. *PloS One*, *11*(4), e0152211–e0152211.

Phelan, P, Nakagawa, M., Wilkin, M. B., Moffat, K. G., O'Kane, C. J., Davies, J. A., & Bacon, J. P. (1996). Mutations in shaking-B prevent electrical synapse formation in the Drosophila giant fiber system. *The Journal of Neuroscience : The Official Journal of the Society for Neuroscience*, *16*(3), 1101–1113.

Phelan, Pauline. (2005). Innexins: Members of an evolutionarily conserved family of gap-junction proteins. *Biochimica et Biophysica Acta - Biomembranes*, *1711*(2 SPEC. ISS.), 225–245.

Phelan, Pauline, Goulding, L. A., Tam, J. L. Y., Allen, M. J., Dawber, R. J., Davies, J. A., & Bacon, J. P. (2008). Molecular Mechanism of Rectification at Identified Electrical Synapses in the Drosophila Giant Fiber System. *Current Biology*, *18*(24), 1955–1960.

Phelan, Pauline, & Starich, T. A. (2001). Innexins get into the gap. *BioEssays*, *23*(5), 388–396.

Phelan, Pauline, Stebbings, L. A., Baines, R. A., Bacon, J. P., Davies, J. A., & Ford, C. (1998). Drosophila Shaking-B protein forms gap junctions in paired Xenopus oocytes. *Nature*, *391*(6663), 181–184.

Preische, O., Schultz, S. A., Apel, A., Kuhle, J., Kaeser, S. A., Barro, C., … Network, D. I. A. (2019). Serum neurofilament dynamics predicts neurodegeneration and clinical progression in

presymptomatic Alzheimer's disease. *Nature Medicine*, *25*(2), 277–283.
Rahayel, S., Frasnelli, J., & Joubert, S. (2012). The effect of Alzheimer's disease and Parkinson's disease on olfaction: A meta-analysis. *Behavioural Brain Research*, *231*(1), 60–74.
Rash, J. E., Dillman, R. K., Bilhartz, B. L., Duffy, H. S., Whalen, L. R., & Yasumura, T. (1996). Mixed synapses discovered and mapped throughout mammalian spinal cord. *Proceedings of the National Academy of Sciences of the United States of America*, *93*(9), 4235–4239.
Revett, T. J., Baker, G. B., Jhamandas, J., & Kar, S. (2013). Glutamate system, amyloid β peptides and tau protein: Functional interrelationships and relevance to Alzheimer disease pathology. *Journal of Psychiatry and Neuroscience*, *38*(1), 6–23.
Rincon-Limas, D. E., Jensen, K., & Fernandez-Funez, P. (2012). Drosophila models of proteinopathies: the little fly that could. *Current Pharmaceutical Design*, *18*(8), 1108–1122.
Root, C. M., Masuyama, K., Green, D. S., Enell, L. E., Nässel, D. R., Lee, C.-H., & Wang, J. W. (2008). A presynaptic gain control mechanism fine-tunes olfactory behavior. *Neuron*, *59*(2), 311–321.
Root, C. M., Semmelhack, J. L., Wong, A. M., Flores, J., & Wang, J. W. (2007). *PNAS-2007-Root-11826-31*. *2007*.
Rubin, B. D., & Katz, L. C. (1999). Optical imaging of odorant representations in the mammalian olfactory bulb. *Neuron*, *23*(3), 499–511.
Scheltens, P., Blennow, K., Breteler, M. M., De strooper, B., Frisoni, G. B., Salloway, s. & van der Flier, W. M. 2016. Alzheimer's disease. *Lancet*.
Seki, Y., Dweck, H. K. M., Rybak, J., Wicher, D., Sachse, S., & Hansson, B. S. (2017). Olfactory coding from the periphery to higher brain centers in the Drosophila brain. *BMC Biology*, *15*(1), 18–22.
Shang, Y., Claridge-Chang, A., Sjulson, L., Pypaert, M., & Miesenböck, G. (2007). Excitatory local circuits and their implications for olfactory processing in the fly antennal lobe. *Cell*, *128*(3), 601–612.
Sheng, M., Sabatini, B. L., & Südhof, T. C. (2012). Synapses and Alzheimer's disease. *Cold Spring Harbor Perspectives in Biology*, *4*(5), 10.
Shimohigashi M, Meinertzhagen IA. (1998). The shaking B gene in Drosophila regulates the number of gap junctions between photoreceptor terminals in the lamina. *J Neurobiology*. Apr;35(1):105-17.
Silbering, A. F., Okada, R., Ito, K., & Galizia, C. G. (2008). Olfactory Information Processing in the Drosophila Antennal Lobe: Anything Goes? *Journal of Neuroscience*, *28*(49), 13075–13087.
Silbering, Ana F, & Galizia, C. G. (2007). Processing of odor mixtures in the Drosophila antennal lobe reveals both global inhibition and glomerulus-specific interactions. *The Journal of Neuroscience : The Official Journal of the Society for Neuroscience*, *27*(44), 11966–11977.
Söhl, G., Maxeiner, S., & Willecke, K. (2005). Expression and functions of neuronal gap junctions. *Nature Reviews Neuroscience*, *6*(3), 191–200.
Stebbings, L. A., Todman, M. G., Phillips, R., Greer, C. E., Tam, J., Phelan, P., … Davies, J. A. (2002). Gap junctions in Drosophila: Developmental expression of the entire innexin gene family. *Mechanisms of Development*, *113*(2), 197–205.
Stocker RF, Heimbeck G, Gendre N, de Belle JS. (1997) Neuroblast ablation in Drosophila P[Gal4] lines reveals origins of olfactory interneurons. J Neurobiol, May; 32 (5):443-56
Stefani, M. (2010). Biochemical and biophysical features of both oligomer/fibril and cell membrane in amyloid cytotoxicity. *FEBS Journal*, *277*(22), 4602–4613.
Su, C. Y., Menuz, K., & Carlson, J. R. (2009). Olfactory Perception: Receptors, Cells, and Circuits. *Cell*, *139*(1), 45–59.
Sun, Y. A., & Wyman, R. J. (1996). Passover eliminates gap junctional communication between neurons of the giant fiber system in Drosophila. *Journal of Neurobiology*, *30*(3), 340–348.
Szabo, T. M. (2004). Transient Electrical Coupling Delays the Onset of Chemical Neurotransmission at Developing Synapses. *Journal of Neuroscience*, *24*(1), 112–120.

Tanaka, N. K., Tanimoto, H., & Ito, K. (2008). Neuronal assemblies of the Drosophila mushroom body. *Journal of Comparative Neurology*, *508*(5), 711–755.

Thomas, J. B., & Wyman, R. J. (1984). Mutations altering synaptic connectivity between identified neurons in Drosophila. *The Journal of Neuroscience : The Official Journal of the Society for Neuroscience*, *4*(2), 530–538.

Todd, K. L., Kristan Jr, W. B., & French, K. A. (2010). Gap junction expression is required for normal chemical synapse formation. *The Journal of Neuroscience : The Official Journal of the Society for Neuroscience*, *30*(45), 15277–15285.

Trimarchi, J. R., & Murphey, R. K. (1997). The shaking-B2 mutation disrupts electrical synapses in a flight circuit in adult Drosophila. *The Journal of Neuroscience : The Official Journal of the Society for Neuroscience*, *17*(12), 4700–4710.

Turner, A. J., Fisk, L., & Nalivaeva, N. N. (2004). Targeting amyloid-degrading enzymes as therapeutic strategies in neurodegeneration. *Annals of the New York Academy of Sciences*, *1035*, 1–20.

Uchida, N., Takahashi, Y. K., Tanifuji, M., & Mori, K. (2000). Odor maps in the mammalian olfactory bulb: domain organization and odorant structural features. *Nature Neuroscience*, *3*(10), 1035–1043.

Vervaeke, K., Lorincz, A., Nusser, Z., & Silver, R. A. (2012). Gap junctions compensate for sublinear dendritic integration in an inhibitory network. *Science*, *335*(6076), 1624–1628.

Vivar, C., Traub, R. D., & Gutiérrez, R. (2012). Mixed electrical-chemical transmission between hippocampal mossy fibers and pyramidal cells. *The European Journal of Neuroscience*, *35*(1), 76–82.

Volff, J. N. (2005). Genome evolution and biodiversity in teleost fish. *Heredity*, *94*(3), 280–294.

Vosshall, L. B. (2007). Into the mind of a fly. *Nature*, *450*(7167), 193–197.

Vosshall, L. B., Amrein, H., Morozov, P. S., Rzhetsky, A., & Axel, R. (1999). A spatial map of olfactory receptor expression in the Drosophila antenna. *Cell*, *96*(5), 725–736.

Wachowiak, M., & Cohen, L. B. (2001). Representation of odorants by receptor neuron input to the mouse olfactory bulb. *Neuron*, *32*(4), 723–735.

Walsh, D. M., Klyubin, I., Fadeeva, J. V, Cullen, W. K., Anwyl, R., Wolfe, M. S., … Selkoe, D. J. (2002). Naturally secreted oligomers of amyloid β protein potently inhibit hippocampal long-term potentiation in vivo. *Nature*, *416*(6880), 535–539.

Wilson, R. I. (2013). Early olfactory processing in Drosophila: mechanisms and principles. *Annual Review of Neuroscience*, *36*, 217–241.

Wolff, G. H., & Strausfeld, N. J. (2015). Genealogical correspondence of mushroom bodies across invertebrate phyla. *Current Biology*, *25*(1), 38–44.

Wolszon, L. (1995). Cell–cell interactions define the innervation patterns of central leech neurons during development. *Journal of Neurobiology*, *27*(3), 335–352.

Wong, A. M., Wang, J. W., & Axel, R. (2002). Spatial representation of the glomerular map in the Drosophila protocerebrum. *Cell*, *109*(2), 229–241.

Yaksi, E., & Wilson, R. I. (2010). Electrical coupling between olfactory glomeruli. *Neuron*, *67*(6), 1034–1047.

Yu, Y.-C., He, S., Chen, S., Fu, Y., Brown, K. N., Yao, X.-H., … Shi, S.-H. (2012). Preferential electrical coupling regulates neocortical lineage-dependent microcircuit assembly. *Nature*, *486*(7401), 113–117.

Z Mentis, G., Diaz, E., Moran, L., & Navarrete, R. (2002). Increased incidence of gap junctional coupling between spinal motoneurons following transient blockade of NMDA receptors in neonatal rats. In *The Journal of physiology* (Vol. 544).

Zetterberg, H., & Schott, J. M. (2019). Biomarkers for Alzheimer's disease beyond amyloid and tau. *Nature Medicine*, *25*(2), 201–203.

Zhang, Z., Curtin, K. D., Sun, Y. A., & Wyman, R. J. (1999). Nested transcripts of Gap junction gene have distinct expression patterns. *Journal of Neurobiology*, *40*(3), 288–301.

Zorović, M., & Hedwig, B. (2013). Descending brain neurons in the cricket Gryllus bimaculatus

(de Geer): auditory responses and impact on walking. *Journal of Comparative Physiology. A, Neuroethology, Sensory, Neural, and Behavioral Physiology*, *199*(1), 25–34.

Zuber, B., Nikonenko, I., Klauser, P., Muller, D., & Dubochet, J. (2005). The mammalian central nervous synaptic cleft contains a high density of periodically organized complexes. *Proceedings of the National Academy of Sciences of the United States of America*, *102*(52), 19192–19197.

AGRADECIMIENTOS/ACKNOWLEDGEMENTS

Me gustaría agradecer a todas esas personas que han participado en la realización de esta tesis doctoral y que han contribuido al sueño de por fin, verla hecha realidad:

A Ángel, por darme la oportunidad de iniciar este proyecto y presentarme a las que siempre serán “mis niñas”.

A todos los integrantes del laboratorio, jamás me cansaré de darles las gracias por tantísima ayuda en todos estos años, por cada palabra de ánimo, por las miles de sonrisas y buenos momentos compartidos, por hacer que todo fuese un poco más fácil. Gracias a todos: Nati, Cati, Héctor, José Luis, Daniel, Alberto, Natalia, Germán, Roger, Silvia, Elva, Belinda, David, Laura, Ricardo, Álex y Brian. Gracias también a Diego y Teresa, por hacerme sentir una más del grupo.

A Guadalberto, gracias por todos tus consejos, por tener siempre un momento para escucharme, por confiar tanto en mí y en que sería capaz de llegar hasta el final. Aún me sigo preguntado a dónde iré con mantón de manila…gracias por tanto cariño, de corazón.

A Héctor, gracias por ser tú, así, sin más. Gracias por haberme acompañado en la aventura, por animarme a querer ser mejor, por saber siempre qué decir, por muy duro que sea. Gracias por hacerme reaccionar y no dejarme caer. Gracias por ser de esas personas que te abrazan y te reinician, por hacerme siempre sonreír, por ponerle hilo musical a las largas tardes de análisis, por los veranos en el laboratorio, por las llamadas interminables en USA, gracias por cuidarme tanto y por todo lo que me has enseñado. Esto también es tuyo. Ahora sí, trá trá!

A Silvi, gracias por tu experiencia, tu sensibilidad y tu cariño. Gracias por tu paciencia, tus consejos, por tener siempre un momento para escucharme, por hacerme ver el “focus”. Gracias por haber estado a mi lado.

A Elva, gracias por estar siempre dispuesta a cuidarme mis niñas, por nuestros inolvidables bailes de calentamiento antes de los tests. Gracias por animarme a seguir adelante.

Me gustaría también agradecer al laboratorio del profesor Alberto Ferrús: Alberto, Sergio, Elena, Clemen y Paco, gracias por haberme enseñado nuevas técnicas y haberme hecho sentir una más. Thanks to all of members at Prof. Santa-Marías´s lab: Ismael, Euge, Yoon and Jêrome, that made me feel as part of the lab and helped me with my project. Thanks for giving me back the illusion of doing science.

A Merce, por tu ayuda incondicional y tus consejos. Gracias por cuidarme tanto esos meses, por hacerme sentir una New-Yorker más: “If you can do it in New York, you can do it everywhere”. Gracias por creer tanto en mí.

A Pablo, por ser el mejor masterchef de la papilla. Gracias por tu generosidad durante todos estos años.

A mis queridos Guille y Eva, gracias por preguntarme cada día por el estado de mis mosquitas, por animarme siempre, por todo vuestro cariño y vuestro apoyo. Gracias por haberme enseñado tanto.

A Dani, por haberte lanzado a vivir conmigo todo lo que una tesis significa. Gracias por haber llevado los momentos más difíciles con la mejor de las sonrisas, con mucha paciencia y cariño. Gracias por hacerme feliz cada día.

A mi doctora preferida, por haberme acompañado siempre en esas largas noches de estudio. Donde quiera que estés, tu huellita no se borrará jamás.

A mi hermana, gracias por todo esos "porque puedes" tan tuyos y darme siempre la tranquilidad que necesito. Gracias por transmitirme tanta fuerza y animarme siempre en todo lo que hago. Un pedacito de esto también es tuyo.

A mis padres, gracias por estar siempre ahí, por haberme acompañado en esta intensa aventura. Gracias por no permitir que me rindiera, por animarme siempre a conseguir mis sueños, y por creer y confiar siempre en mí. Gracias por emocionaros conmigo cuando las mosquitas se "portaban" bien, por querer escuchar siempre cómo iban los experimentos o la investigación y al final, terminar queriendo a las mosquitas casi tanto como yo. Gracias por vuestro apoyo incondicional, no habría llegado hasta aquí sin vuestra ayuda. Esto es de ustedes.

Gracias también a ti, por haberle dedicado un tiempo a leer esta tesis.

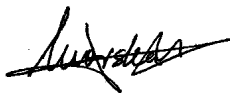

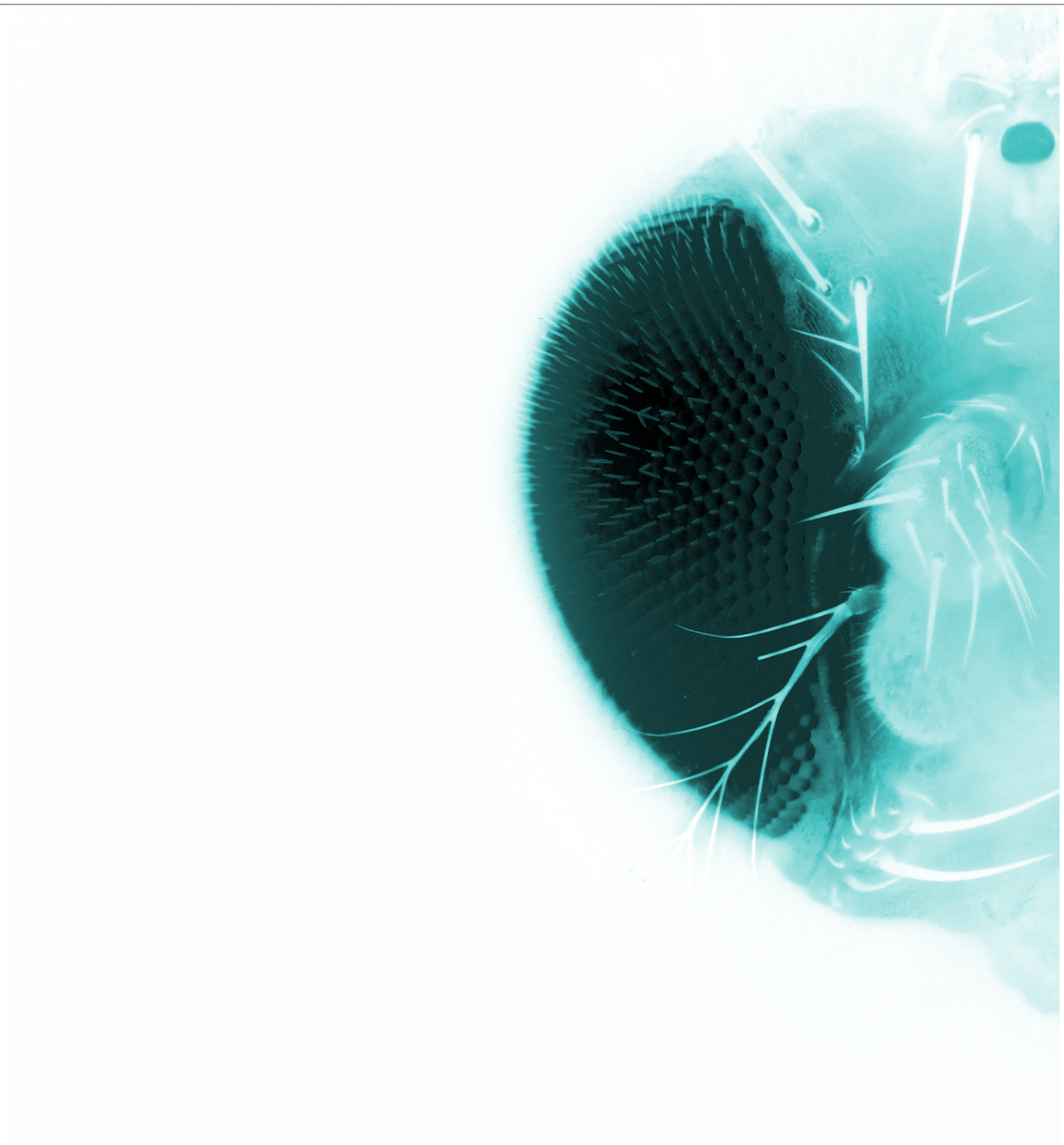

Image modified from:
Drosophila expressing GFP
Macroscopic Solutions (CC BY-NC)